

**NMR STUDY OF AQUEOUS
TETRAALKYLAMMONIUM SILICATES**

by

Raymond T. Syvitski

submitted to

**The Department of Chemistry, Lakehead University,
in Partial Fulfilment of the Requirements for
the Degree of Master of Science.**

Supervisor: Dr. S. D. Kinrade

**©Raymond T. Syvitski
Department of Chemistry, Lakehead University
Thunder Bay, Ontario, Canada, P7B 5E1
August, 1994.**

ProQuest Number: 10611896

All rights reserved

INFORMATION TO ALL USERS

The quality of this reproduction is dependent upon the quality of the copy submitted.

In the unlikely event that the author did not send a complete manuscript and there are missing pages, these will be noted. Also, if material had to be removed, a note will indicate the deletion.



ProQuest 10611896

Published by ProQuest LLC (2017). Copyright of the Dissertation is held by the Author.

All rights reserved.

This work is protected against unauthorized copying under Title 17, United States Code
Microform Edition © ProQuest LLC.

ProQuest LLC.
789 East Eisenhower Parkway
P.O. Box 1346
Ann Arbor, MI 48106 - 1346



National Library
of Canada

Acquisitions and
Bibliographic Services Branch

395 Wellington Street
Ottawa, Ontario
K1A 0N4

Bibliothèque nationale
du Canada

Direction des acquisitions et
des services bibliographiques

395, rue Wellington
Ottawa (Ontario)
K1A 0N4

Your file *Votre référence*

Our file *Notre référence*

THE AUTHOR HAS GRANTED AN IRREVOCABLE NON-EXCLUSIVE LICENCE ALLOWING THE NATIONAL LIBRARY OF CANADA TO REPRODUCE, LOAN, DISTRIBUTE OR SELL COPIES OF HIS/HER THESIS BY ANY MEANS AND IN ANY FORM OR FORMAT, MAKING THIS THESIS AVAILABLE TO INTERESTED PERSONS.

L'AUTEUR A ACCORDE UNE LICENCE IRREVOCABLE ET NON EXCLUSIVE PERMETTANT A LA BIBLIOTHEQUE NATIONALE DU CANADA DE REPRODUIRE, PRETER, DISTRIBUER OU VENDRE DES COPIES DE SA THESE DE QUELQUE MANIERE ET SOUS QUELQUE FORME QUE CE SOIT POUR METTRE DES EXEMPLAIRES DE CETTE THESE A LA DISPOSITION DES PERSONNE INTERESSEES.

THE AUTHOR RETAINS OWNERSHIP OF THE COPYRIGHT IN HIS/HER THESIS. NEITHER THE THESIS NOR SUBSTANTIAL EXTRACTS FROM IT MAY BE PRINTED OR OTHERWISE REPRODUCED WITHOUT HIS/HER PERMISSION.

L'AUTEUR CONSERVE LA PROPRIETE DU DROIT D'AUTEUR QUI PROTEGE SA THESE. NI LA THESE NI DES EXTRAITS SUBSTANTIELS DE CELLE-CI NE DOIVENT ETRE IMPRIMES OU AUTREMENT REPRODUITS SANS SON AUTORISATION.

ISBN 0-315-97069-3

Canada

Abstract

Silicon-29 nuclear magnetic resonance (NMR) spectroscopy has been used to investigate the equilibrium distribution and kinetics of silicate oligomers in aqueous tetraalkylammonium silicate solutions. Certain tetraalkylammonium cations (particularly tetramethylammonium cation) stabilize specific silicate oligomers, such as the cubic octamer and prismatic hexamer, by forming a protective shell that shields these oligomers from interaction with paramagnetic ions and impedes Si-Si chemical exchange. For tetramethylammonium silicate solutions, the dependence of the initial rate of cubic octamer formation on alkalinity, silica concentration and tetramethylammonium cation concentration has been investigated and a mechanism for the formation of cubic octamer proposed.

For tetraalkylammonium silicate solutions with $\text{OH}^-:\text{Si}^{\text{IV}} \leq 1:1$ which favour the cubic octamer, at least four resonances which occur down-frequency of the cubic octamer resonance have been attributed to stable protonated states of the cubic octamer.

Alkali-metal cations added to tetramethylammonium silicate solutions destabilize the cubic octamer probably by displacing tetramethylammonium cations which surround the oligomer.

Acknowledgements

I would like to express sincere thanks to my supervisor, Dr. S. D. Kinrade, for his guidance, thoughtful discussions and generous help throughout my graduate studies. My gratitude goes out to: Messrs. A. McKenzie, K. Pringnitz and A. Raitsakas, of the Science Instrumentation Laboratory, for instrumental measurements and for instructions on the use of the NMR and FTIR; Messrs. A.J. Harding, D. Corbett, B.K. Morgan and A. Bharath for technical help; Mr. E. Drotar and Mr. R. Mazzaferro, of the science workshop, for their excellent work in constructing the high pressure NMR tube assembly and various other equipment; and Mr. K. Marat and Mr. T. Woliec, of The Prairie Regional NMR Facility, for acquiring spectra, for their patient assistance when I was operating the Bruker AMX 500 spectrometer in Winnipeg and for constant guidance with the NMR processing program UXNMR/P.

Special thanks and consideration must be given to Mr. J. DeINin, Mr. G. Hill and Mr. S. Whatley for their interesting and thought provoking discussions and, Mr. D.L. Pole, who began preliminary studies on this research and guided me through the first couple of months.

This research was supported by graduate scholarships (1991-93) from the Ontario Ministry of Colleges and Universities, assistantships from the Faculty of Research and Graduate Studies and the Department of Chemistry and, the Natural Sciences and Engineering Research Council of Canada.

Symbols and Abbreviations

ATR	attenuated total reflection
DMSO	dimethylsulfoxide (methylsulfoxide)
ETMA ⁺	(β -hydroxyethyl)trimethylammonium cation
FEP	fluorinated ethylene propylene
FID	free induction decay
FTIR	Fourier transform infrared (spectroscopy)
I	ionic strength
ICP	inductively coupled plasma (spectroscopy)
I.D.	inside diameter
k	rate coefficient
k_f	forward rate coefficient
k_r	reverse rate coefficient
MHz	megahertz
mm	millimetres
MPa	megapascals
Na ₂ H ₂ EDTA	disodium ethylenediaminetetraacetic acid
NMR	nuclear magnetic resonance (spectroscopy)
O.D.	outside diameter
$\text{OH}^-:\text{Si}^{\text{IV}}$	molal concentration ratio between OH^- and dissolved Si^{IV}
P	pressure
PEEK	polyetheretherketone

pH	negative log of the hydrogen ion concentration
pKa	negative logarithm of acid dissociation constant
ppm	parts per million
Q_z^y	tetrahedral SiO_4 centre with 4- y terminal hydroxyl groups. When applicable, z indicates the number of equivalent centres in totally symmetric species.
$^*Q^y$	activated silicate centre with y coordinated silicate groups
R	gas constant (<i>i.e.</i> , $8.314 \text{ J K}^{-1} \text{ mol}^{-1}$)
SBU	secondary building unit (theory)
SEM/EDS	scanning electron microscope with X-ray microanalyser
SIR	selective inversion recovery
T	temperature
t	time
T_1	nuclear spin-lattice relaxation time
T_2	nuclear spin-spin relaxation time
TAA ⁺	tetraalkylammonium cation
TBA ⁺	tetra(<i>n</i> -butyl)ammonium cation
TEA ⁺	tetraethylammonium cation
TFE	tetrafluoroethylene
TMA ⁺	tetramethylammonium cation
TMS	tetramethylsilane
TPA ⁺	tetra(<i>n</i> -propyl)ammonium
\bar{V}	partial molar volume

ΔV^\ddagger	activation volume
X^+	cation other than TMA^+
X_{TMA^+}	mole fraction of cations which are TMA^+
X_{X^+}	mole fraction of cations which are X^+
ZnSe	zinc selenide
$\Delta\delta$	difference in δ (usually with respect to Q^0 resonance)
δ	chemical shift in ppm (value is positive for up-frequency shift)

Contents

Abstract	i
Acknowledgements	ii
Symbols and Abbreviations	iii
Contents	vi
Chapter I. Introduction	
1.1. Preface	1
1.2. Aqueous Silicate Chemistry	1
1.2.1. Overview	1
1.2.2. Early Studies	2
1.2.3. ²⁹ Si NMR Studies	2
1.2.4. Alkali-Metal Silicates	7
1.2.5. Tetraalkylammonium Silicates	8
1.3. Zeolite Synthesis	12
1.3.1. Zeolites	12
1.3.2. Theories of Zeolite Crystallization	13
1.4. Objectives	14
Chapter II. Experimental Procedure	
2.1 Reagents	15
2.2. Sample Preparation	16
2.3. NMR Measurements	17
2.4. pH Measurements	21
2.5. Attenuated Total Reflection Infrared Measurements	22

Chapter III. Experimental Findings

3.1. Silicate Equilibria	23
3.1.1. Analysis of Previous Studies	23
3.1.2. TMA Silicate Equilibria	24
3.1.3. Mixed Cation Silicate Equilibria	29
3.1.4. TAA Silicate Equilibria at $\text{OH}^-:\text{Si}^{\text{IV}} < 1:1$	34
3.2. Silicate Kinetics	41
3.2.1. Analysis of Previous Studies	41
3.2.2. Method of Initial Rates	41
3.2.3. Effect of Pressure on Silicate Kinetics	45
3.2.4. Kinetics of TMA Silicate Solutions	45
3.2.5. Transient Species in TMA Silicate Solutions	48
3.2.6. Transient Species in Other TAA Silicate Solutions	51
3.2.7. Effect of Na^+ Ions on TMA Silicate Solutions	54
3.2.8. Germanosilicates	54
3.3. Analysis of Kinetic Data	57

Chapter IV. Discussion

4.1. Current Theories of Q_8^3 Stabilization	65
4.2. Evidence for a Direct Association Between Q_8^3 and TMA^+ Ions	66
4.3. Nature of the Solution Phase $\text{Q}_8^3(\text{and Q}_6^3)/\text{TMA}^+/\text{H}_2\text{O}$ Cluster	69
4.4. Mechanism of $\text{Q}_8^3/\text{TMA}^+/\text{H}_2\text{O}$ Cluster Formation	72

4.5. Implications to the Mechanism of Zeolite Synthesis	75
4.6. Conclusions	76
Chapter V. Future Studies	
5.1. Kinetics of $Q_8^3/TMA^+/H_2O$ Cluster Formation	78
5.2. Metal Substitution in Silicate Oligomers	78
5.3. Identification of Silicate Anions	79
5.4. Investigation of Protonated Q_8^3 Clusters	79
References	80
Appendix to Chapter 3 Section 3.2	
Selective Population Transfer NMR	86

Chapter I. Introduction

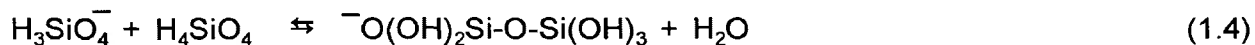
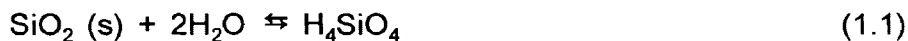
1.1. Preface

Although silicon is the second most abundant element, by mass, in the earth's crust, its chemistry is relatively unexplored. Silicon is commonly found as a dioxide and usually in a tetrahedral configuration. However, it also can be incorporated into many organic and inorganic compounds in which the silicon atom is central in a trigonal, trigonal bipyramidal, square planar or octahedral structure.^[1] Silicon dioxide is relatively unreactive with neutral aqueous solutions, chlorine gas, hydrogen gas, most acids, and most metals at moderate or slightly elevated temperatures. It is reactive with aqueous hydroxides, fluorine, hydrofluoric acid and fused carbonates.^[1]

1.2. Aqueous Silicate Chemistry

1.2.1. Overview

Amorphous silica (SiO_2) readily dissolves in aqueous hydroxide solutions. Equations 1.1 to 1.3 characterize formation of silicic acid and its subsequent ionization (pKa's are at 298 K and ionic strength = 0.6 mol L^{-1} ^[2]). Once dissolved, silicic acid can form a number of oligomeric silicate anions (up to 20 or more) rapidly and reversibly via condensation (Equation 1.4 to 1.6).



The occurrence of straight chains longer than four silicic acid units is unusual as silicate oligomers tend to form structures which are cyclic or cage-like in nature^[3,4,5] (Table I-I).

In the system of nomenclature initially used by Engelhardt *et al.*,^[6] a Quadrifunctional silicon centre with y siloxane (Si-O-Si) linkages (commonly referred to as the "*degree of connectivity*") is represented by Q^Y . Totally symmetric oligomers can be denoted by including as a subscript the corresponding number of equivalent tetrahedra *e.g.*, Q_X^Y (Table I-I).

1.2.2. Early Studies

Early studies employed wet chemical techniques (*i.e.*, trimethylsilylation,^[7,8,9] paper chromatography^[10] and reactions with molybdic acid^[11,12]) to investigate the chemistry of aqueous silicate oligomers. These techniques revealed a predominance of small, globular oligomers made up of rings and cages. Investigators^[13,14,15] later determined that such methods can alter the distribution and structure of oligomers. Infrared and Raman spectroscopy^[16,17,18] also have been employed. However, the detected vibrational modes are not uniquely characteristic of individual oligomers.

1.2.3. ²⁹Si NMR Studies

In contrast, ²⁹Si NMR spectroscopy has provided extensive information on aqueous silicate chemistry. Definitive evidence for the existence of eighteen silicate oligomers in aqueous alkaline solution has been provided using one- and two-dimensional techniques.^[19-24] Five other species were identified with less certainty. Selected ²⁹Si NMR assignments for a solution containing 0.9 mol kg⁻¹ SiO₂ and 0.9 mol kg⁻¹ NaOH are depicted in Figure 1-1.

The natural isotopic abundance of the spin 1/2 ²⁹Si nucleus is 4.7%.

Table I-I.^a Silicate anion names, molecular formula^b, structures, nomenclature, and assignments

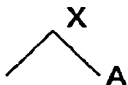
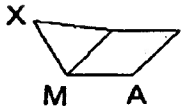

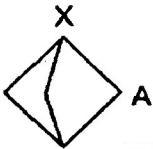
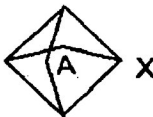

Species	Structure ^c	Si-Centre	Assignment ^d ($\Delta\delta$ /ppm)
Monomer H_3SiO_4^-	•	Q^0	0.00
Dimer $\text{H}_4\text{Si}_2\text{O}_7^{2-}$	—	Q_2^1	-8.5
Linear trimer $\text{H}_5\text{Si}_3\text{O}_{10}^{3-}$		Q^1 (A) Q^2 (X)	-8.1 -16.7
Bicyclic pentamer $\text{H}_3\text{Si}_5\text{O}_{14}^{5-}$		Q^2 (X) Q^2 (A) Q^3 (M)	-9.9 -16.3 -17.2
Tricyclic hexamer (1) $\text{H}_2\text{Si}_6\text{O}_{16}^{6-}$		Q^2 (A) Q^3 (X)	-10.4 -16.6
Bridged cyclic tetramer $\text{H}_3\text{Si}_5\text{O}_{14}^{5-}$		Q^2 (A) Q^3 (X)	-14.2 -21.9
Doubly bridged cyclic tetramer $\text{H}_2\text{Si}_6\text{O}_{16}^{6-}$		Q^2 (A) Q^3 (X)	-14.5 -21.4
Cyclic trimer $\text{H}_3\text{Si}_3\text{O}_9^{3-}$		Q_3^2	-10.2

Table I-I. (con't)

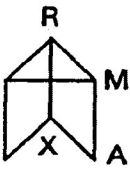
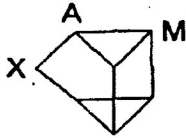
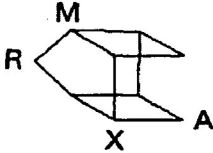
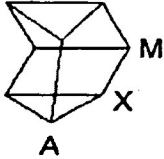

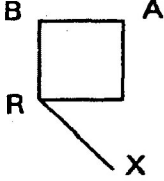
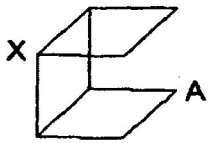

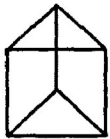
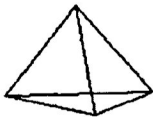
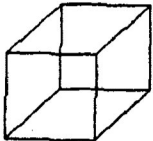
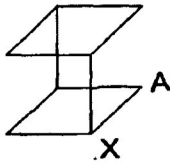
<p>Tricyclic hexamer (2) $H_2Si_6O_{16}^{6-}$</p>		<p>Q^2 (A) Q^3 (R) Q^3 (M) Q^3 (X)</p>	<p>-16.0 -16.6 -17.5 -24.7</p>
<p>Pentacyclic heptamer $HSi_7O_{18}^{7-}$</p>		<p>Q^2 (X) Q^3 (M) Q^3(A)</p>	<p>-16.9 -17.9 -18.9</p>
<p>Pentacyclic nonamer $H_3Si_9O_{20}^{9-}$</p>		<p>Q^2 (A) Q^2 (R) Q^3 (M) Q^3 (X)</p>	<p>-15.7 -16.6 -18.1 -24.9</p>
<p>Hexacyclic octamer $Si_8O_{20}^{8-}$</p>		<p>Q^3 (X) Q^3 (A) Q^3 (M)</p>	<p>-17.8 -20.4 -26.7</p>
<p>Bicyclic hexamer $H_4Si_6O_{17}^{6-}$</p>		<p>Q^2 (A) Q^3 (X)</p>	<p>-16.2 -24.1</p>
<p>Substituted cyclic tetramer $H_5Si_5O_{15}^{5-}$</p>		<p>Q^1 (X) Q^2 (B) Q^2 (A) Q^3 (R)</p>	<p>-7.9 -15.8 e -24.2</p>

Table I-I. (con't)

Tricyclic octamer (1) $H_4Si_8O_{22}^{8-}$		Q^2 (A) Q^3 (X)	-15.5 -24.5
Cyclic tetramer $H_4Si_4O_{12}^{4-}$		Q_4^2	-16.1
Prismatic hexamer $Si_6O_{15}^{6-}$		Q_6^3	-17.2
Tetrahedral tetramer $Si_4O_{10}^{4-}$		Q_4^3	-25.7
Cubic octamer $Si_8O_{20}^{8-}$		Q_8^3	-27.3
Tricyclic octamer (2) $H_4Si_8O_{22}^{8-}$		Q^2 (A) Q^3 (X)	-15.6 -25.2

^aList is not exhaustive.

^bThe charge on the anion is dependant on solution alkalinity.

^cStructures are represented by stick figures in which lines represent Si-O-Si linkages. For convenience, terminal hydroxyl groups are not shown.

^dAssignments are from references 19-24 and correspond to resonances in Figure 1-1 and Figure 1-2; chemical shifts are dependant on solution composition and temperature.

^e Resonance is unidentified^[5]

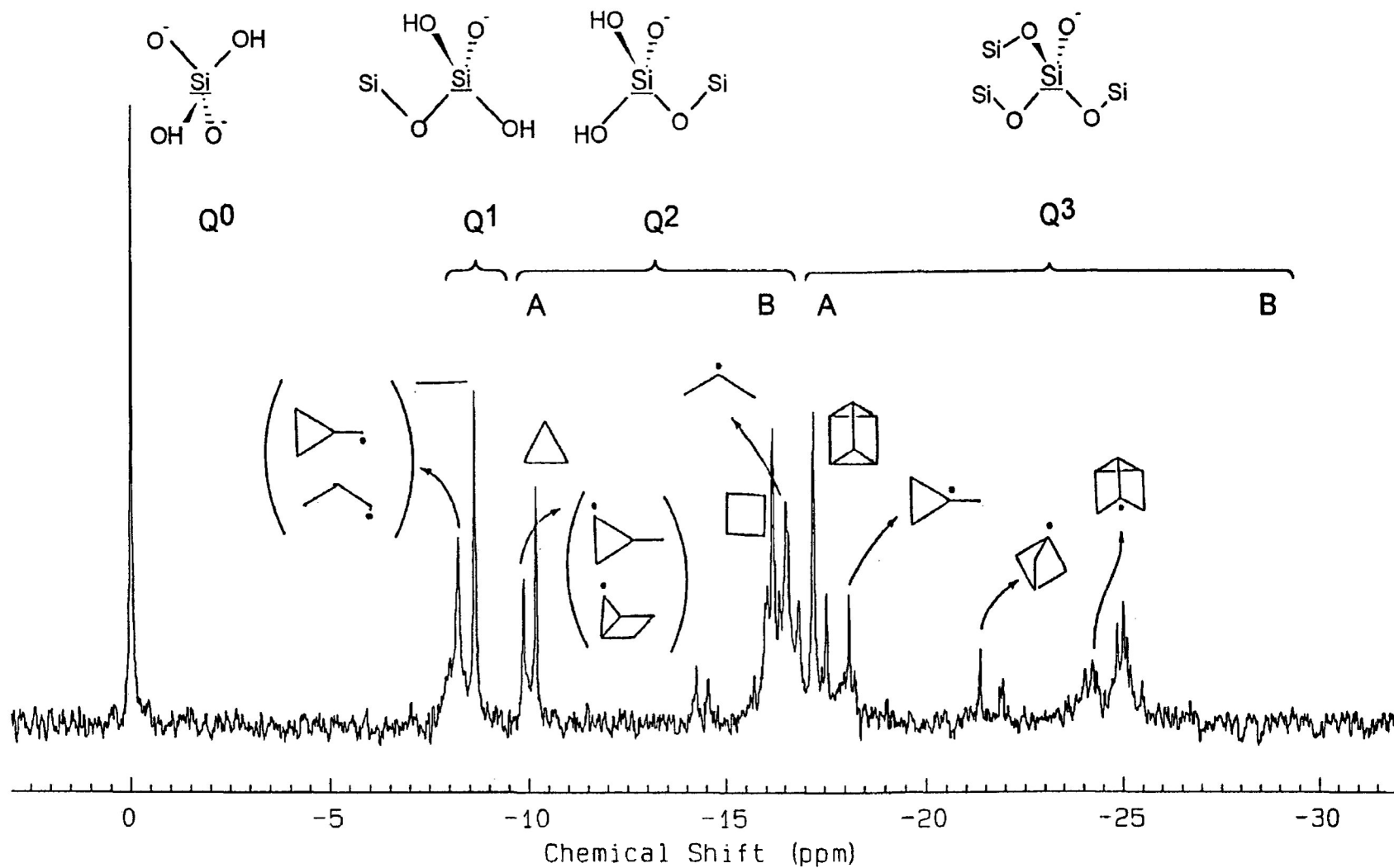


Figure 1 – 1. ^{29}Si NMR spectrum of a $0.9 \text{ mol kg}^{-1} \text{ SiO}_2$ and $0.9 \text{ mol kg}^{-1} \text{ NaOH}$ solution at 296.1 K. The dot indicates the resonating silicon centre. Structures are represented as in Table I–I. The spectrum is referenced to the monomer (0 ppm) which is approximately 71 ppm down-frequency of tetramethylsilane.

This low natural abundance virtually eliminates ^{29}Si – ^{29}Si coupling unless solutions are isotopically enriched. Rapid exchange of hydroxyl protons, relative to the NMR time scale, precludes detection of either ^{29}Si – ^1H coupling or time-resolved silicate ^1H resonances.

In ^{29}Si NMR spectra, resonances are shifted in accordance with the degree of connectivity on the resonating silicate centre (Figure 1-1). Resonances occurring within the Q^2 and Q^3 regions can be grouped further into two subregions (labelled A and B) owing primarily to the degree of ring strain.^[25,26]

1.2.4. Alkali-Metal Silicates

Alkali-metal silicate solutions can contain a wide variety of silicate oligomers. The equilibrium distribution is affected by a variety of factors. As temperature or alkalinity is increased, the extent of polymerization and the variety of silicate oligomers decrease.^[24,27-29] The extent of polymerization increases when organic solutes are added^[30] and with the mass of the alkali-metal cation (*i.e.*, as in the order: $\text{Na}^+ < \text{K}^+ < \text{Rb}^+ < \text{Cs}^+$). The latter influence has been attributed to changes in the extent of silicate-metal ion-pairing.^[31-33]

The rate of Si-Si exchange decreases uniformly for all Si centres as alkalinity is increased.^[29] Direct attack by one silicate anion (*e.g.* H_3SiO_4^-) on a second silicate anion would be electrostatically improbable as compared with attack by a neutral species (*e.g.* H_4SiO_4). It therefore has been suggested, because of its relatively high mobility (*i.e.*, small size), that an activated monomer species, H_4SiO_4 , is the principal vehicle of intermolecular Si-Si exchange.^[29] When alkalinity is increased, there would be an equilibrium shift

away from the activated monomer (Equations 1.1 to 1.3) and a subsequent decrease in the Si-Si exchange rate.^[29]

All alkali-metal silicate ²⁹Si resonances shift to higher frequencies as alkalinity is increased (probably due to deprotonation of silicate oligomers)^[2,19,27] or temperature^[24] is increased. As well, all ²⁹Si resonances shift to lower frequencies as the alkali-metal cation is changed from Na⁺ to K⁺ to Rb⁺.^[24]

1.2.5. Tetraalkylammonium Silicates

The relative abundance of certain silicate anions, especially the cubic octamer and prismatic hexamer, can be significantly enhanced in solutions containing tetraalkylammonium cation.^[34-38] Tetramethylammonium cations exert the greatest influence; the concentration of cubic octamer systematically decreases when methyl groups are substituted with larger alkyl (or aryl) groups.^[35-38] In addition, the 2-hydroxyethyl group imparts a structure-directing influence only slightly lower than that of the methyl group^[35] (Figure 1-2).

One theory for the stabilization of the cubic octamer and prismatic hexamer is based on gaseous^[39-41] and solid^[42] phase structures of hydrated tetramethylammonium cations and on the crystal structure of hydrated tetramethylammonium silicate containing the cubic octamer.^[43] In the gas and solid phases of hydrated tetramethylammonium cations, a polyhedral framework of water molecules and hydroxide ions surround tetramethylammonium cations. In solution, labile water-structures that resemble such polyhedral frameworks are probably formed around tetramethylammonium cations.^[3,44-48] Framework water molecules and hydroxide ions would be expected to exchange with non-framework water molecules and hydroxide ions. Since orthosilicate anions are of similar size and chemistry to that of water,^[49] they too would be expected

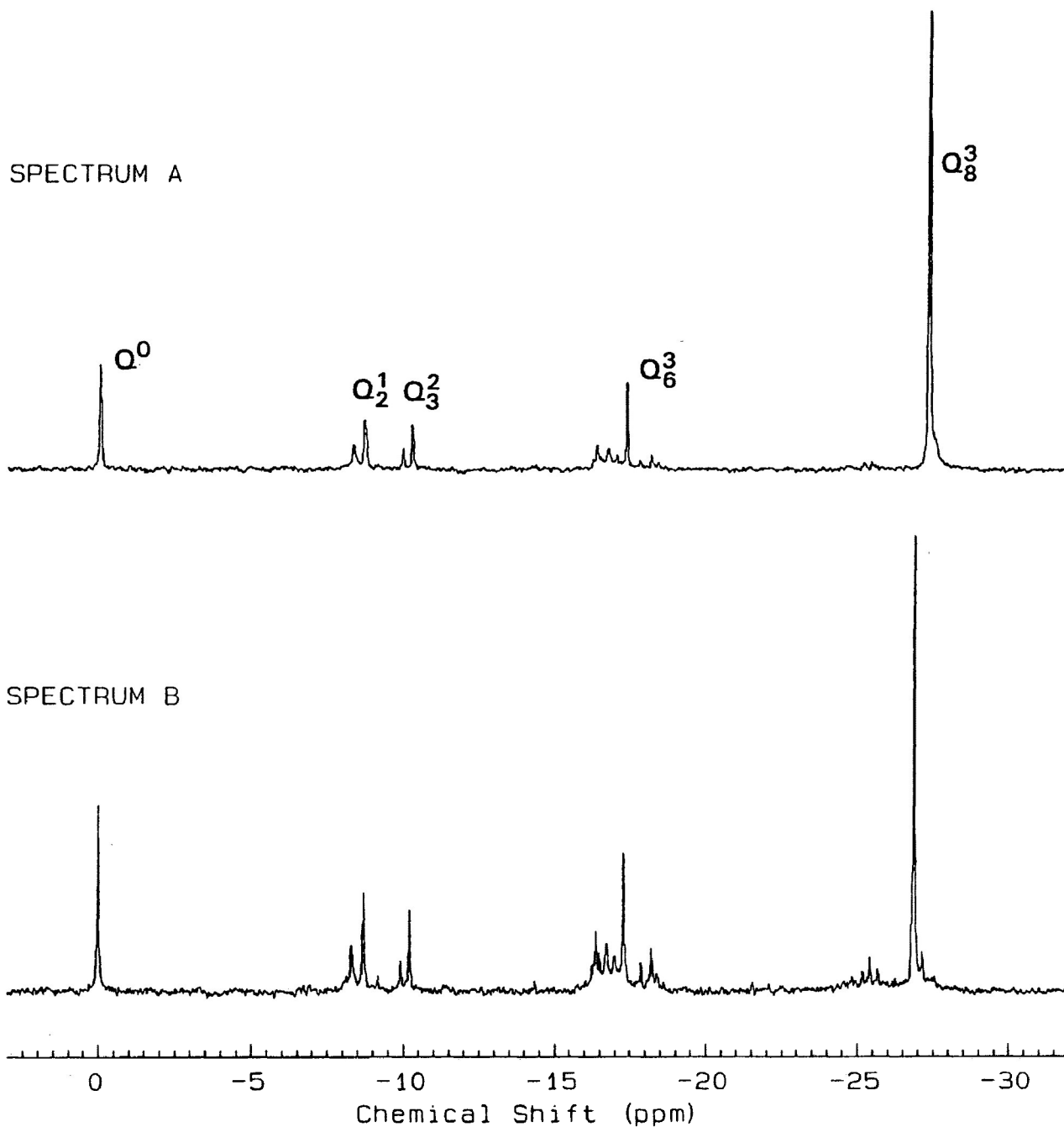


Figure 1 – 2. ^{29}Si NMR spectra of A) $0.9 \text{ mol kg}^{-1} \text{ SiO}_2$ and 0.9 mol kg^{-1} tetramethylammonium hydroxide and, B) $0.9 \text{ mol kg}^{-1} \text{ SiO}_2$ and 0.9 mol kg^{-1} 2-hydroxyethyltrimethylammonium hydroxide solution at 296.1 K. The dominant resonance corresponds to the cubic octamer.

to exchange with framework water molecules.^[3] Held in close proximity, the orthosilicate ions would readily condense into small oligomers which, owing to electrostatic attraction, would be associated with multiple TMA⁺ ions. Ultimately, cage-like structures (*i.e.*, cubic octamer and prismatic hexamer) would be formed with hydrated tetramethylammonium cations surrounding them.^[3,47] Groenen *et al.*^[50] suggest that, since attenuated total reflection infrared spectra of solution phase cubic octamer and crystalline phase hydrated tetramethylammonium/cubic octamer clusters are almost identical, the structure of the immediate environment around the solution species is probably very similar to that of the crystalline cluster.

Hendricks *et al.*,^[32] however, have suggested that formation of the cubic octamer results from the particular size of tetraalkylammonium cations. Cation-anion pairing is insignificant due to the small charge to radius ratio of tetraalkylammonium cations. When the size of tetraalkylammonium cations is increased, the extent of hydrophobic water structuring increases which promotes condensation. On the other hand, "ion crowding" produces an "electrostatic stress" that can only be compensated by a reduction in silicate anion size resulting in depolymerization.^[32] It is proposed that the combined effects favour formation of the cubic octamer with tetramethylammonium cations but not with larger tetraalkylammonium cations.

If the solution contains organic solutes, however, larger tetraalkylammonium cations (*e.g.* tetrapropylammonium and tetrabutylammonium cations) can favour cage-like silicate oligomers.^[51-53] Hendricks *et al.*^[51] suggest that displacement of silicate oligomers towards the cubic octamer is due to "mass action equilibration" and water structuring. Silicates oligomerize via a

condensation reaction (Equations 1.4 to 1.6). If the effective water concentration in these equilibria is decreased, owing to addition of an organic solute, the extent of polymerization would increase due to the mass action effect. They attempted to calculate the extent of this effect and concluded that it alone could not fully account for the observed increase in the extent of oligomerization. The excess degree of oligomerization was then attributed to increased water structuring by the organic molecule since this would further decrease the effective concentration of water.

When temperature is increased, the cubic octamer resonance shifts slightly up-frequency (relative to monomer).^[20,54] Addition of tetramethylammonium hydroxide causes a slight down-frequency shift of the cubic octamer resonance and prismatic hexamer resonance, but all other silicate resonances shift up-frequency.^[54] When sodium cations were added to tetramethylammonium silicate solutions, the cubic octamer concentration decreased and its resonance shifted to a higher frequency.^[36] Engelhardt and Rademacher^[55] had comparable observations. Therefore, it was suggested^[36,55] that successive exchange of tetramethylammonium cations with sodium cations destabilizes the cubic octamer and thus shifts its resonance up-frequency.

Another unusual phenomenon observed with tetramethylammonium silicate solutions is the slow Si-Si exchange rate between the cubic octamer and other silicate oligomers. Knight *et al.*^[56] were first to observe this. They employed a boil-freeze-thaw technique whereby the sample ($1.0 \text{ mol kg}^{-1} \text{ SiO}_2$, 2.0 mol kg^{-1} tetramethylammonium hydroxide and 20% v/v CD_4OD) was boiled to perturb the equilibria, frozen in liquid nitrogen, thawed and monitored by ^{29}Si NMR at 20 °C. Over the first two hours the cubic octamer resonance was not detected although

there were resonances corresponding to almost all other oligomers. Several weeks at ambient temperature were required for the chemical system to regain equilibrium. They reported that in similar studies with alkali-metal silicate solutions, which do not contain large concentrations of cubic octamer, an equilibrium distribution of oligomers was attained in less than a few minutes.

1.3. Zeolite Synthesis

1.3.1. Zeolites

Zeolites are tectoaluminosilicates which exhibit a remarkable variety of framework structures consisting of very regular channels and cavities in which ions and molecules, depending on size and charge, can be adsorbed.^[1] The adsorbed species have considerable freedom of movement in and out of the cavities and channels. The well-known ion-exchange and catalytic properties of zeolites depend on this mobility. Most importantly, the size and shape of reactants and products can be controlled by use of zeolitic catalysts having the appropriate framework structure.^[57]

There are some thirty-seven natural zeolite minerals and well over one hundred synthetic zeolites.^[1] Although the structure of zeolites^[57-64] and solution composition of zeolite synthesis mixtures^[3,44,65,66] are known, the mechanism of zeolite formation is not well understood. Since zeolites are usually synthesized from aluminosilicate gels which can contain any variety of alkali-metal cations, transition metals, quaternary ammonium cations and/or miscible organic solutes,^[58] it has been suggested that the nucleation and crystallization of a zeolite occurs directly in the gel phase.^[67] Subsequent growth would then proceed via depolymerization and rearrangement of the gel network, mediated by hydroxide ions. However, zeolites also crystallize directly from true

homogeneous solutions.^[3,65] Barrer^[61] has noted that even if nucleation were to occur in a gel phase, the higher density zeolite would retreat from contact with the gel. The cavity which is created would then fill with solution, and for further growth to occur, the aluminosilicate species in the gel would need to dissolve to reach the growing crystal surfaces. Nucleation could occur in solution, on the gel surface or within gel particles,^[61,68,69] but crystal growth has to occur by condensation polymerization of dissolved species on the surface of the crystal. Therefore, the solution chemistry of dissolved silicate and aluminate species is important to the study of zeolite crystallization.

1.3.2. Theories of Zeolite Crystallization

Two theories have been proposed to explain zeolite crystallization from solution, the secondary building unit (SBU) theory^[70] and the cation templating theory.^[65] In the SBU theory, a zeolite framework is constructed through condensation polymerization of large cage or ring aluminosilicate species which exist in solution. Aluminosilicate species could provide both the nucleation point and, by their sequential addition, the mode of growth.

In the cation templating theory, the zeolite framework is influenced by the size and shape of a hydrated cation. An ordered water structure forms around small cations; zeolite synthesis would be initiated by the exchange of water molecules for aluminate or silicate anions. The anions would be held in position for sufficient time to form siloxy or alumino-siloxy linkages which would ultimately result in nucleation and growth of a zeolite. Knight^[65] along with other researchers^[44,55,61,63] have given persuasive arguments against the SBU theory and suggest that the cation templating theory effectively explains zeolite synthesis. However, it is quite evident from a recent report that the mechanism

of zeolite crystallization is still very much open for debate.^[71]

Nonetheless, it is certain that the interaction between cations and silicate anions determines the structure of zeolites as well as the structure of silicate oligomers in solution. By studying dissolved aqueous aluminosilicates and silicates, the structure-directing role of cations can be better understood and thus used to help elucidate a mechanism for zeolite synthesis.

1.4. Objectives

The objectives of the present study were to investigate, using ^{29}Si NMR, the equilibria and kinetics of aqueous tetraalkylammonium silicate solutions. In particular, we hoped to elucidate factors responsible for the unusual behaviour of these solutions relative to alkali-metal silicate solutions.

Chapter II. Experimental Procedure

2.1. Reagents

Aqueous hydroxide solutions were prepared from: tetramethylammonium (TMA⁺) hydroxide (Aldrich, pentahydrate, 99% or Johnson Matthey, 25 wt% aqueous solution); tetraethylammonium (TEA⁺) hydroxide (Aldrich, 40 wt% aqueous solution); tetra(*n*-propyl)ammonium (TPA⁺) hydroxide (Johnson Matthey, 40 wt% aqueous solution); tetra(*n*-butyl)ammonium (TBA⁺) hydroxide (Aldrich, 40 wt% aqueous solution); (2-hydroxyethyl)- trimethylammonium (ETMA⁺) hydroxide (Aldrich, 20 wt% aqueous solution); sodium hydroxide (Aldrich, 99.99%); or cesium hydroxide (Aldrich, monohydrate or 50 wt% aqueous solution). Chloride sources were tetramethylammonium chloride (Aldrich, 97%), and sodium chloride (Johnson Matthey, 99.99%).

Amorphous silicon dioxide was prepared by hydrolysis of freshly distilled silicon tetrachloride (Aldrich, 99.999%). The resulting silica gel was dried at 150 °C, crushed and repeatedly washed until a neutral pH of the washing was obtained. Germanium dioxide was similarly prepared from germanium tetrachloride (Johnson Matthey, 99.9999%) or was purchased as electronic grade material (99.9999%, Johnson Matthey).

Silica that was 95% isotopically enriched in ²⁹Si was recovered from samples employed in previous studies^[72] using the method of DeFretas *et al.*^[73] The muffle furnace used in the recovery process was pre-heated at 1100 °C to remove volatile material which might contaminate the recovered silica. During the recovery process the furnace was kept below 850 °C; tests revealed that amorphous silica is transformed to comparatively insoluble cristobalite above *ca.* 850 °C. No more than 55 mg of silica was recovered

at any one time. A total of 160 mg of enriched silica was recovered. The original isotopically enriched silica contained Na, Mg, and Ti in trace amounts (<0.01%), while another 52 elements were undetectable.^[72] ICP analysis of the recovered silicon dioxide revealed only traces (<0.01%) of Fe, Mn, and Na. SEM/EDS analysis also revealed particles of solid Pt (from the crucible). The bulk of Pt was later removed by filtration of solutions prepared from the recovered silica.

2.2. Sample Preparation

For aqueous silicate solutions, alkalinity is conveniently characterized by the $OH^-:Si^{IV}$ molal concentration ratio. The calculation of molal concentration includes the mass of H₂O, D₂O and/or organic solutes. Molal concentrations are represented by square brackets *e.g.* [SiO₂]. Solutions were prepared using distilled/deionized (≥17.8 Mohm) water and only contacted surfaces of low density polyethylene. Solutions were stored under nitrogen in low-density polyethylene screw-top bottles or in Teflon FEP[®] NMR tube liners sealed with Teflon TFE[®] caps. All lab-ware was carefully cleaned by soaking in successive dilute solutions of nitric acid, hydrochloric acid and Na₂H₂EDTA solution to minimize contamination from paramagnetic metal ions which can affect NMR measurements. Silicate and germanosilicate solutions were prepared by dissolving a known quantity of amorphous silicon dioxide or germanium dioxide, which had been dried at 180 °C for 12 hours, in standardized aqueous hydroxide solutions. If required, the solvent was 20 wt% enriched with deuterium oxide to provide an internal NMR field/frequency lock. Samples were then warmed at 50 °C until dissolved. Non-enriched silicon dioxide dissolved readily and completely in all solutions containing

tetraalkylammonium hydroxide except those with $\text{OH}^-:\text{Si}^{\text{IV}} < 0.6:1$; the silicon dioxide did not completely dissolve in solutions containing alkali-metal hydroxides with $\text{OH}^-:\text{Si}^{\text{IV}} < 1:1$.^[24,29] The isotopically enriched silicon dioxide required a comparatively long time to dissolve and would only completely dissolve in solutions containing tetraalkylammonium hydroxides with $\text{OH}^-:\text{Si}^{\text{IV}} \geq 1:1$. Germanium dioxide completely dissolved in solutions containing tetraalkylammonium hydroxide with $\text{OH}^-:(\text{Si}^{\text{IV}}+\text{Ge}^{\text{IV}}) \geq 0.6:1$; the germanium dioxide was only sparingly soluble in alkali-metal hydroxide solutions.^[29] Low $\text{OH}^-:\text{Si}^{\text{IV}}$ ratios ($< 1:1$) were attained by adding standardized HCl (Caledon Lab) drop-wise with vigorous mixing to silicate solutions originally prepared with $\text{OH}^-:\text{Si}^{\text{IV}} \geq 1:1$. Solutions containing slight precipitate were filtered through 25 μm polyethylene membranes. Methanol (BDH, 99.8%) or dimethyl sulfoxide (Aldrich, 99.97%) was added as a solute to selected samples. Solute and D_2O concentrations are expressed as a weight percent (wt%) of the total mass of solution.

2.3. NMR Measurements

Silicon-29 NMR spectra of *ca.* 350 different solutions were obtained on Bruker AC-E 200 and AMX 500 Fourier transform NMR spectrometers operating at 39.73 and 99.36 MHz, respectively. As well, germanium-73 NMR spectra of selected samples were obtained on the AMX 500 operating at 17.44 MHz. Glass sample tubes and coil supports in the probes were replaced with equivalent Vespel SP-1^{®[74]} components in order to eliminate ^{29}Si background signals. Vespel is a high mechanical strength, silicon- and aluminum-free polyimide resin which is able to withstand high temperatures and pressures. Pressurizable NMR tube assemblies,^[72] 15 mm and 10 mm O.D., were

constructed of Vespel and teflon FEP/TFE for use with the AC-E 200 and AMX 500 NMR spectrometers, respectively (a slight modification from the assembly described in reference 72 was to replace the valve-head with one constructed from Kel-F^[75] which is chemically inert toward alkaline solutions). For spectra acquired at temperatures > 30 °C, the solutions were pre-pressurized with N₂ to 0.4 MPa to prevent degassing.

An additional 15 mm O.D. NMR tube assembly was designed and constructed for use at pressures to ca. 50 MPa (Figure 2-1). It was leak-free during repeated pressurizing cycles of up to 60 MPa and 300 K but eventually failed at 50 MPa and 300 K. Hexane was chosen as the pressurizing fluid because it is inert to Vespel, immiscible with the aqueous samples and would readily evaporate if the assembly failed in the spectrometer. The pressure was transmitted to the sample via 1/16" O.D. flexible tubing of polyetheretherketone (PEEK)^[76] (0.01" I.D.) or stainless steel (0.03" I.D.) which was connected to the top of the assembly by a PEEK coupling.

As noted in previous studies,^[56] the distribution of tetramethylammonium silicate oligomers may require up to two weeks to attain equilibrium. For this reason, samples used to study the equilibrium distribution of oligomers were prepared and then subsequent NMR spectra acquired two to three weeks later. The "boil-freeze-thaw" procedure, described by Knight *et al.*,^[56] was used to monitor the non-equilibrium distribution of silicate oligomers. Samples (in FEP NMR tube liners) were heated in boiling water for ca. 3 minutes, immersed in liquid nitrogen, thawed in a water bath, and immediately placed in the spectrometer to obtain successive ²⁹Si NMR spectra (*e.g.*, Figure 2-2). The samples always appeared mono-phasic on thawing.

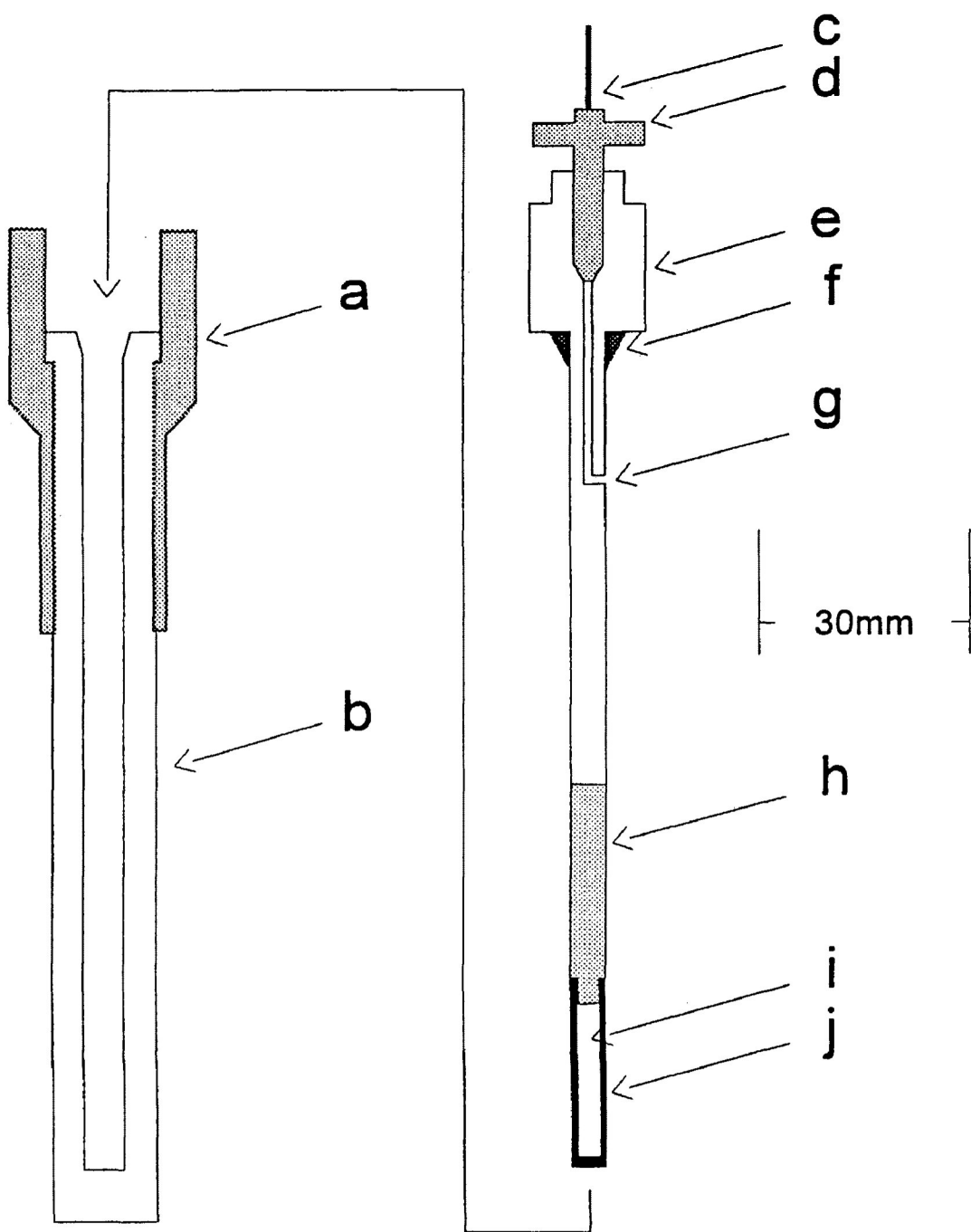


Figure 2 – 1. 15 mm Pressurizable NMR Tube Assembly. (a) Vespel spinner. (b) Vespel pressure jacket. (c) Stainless steel or PEEK tube. (d) PEEK fitting and ferrule. (e) Vespel pressure head threaded onto a. (f) Vespel ferrule. (g) Drilled hole for pressurizing fluid. (h) Kel-F^[75] shaft threaded onto e. (i) Sample compartment. (j) Teflon FEP liner friction fit onto h. System is pressurized by a hand pump (max. 200 MPa) using n-hexane. Pressure monitored using an Omega analog gauge (PGJ-60B-10 000).

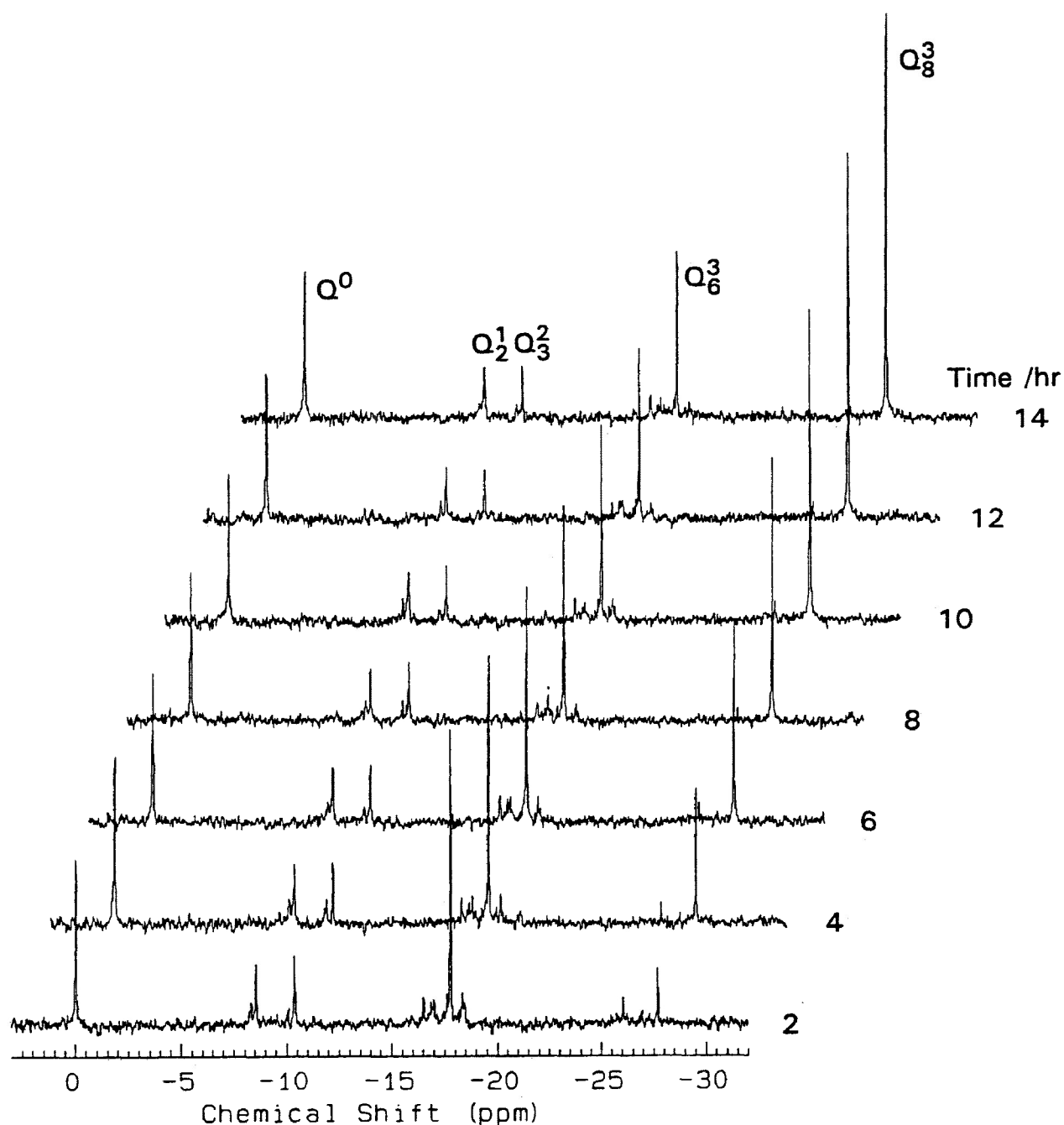


Figure 2 – 2. ^{29}Si NMR spectra of a 1.0 mol kg^{-1} SiO_2 , 1.4 mol kg^{-1} TMAOH and 0.6 mol kg^{-1} TMACl solution at 296.1 K following perturbation by the "boil-freeze-thaw" method. The times listed correspond to the interval between sample thawing and the end of spectral acquisition.

Temperature calibrations on both spectrometers were performed periodically using the ^1H spectrum of neat ethylene glycol.^[77] All spectra were acquired with an artificial line broadening of 1.0 Hz and at 296.1 K unless otherwise stated. Since optimum control over temperature is required during kinetic studies, the air pressure and spin rate were kept constant throughout the experiments. It is believed that the solution temperature varied by no more than 0.5 K over each acquisition.

The ^{29}Si 90° pulse width was determined periodically with hexamethyldisiloxane and a $3.0 \text{ mol kg}^{-1} \text{ SiO}_2$ and $5.0 \text{ mol kg}^{-1} \text{ NaOH}$ solution. For the AC-E 200 and AMX 500 it was calculated to be 34 μs and 20 μs , respectively. All spectra were acquired with a resolution of 0.3 Hz. Spectra acquired for samples at equilibrium had typically 700 to 800 scans and spectra acquired using the "boil-freeze-thaw" method had 160 scans. The ^{73}Ge 90° pulse width was determined to be 62 μs and spectra typically were acquired with 30000 scans and 4.0 Hz resolution.

Since quantitative spectral integrations (relative error is estimated at $\pm 5\%$) were required for the determination of silicate oligomer concentrations, the ^{29}Si 90° pulses were cycled over periods greater than 3 to 5 times the maximum T_1 value. The longest T_1 value was measured to be near 15 seconds. All ^{29}Si assignments are from previous studies unless stated otherwise.

2.4. pH Measurements

pH measurement of representative silicate solutions were conducted at $298.0 \pm 0.5 \text{ K}$ using an Orion glass membrane electrode and Ag/AgCl double junction reference half cell containing 1.0 mol kg^{-1} tetramethylammonium

hydroxide in the outer compartment (to minimized liquid-liquid junction potential). The meter was calibrated with three buffers, pH of 10.01, 12.00, and 12.45 (saturated $\text{Ca}(\text{OH})_2$). Samples were pre-equilibrated in a thermostatic bath for ca. 7-10 minutes such that the pH did not fluctuate more than ± 0.007 of a pH unit. Solvents were not isotopically enriched in ^2H .

2.5. Attenuated Total Reflection Infrared Measurements

ATR infrared spectra (1 cm^{-1} resolution) were obtained for tetramethylammonium silicate solutions using a Bruker IFS-66 Fourier transform infrared spectrometer. A ZnSe crystal was used as the support in the ATR apparatus because it is chemically resistant to strong alkaline solutions. Samples were prepared with 100% ^2H isotopically enriched water so as to avoid overlap of O-H bending with Si-O stretching signals.

Chapter III. Experimental Findings.

3.1. Silicate Equilibria

3.1.1. Analysis of Previous Studies

The distribution of aqueous tetramethylammonium (TMA) silicate oligomers has been studied extensively since the mid 1960's.^[7-11] Not until 1986, however, was it reported that a TMA silicate solution can require two weeks to equilibrate.^[56] Thus previous observations can be considered, at best, only qualitative. Nevertheless, investigators were able to determine that the Q_8^3 concentration^[34,36] increases and the Q_8^3 and Q_6^3 resonances^[20,54] shift down frequency as the TMAOH concentration is increased or temperature is decreased. The effects of alkalinity (*i.e.*, $OH^-:Si^{IV}$ ratio) and TMA^+ ion concentration, however, were not examined independently.

Alkali-metal silicates contain a wide distribution of silicate oligomers but only a small or negligible concentration of Q_8^3 .^[19-22] In solutions containing both alkali-metal and TMA cations,^[36,55] the Q_8^3 concentration increases and the Q_8^3 resonance shifts down-frequency as the mole fraction of TMA^+ ions is increased. Therefore, different groups of investigators^[36,55] have concluded that the chemical shift of the Q_8^3 resonance is related to the stability of Q_8^3 .

Organic solutes added to TAA silicate solutions further promote the formation of Q_8^3 .^[53] Several groups have indicated that certain TAA silicate solutions which contain organic solutes yield at least two small resonances, attributed to double five and double six ring silicate structures,^[4,78,79] down-frequency of the Q_8^3 resonance. Boxhoorn *et al.*^[80] have suggested that, in a TPA/Na alumino-silicate solution containing 50% v/v DMSO, the double five ring is the dominant oligomer. Double five and double six ring oligomers

appear structurally similar to the "secondary building units" described for zeolites. The possible existence of these species in solution has therefore been used to promote the feasibility of the SBU theory of zeolite formation. Kinrade and Whatley^[53] have noted that these two resonances appear only at $\text{OH}^-:\text{Si}^{\text{IV}} \leq 1:1$ and that, as the $\text{OH}^-:\text{Si}^{\text{IV}}$ ratio is decreased, possibly two more resonances appear further down-frequency. It does not appear that the correlation with low alkalinity had been explicitly drawn previously.

3.1.2. TMA Silicate Equilibria

The effects of $\text{OH}^-:\text{Si}^{\text{IV}}$ ratio and TMA^+ ion concentration on the equilibrium distribution and chemical shift of silicate oligomers in TMA silicate solutions were investigated. If the TMA^+ ion concentration was constant, increasing the $\text{OH}^-:\text{Si}^{\text{IV}}$ ratio had no significant effect on Q_8^3 concentration (Figure 3-1a) while other oligomers underwent slight depolymerization. The Q_8^3 and Q_6^3 resonances shifted down-frequency, whereas all other resonances shifted up-frequency with increasing $\text{OH}^-:\text{Si}^{\text{IV}}$ ratio (Table III-I). If the $\text{OH}^-:\text{Si}^{\text{IV}}$ ratio was constant, increasing the TMA^+ ion concentration increased the concentration of Q_8^3 (Figure 3-1b) at the expense of all other oligomers. Most resonances shifted slightly down-frequency as the TMA^+ ion concentration was increased (Table III-II). When both the $\text{OH}^-:\text{Si}^{\text{IV}}$ ratio and TMA^+ ion concentration were increased simultaneously, the concentration of Q_8^3 increased as well. It appears from Figures 3-1a and b that at $\text{OH}^-:\text{Si}^{\text{IV}} \geq 1:1$ and $\leq 2:1$ the TMA^+ ion concentration governs the overall stability of Q_8^3 whereas the $\text{OH}^-:\text{Si}^{\text{IV}}$ ratio has only a small effect if any. This contradicts the hypothesis that chemical shift correlates with stability of Q_8^3 (see Section 3.1.1).

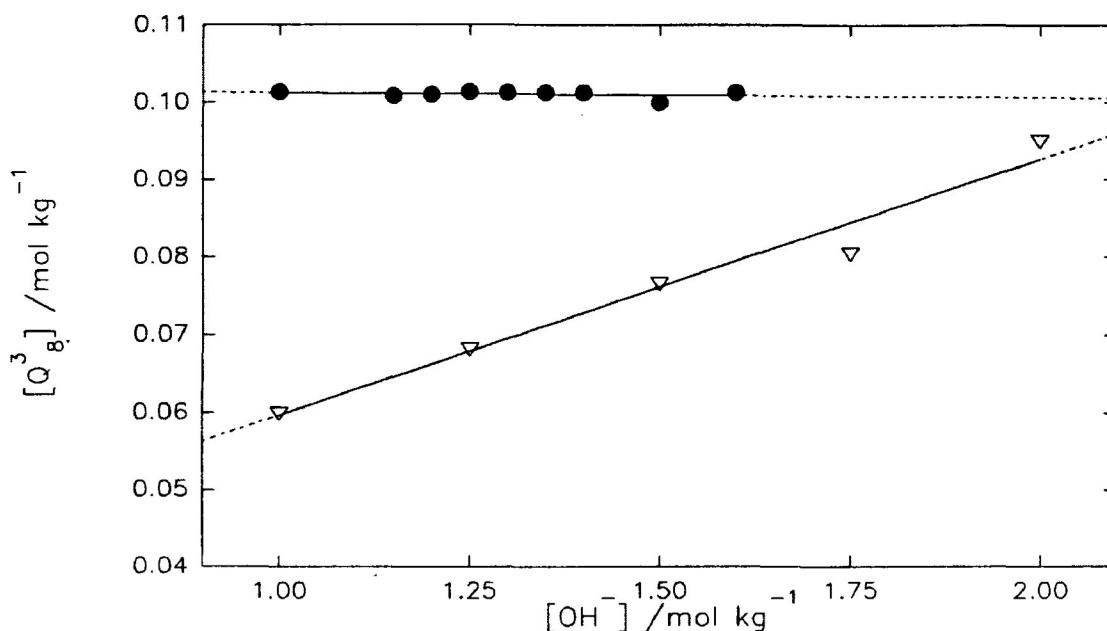


Figure 3 – 1a. Equilibrium concentration of Q_8^3 at 296.1 K as a function of alkalinity. All samples contain $1.0 \text{ mol kg}^{-1} \text{ SiO}_2$. For samples represented by ●, $[TMA^+]$ is fixed at 2.0 mol kg^{-1} by addition of TMACl. For samples represented by ▽, $[TMA^+] = [OH^-]$.

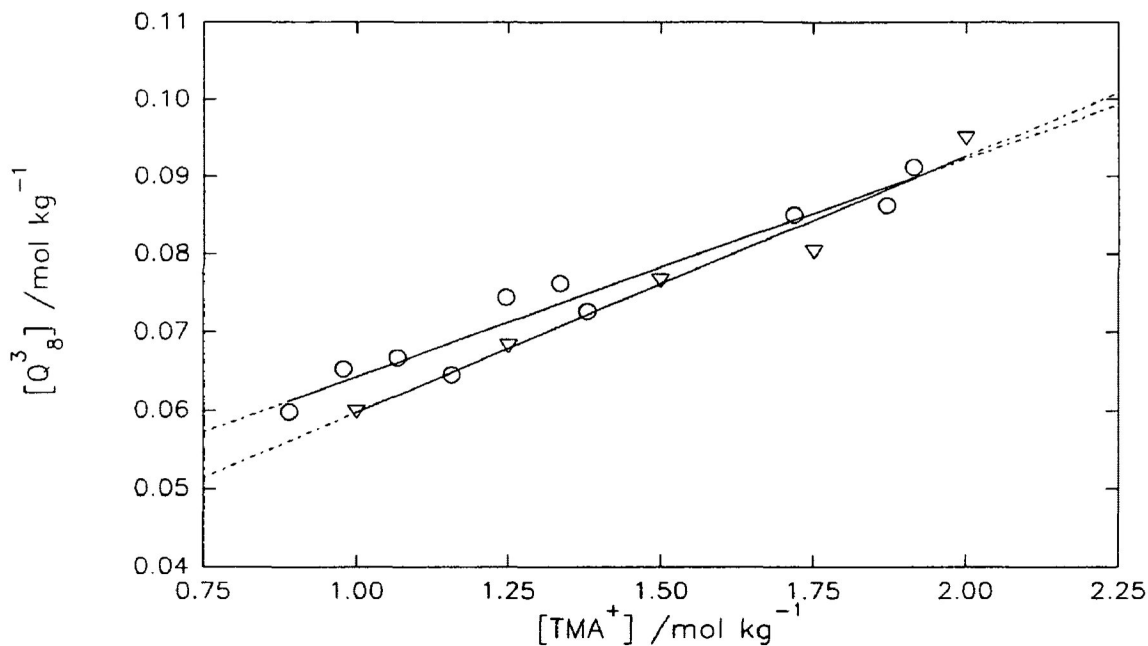


Figure 3 – 1b. Equilibrium concentration of Q_8^3 at 296.1 K as a function of $[TMA^+]$. Samples represented by ▽, contain $1.0 \text{ mol kg}^{-1} \text{ SiO}_2$ and $[OH^-] = [TMA^+]$; samples represented by ○, contain $0.9 \text{ mol kg}^{-1} \text{ SiO}_2$, $0.9 \text{ mol kg}^{-1} \text{ TMAOH}$ and the $[TMA^+]$ was increased by addition of TMACl.

Table III-I. Chemical shift (in ppm) of selected silicate oligomers at various $\text{OH}^-:\text{Si}^{\text{IV}}$ ratios. Solutions contain $1.0 \text{ mol kg}^{-1} \text{ SiO}_2$ and $2.0 \text{ mol kg}^{-1} \text{ TMA}^+$ ions. Chemical shifts are externally referenced to the monomer in a $1.0 \text{ mol kg}^{-1} \text{ SiO}_2$ and $1.0 \text{ mol kg}^{-1} \text{ TMAOH}$ solution.

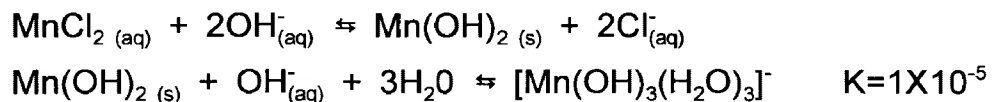
$\text{OH}^-:\text{Si}^{\text{IV}}$	Oligomer				
	Q_8^3	Q_6^3	Q^3 of substituted cyclic trimer	Q_2^1	Q^0
1.00:1	-27.32	-17.34	-18.32	-8.68	0.02
1.25:1	-27.32	-17.34	-18.31	-8.56	0.10
1.50:1	-27.34	-17.38	-18.29	-8.42	0.22
1.75:1	-27.38	-17.43	-18.29	-8.31	0.27
2.00:1	-27.43	-17.47	-18.28	-8.24	0.28

Table III-II. Chemical shift (in ppm) of selected silicate oligomers at various TMA^+ ion concentrations. Solutions contain $0.9 \text{ mol kg}^{-1} \text{ SiO}_2$ and $0.9 \text{ mol kg}^{-1} \text{ TMAOH}$. The TMA^+ ion concentration was increased by adding TMACl . The *total* TMA^+ ion concentrations are indicated in the Table.

$[\text{TMA}^+]$ $/\text{mol kg}^{-1}$	Oligomer				
	Q_8^3	Q_6^3	Q^3 of substituted cyclic trimer	Q_2^1	Q^0
0.90	-27.32	-17.36	-18.30	-8.66	0.03
1.00	-27.32	-17.33	-18.30	-8.68	0.00
1.15	-27.34	-17.35	-18.29	-8.66	0.00
1.35	-27.35	-17.35	-18.29	-8.65	0.00
1.75	-27.37	-17.39	-18.30	-8.64	-0.01
1.90	-27.38	-17.40	-18.28	-8.64	-0.02

It is possible that in solution hydrated TMA^+ ions surround $\text{Q}_8^{3[47,64]}$ (see Section 1.2.5). These TMA^+ ions might well impede silicate exchange.

To test this hypothesis, paramagnetic Mn(II) ions were added to a TMA silicate solution. In alkaline solution MnCl₂ reacts to form the [Mn(OH)₃(H₂O)₃]⁻ ion which contains five unpaired electrons:^[1]



If paramagnetic ions are in proximity to a silicon nucleus the unpaired electrons will increase the transverse relaxation rate (1/T₂) and therefore broaden the corresponding ²⁹Si NMR resonance.^[81] A TMA silicate solution was saturated with manganese chloride. All resonances broadened to some extent (Figure 3-2; Table III-III), however, those corresponding to Q₆³ and Q₈³, which are theorized to be surrounded by hydrated TMA⁺ ions, were significantly less affected even compared with resonances of other Q³ centres (which can not be resolved above noise because of paramagnetic broadening).

Table III-III. Line width measurements at 1/2 peak height in Hz (± 5%) for samples with and without MnCl₂. Both samples contain 0.9 mol kg⁻¹ SiO₂, 0.9 mol kg⁻¹ TMAOH and 0.9 mol kg⁻¹ TMACl.

Sample	Oligomer				
	Q ⁰	Q ₂ ¹	Q ₃ ²	Q ₆ ³	Q ₈ ³
with MnCl ₂	5.1	2.4	1.5	0.7	0.7
no MnCl ₂	0.7	0.7	0.5	0.4	0.4

The ATR infrared spectra of crystalline TMA silicates, which contain Q₈³ oligomers and solution phase Q₈³ (solution containing 1.0 mol kg⁻¹ SiO₂ and TMAOH), were almost identical. Two adsorption bands at 998 and 1107 cm⁻¹

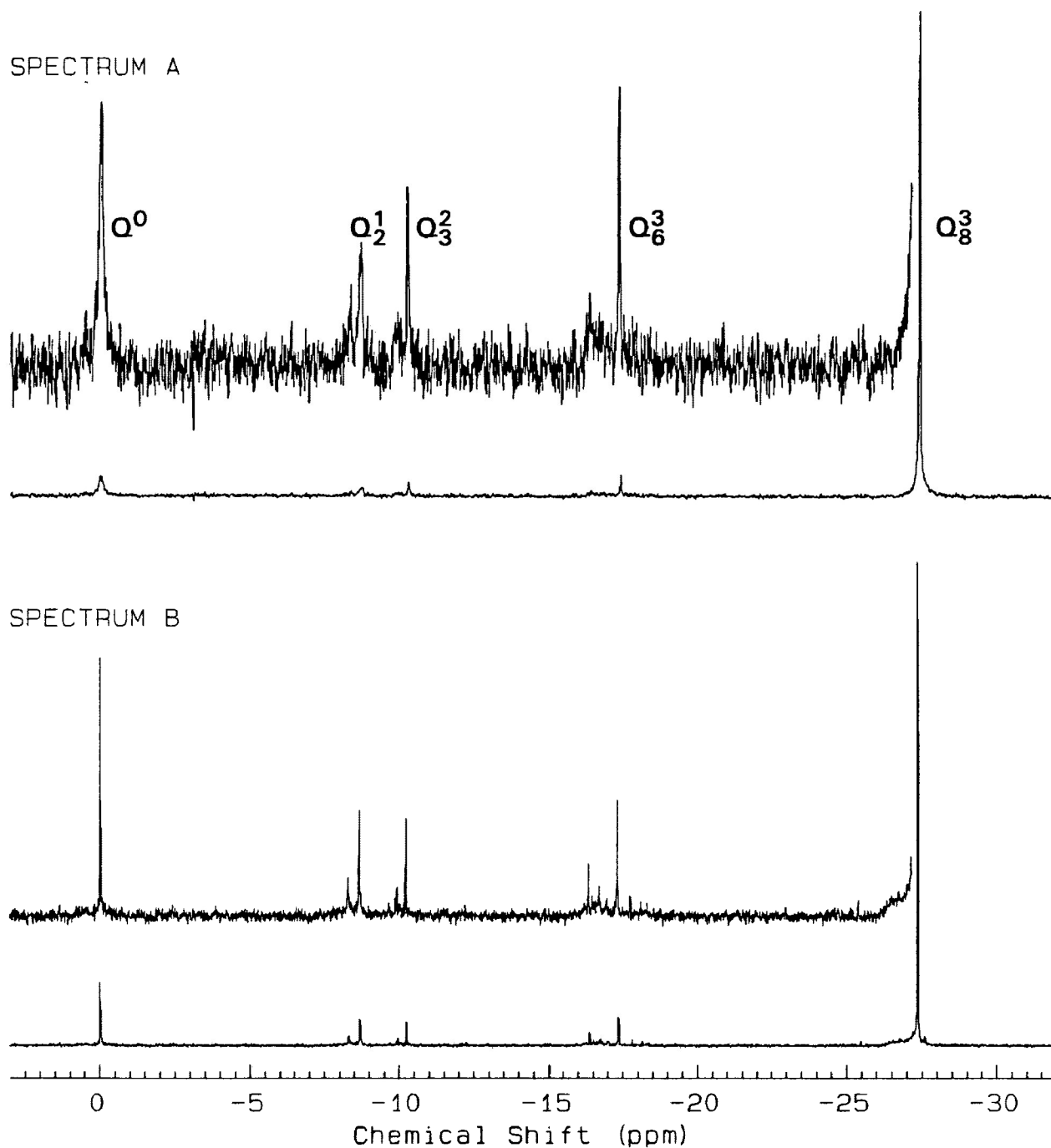


Figure 3 – 2. ^{29}Si NMR spectra of solutions containing $0.9 \text{ mol kg}^{-1} \text{ SiO}_2$, $0.9 \text{ mol kg}^{-1} \text{ TMAOH}$ and $0.9 \text{ mol kg}^{-1} \text{ TMACl}$ at 296.1 K. Spectrum A is saturated with MnCl_2 . Note broadening of resonances in A. (0.1 Hz artificial line broadening). Some resonances in spectrum B can not be resolved above noise because of paramagnetic broadening.

which have been attributed to Si-O⁻ and asymmetric Si-O-Si stretching vibrations,^[82] respectively. Similar observations were reported by Groenen *et al.*^[50]

In the ²⁹Si NMR spectrum of a solution containing 1.0 mol kg⁻¹ SiO₂, 1.0 mol kg⁻¹ TMAOH and 90 wt% methanol, the Q₈³ resonance was the only observable resonance. When the solution was heated to *ca.* 90 °C (to disrupt Q₈³, see Section 2.3) it gelled. In the ²⁹Si NMR spectrum (recorded at 298 K) of the gel, there was a broad band corresponding to colloidal silica and small resonances corresponding to low molecular weight oligomers. The gel slowly reverted back to a monophasic solution. After a week, the Q₈³ resonance was again the only observable resonance at 298 K. When NaOH was used instead of TMAOH, a gel formed. Even after heating, the mixture remained a gel. In the NMR spectrum of the sodium silicate gels, there were low intensity resonances corresponding to low molecular weight oligomers and colloidal silica only.

3.1.3. Mixed Cation Silicate Equilibria

The effects of added X⁺ ions (where X⁺ = Na⁺, Cs⁺, TBA⁺, TEA⁺, or ETMA⁺) on TMA silicate equilibria were investigated. In all cases the nominal silica concentration was 0.9 mol kg⁻¹ and the OH⁻:Si^{IV}:cation concentration ratio = 1:1:1. Solutions are characterized by X_{X⁺} (*i.e.*, mole fraction of X⁺ ions = [X⁺]/([TMA⁺]+[X⁺])). The influence of X_{X⁺} on the distribution of silicate oligomers is typified by spectra in Figures 3-3a and b.

In agreement with similar studies,^[36,37,83] the Q₈³ concentration is dependant on the mole fraction and type of X⁺ ion. When X_{X⁺} = 1.0, except where X⁺ = ETMA⁺, Q₈³ could not be detected. As depicted in Figures 3-4a

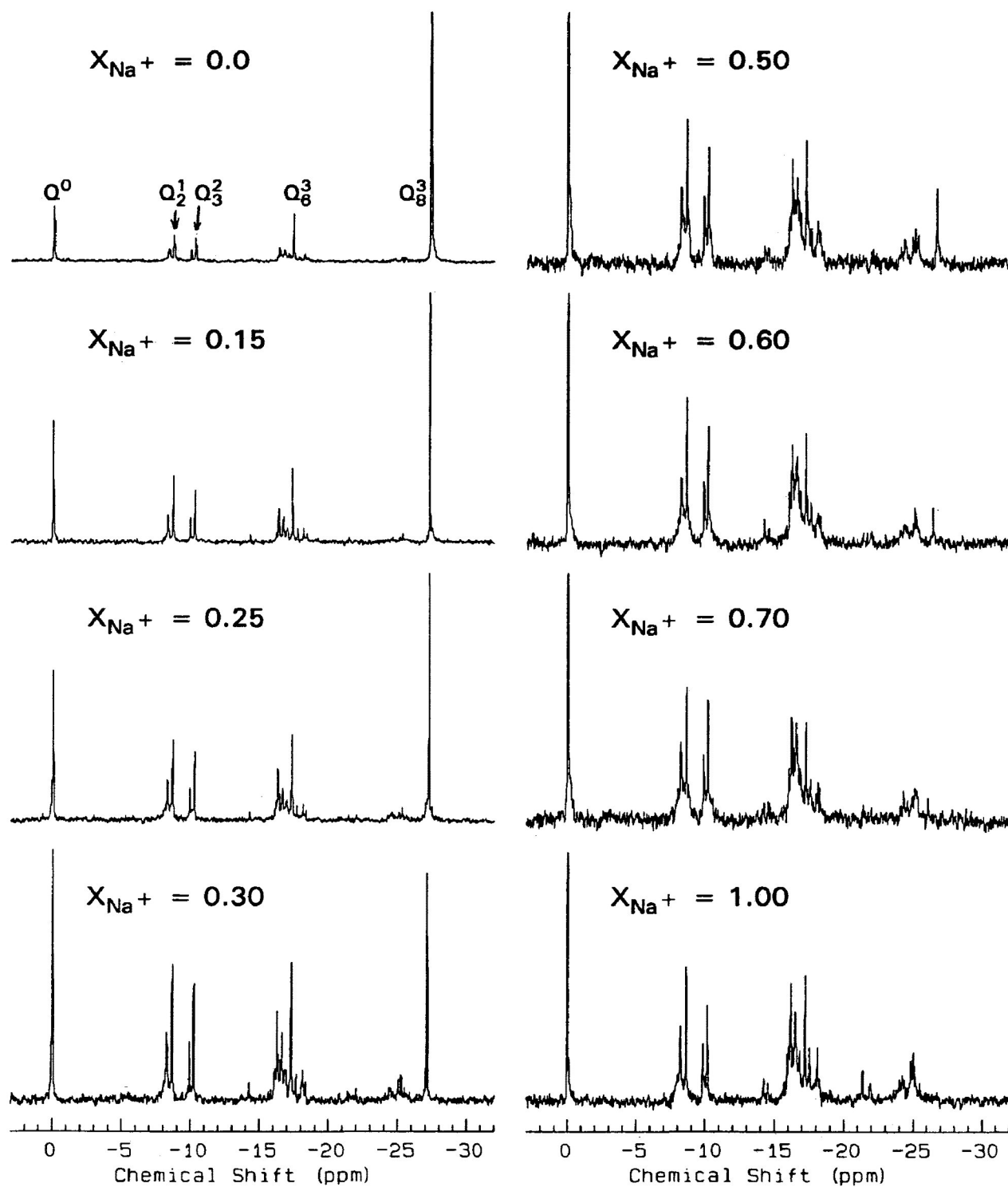


Figure 3 – 3a. ^{29}Si NMR spectra at 296.1 K of solutions containing $0.9 \text{ mol kg}^{-1} \text{ SiO}_2$, $0.9 \text{ mol kg}^{-1} \text{ OH}^-$ and $[\text{TMA}^+ + \text{Na}^+] = 0.9 \text{ mol kg}^{-1}$. Spectra are characterized by mole fraction of Na^+ ions (X_{Na^+}) and are normalized to highest peak.

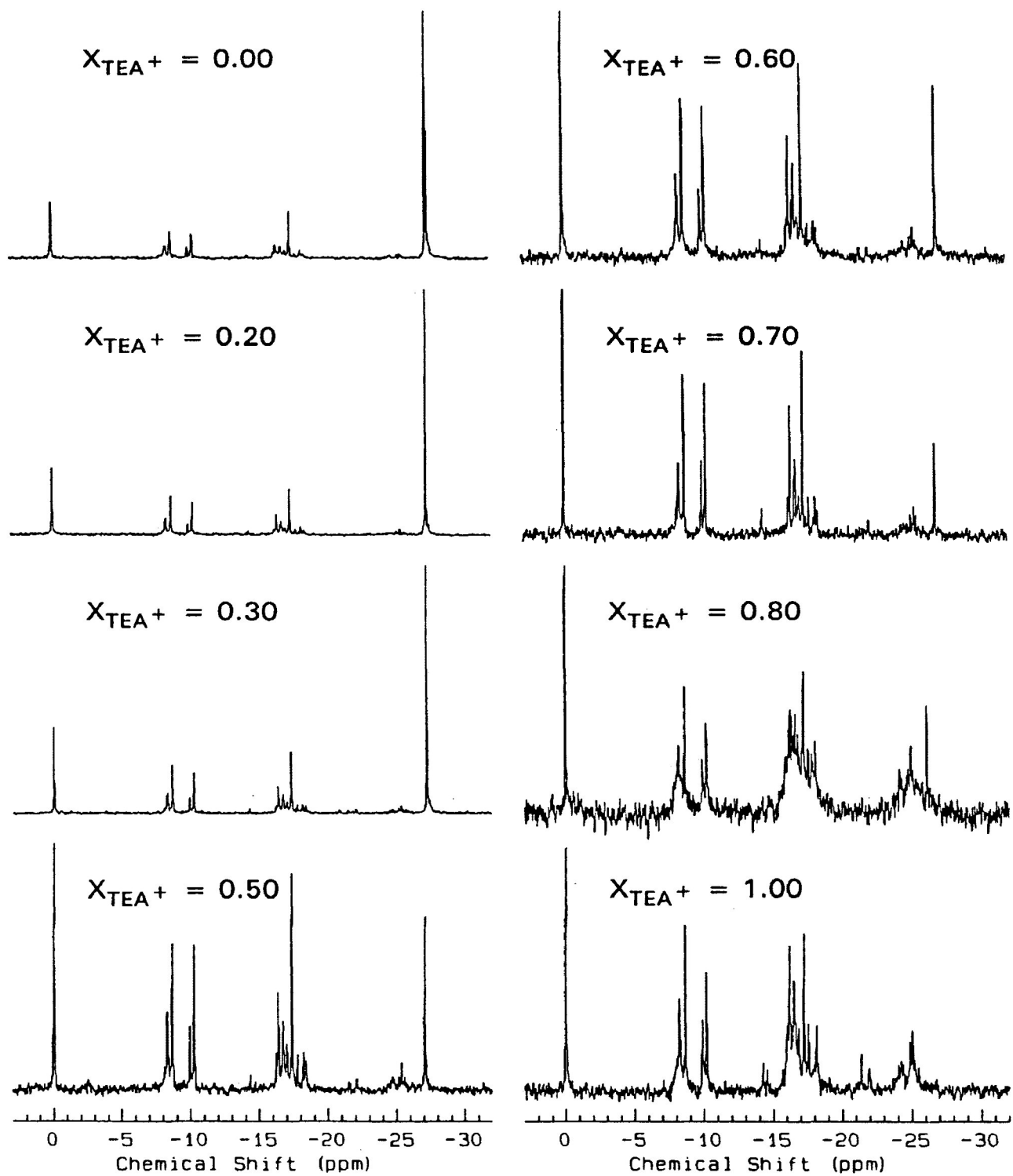


Figure 3-3b. ^{29}Si NMR spectra at 296.1 K of solutions containing $0.9 \text{ mol kg}^{-1} \text{ SiO}_2$, $0.9 \text{ mol kg}^{-1} \text{ OH}^-$ and $[\text{TMA}^+ + \text{TEA}^+] = 0.9 \text{ mol kg}^{-1}$. Spectra are characterized by mole fraction of TEA^+ ions (X_{TEA^+}) and are normalized to highest peak.

and b, the Q_8^3 concentration decreased as X_{X^+} was increased. At Q_8^3 concentrations $\geq 0.01 \text{ mol kg}^{-1}$ (i.e., at $\geq 10\%$ of the dissolved silica), correlation of the data is approximately linear. A best fit line has been drawn through these points and extrapolated to zero Q_8^3 concentration. This intercept yields the *limiting mole fraction of TMA⁺ ion* (i.e., the minimum mole fraction of TMA⁺ ions required to stabilize Q_8^3). In the series where $X^+ = \text{ETMA}^+$, there is no "limiting mole fraction" since ETMA⁺ ions themselves favour Q_8^3 (Figure 3-4b, Figure 1-2). The limiting mole fraction for each series is shown in Table III-IV.

Table III-IV. Limiting mole fraction of TMA⁺ ions in solutions with $[\text{SiO}_2]$ and $[\text{TMAOH} + \text{XOH}] = 0.9 \text{ mol kg}^{-1}$

X ⁺ Ion	Na ⁺	Na ⁺ ^a	Cs ⁺	TEA ⁺	TBA ⁺	ETMA ⁺
Limiting mole fraction	0.56	0.28	0.53	0.35	0.27	—

^a 20 wt% methanol was added to solution

To study further the effects of certain X⁺ ions on TMA silicate equilibria, TMA⁺ ions were added to sodium, cesium and TMA silicate solutions (Figure 3-5). The point at which Q_8^3 concentration increases linearly with increasing concentration of TMA⁺ ions is dependant on the type of X⁺ ion. It can be seen in Figure 3-5 that once this concentration has been reached the slopes of all three lines are very similar regardless of the type of X⁺ ion. The limiting mole fraction of TMA⁺ ion as defined above was calculated to be 0.44 for X⁺ = Na⁺ and 0.33 for X⁺ = Cs⁺.

Sodium chloride was added to TMA silicate solutions in order to

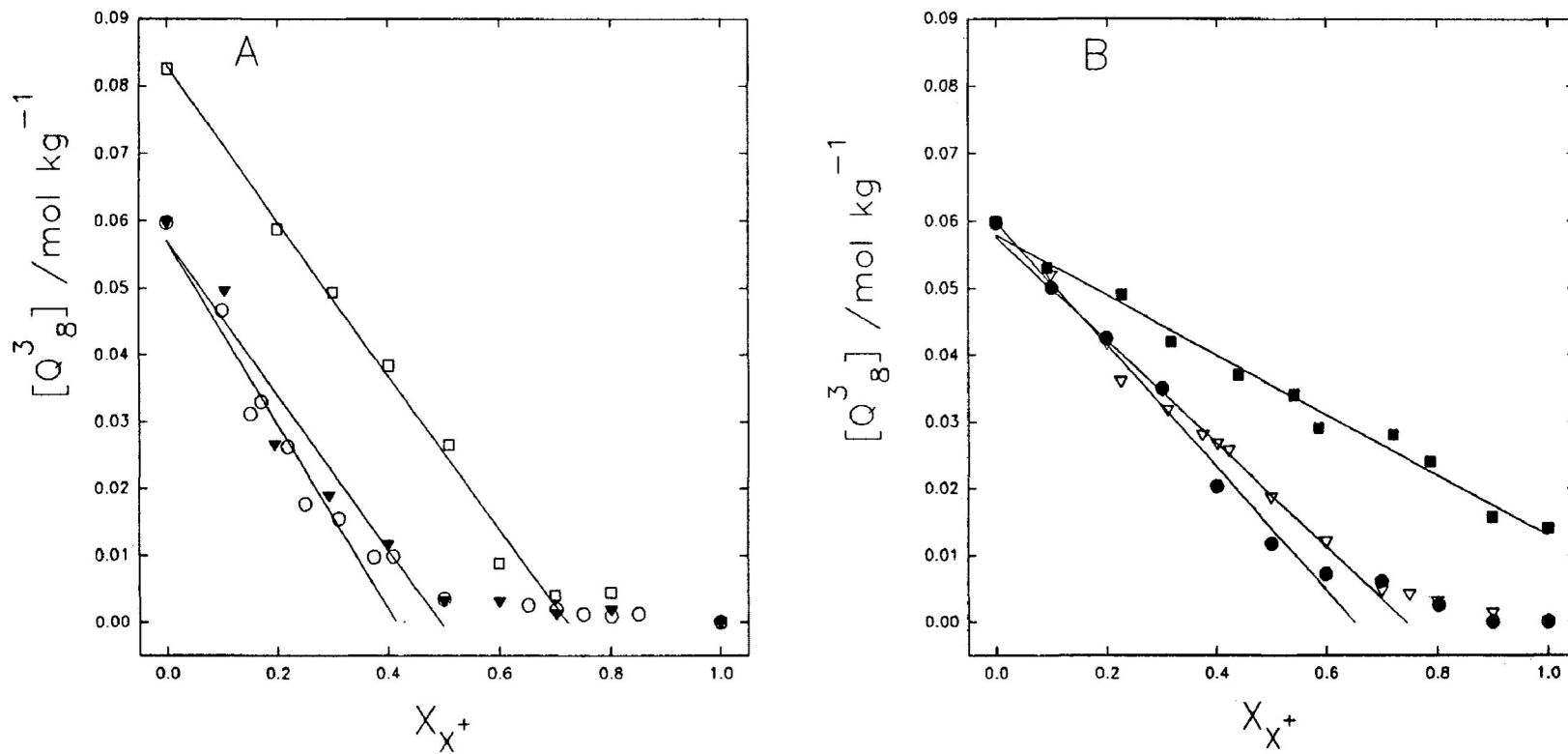


Figure 3-4. Equilibrium concentration of Q_g^3 at 296.1 K as a function of X_{X^+} . The limiting mole fraction of TMA^+ ion = $1 - X_{X^+}$ (see Section 3.1.3). In Graph A, $X^+ = \text{Na}^+$ (O), Cs^+ (▽) or Na^+ with 20 wt% methanol (□). In Graph B, $X^+ = \text{TEA}^+$ (●), TBA^+ (▽), or ETMA^+ (■). The $[\text{SiO}_2] = 0.9 \text{ mol kg}^{-1}$, $[\text{OH}^-] = 0.9 \text{ mol kg}^{-1}$ and $[X^+ + \text{TMA}^+] = 0.9 \text{ mol kg}^{-1}$ in both graphs.

examine the effect of sodium ions on the oligomer distribution. As the NaCl concentration was increased, the concentration of Q_8^3 decreased (Figure 3-6). When the solution contained equimolar amounts of Na^+ and TMA^+ ions, Q_8^3 concentration represented ca. 4% of the dissolved silica and the distribution of silicate oligomers was similar to a $1.0 \text{ mol kg}^{-1} \text{ SiO}_2$ and NaOH silicate solution. The limiting mole fraction of TMA^+ ions as defined above was calculated to be 0.50 for $X^+ = Na^+$.

It is important to note that the $OH^-:Si^{IV}$ ratio of all solutions described in Section 3.2.2 was held constant at 1:1 so that the effects of cations could be monitored independently of alkalinity.

3.1.4. TAA Silicate Equilibria at $OH^-:Si^{IV} < 1:1$

Hydrochloric acid was added to TMA silicate solutions to decrease the nominal $OH^-:Si^{IV}$ ratio. Whereas alkali-metal silicates tend to precipitate as the $OH^-:Si^{IV}$ ratio is decreased to just below 1:1, TMA silicate solutions remain homogeneous to ratios of $\leq 0.68:1$. At lower ratios, a broad ^{29}Si band in the Q^4 region (*i.e.*, < -30 ppm) indicates the presence of colloidal silica. Broad bands near -15 ppm and -27 ppm probably correspond to Q^2 and Q^3 silicate oligomers within the colloidal silicate phase (Figure 3-7a). We observed two resonances at approximately 0.23 and 0.35 ppm down-frequency of the Q_8^3 resonance which previously were attributed^[4,78,79] to double five and double six ring structures (Figure 3-7b). These resonances were also observed when the weak diprotic acid, H_2Na_2EDTA , was added to TMA silicate solutions.^[54] For a solution containing 95% ^{29}Si isotopically enriched silica the resonance at ca. 0.23 ppm down-frequency of the Q_8^3 resonance (Figure 3-8, Spectrum A) is a singlet and therefore must correspond to a symmetrical silicate oligomer. We

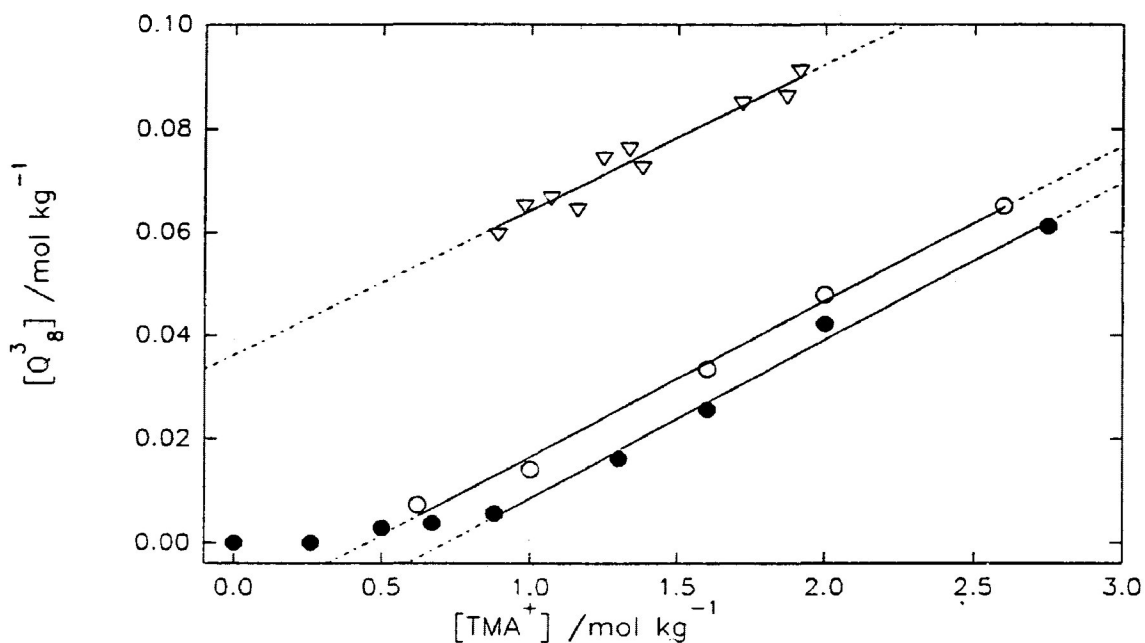


Figure 3-5. Equilibrium concentration of Q_8^3 at 296.1 K as a function of $[TMA^+]$. Solutions contain 0.9 mol kg^{-1} SiO_2 and 0.9 mol kg^{-1} $NaOH$ (●), $CsOH$ (○), or $TMAOH$ (∇). The $[TMA^+]$ was increased by the addition of $TMACl$.

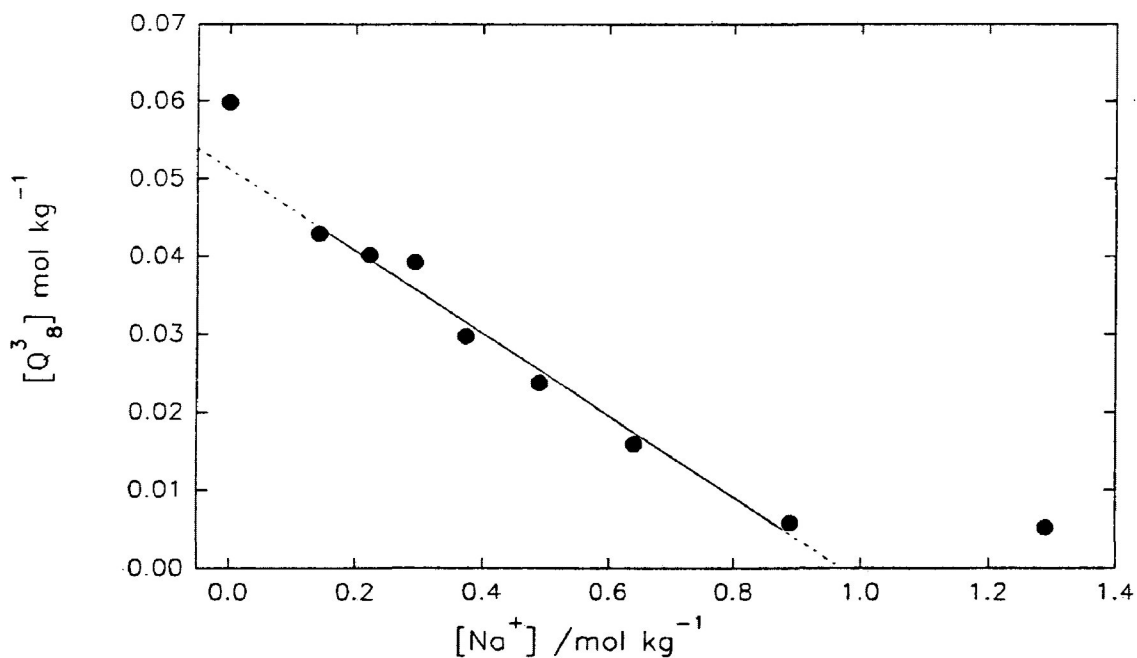


Figure 3-6. Equilibrium concentration of Q_8^3 at 296.1 K as a function of $[Na^+]$ for solutions containing 0.9 mol kg^{-1} SiO_2 and 0.9 mol kg^{-1} $TMAOH$. The $[Na^+]$ was increased by addition of $NaCl$.

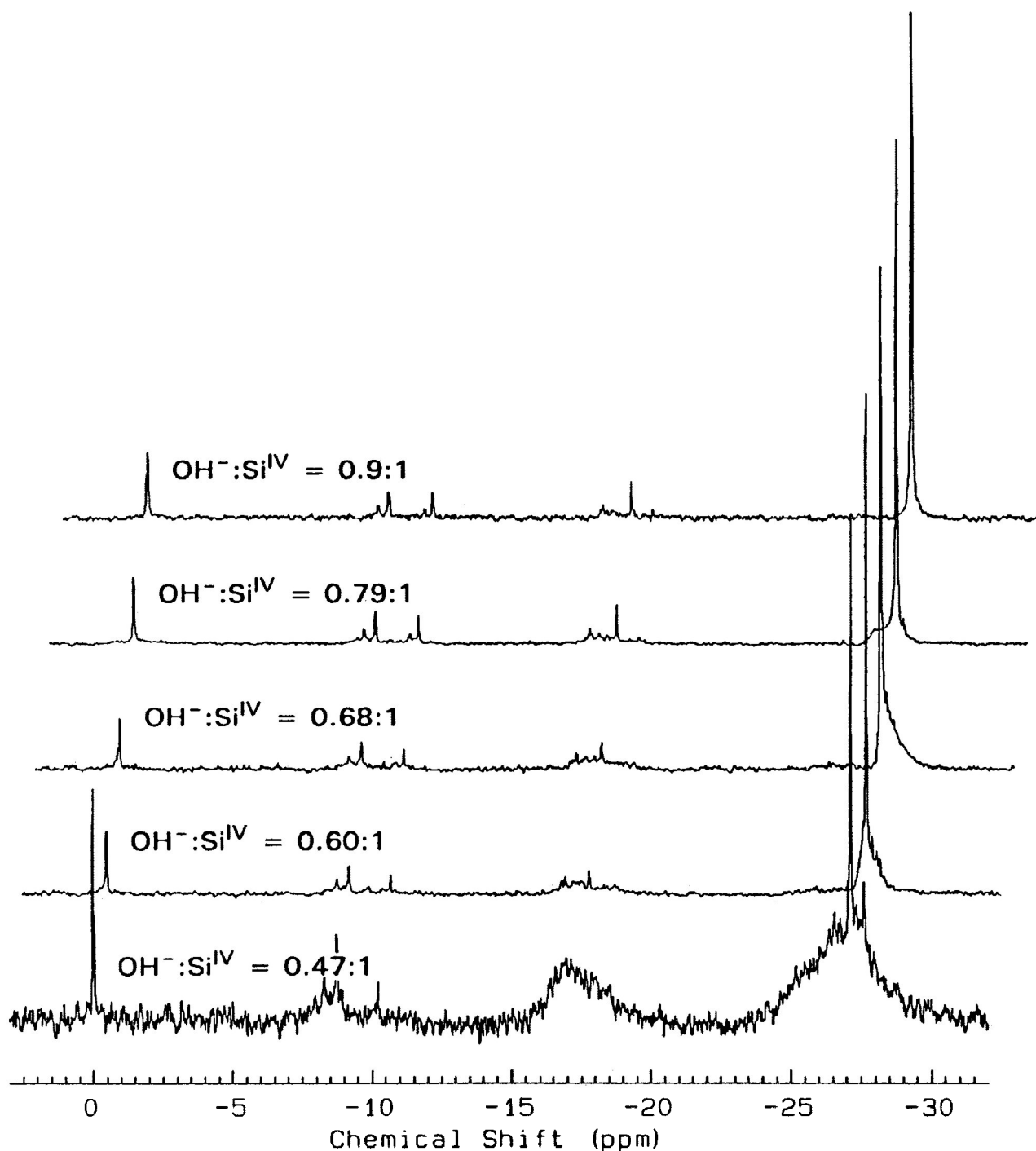


Figure 3–7a. ^{29}Si NMR of solutions containing 1.0 mol kg^{-1} SiO_2 and 1.0 mol kg^{-1} TMAOH at 296.1 K. The $\text{OH}^-:\text{Si}^{\text{IV}}$ ratio was adjusted using concentrated HCl. The Q_3^3 resonance is dominant at $\text{OH}^-:\text{Si}^{\text{IV}} > 0.4:1$. Spectra are scaled to the Q_8 resonance and are offset by 0.5 ppm for clarity.

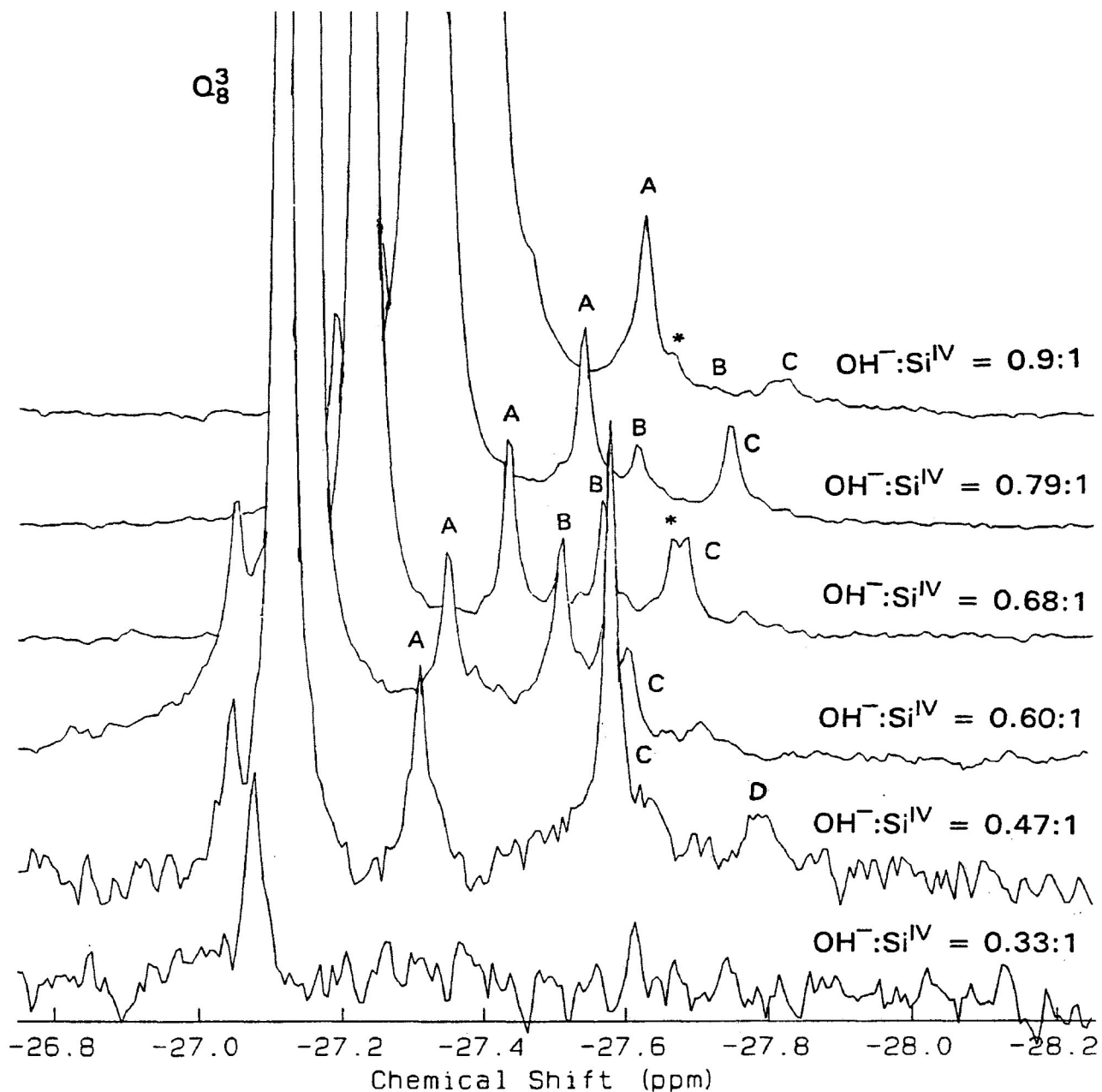
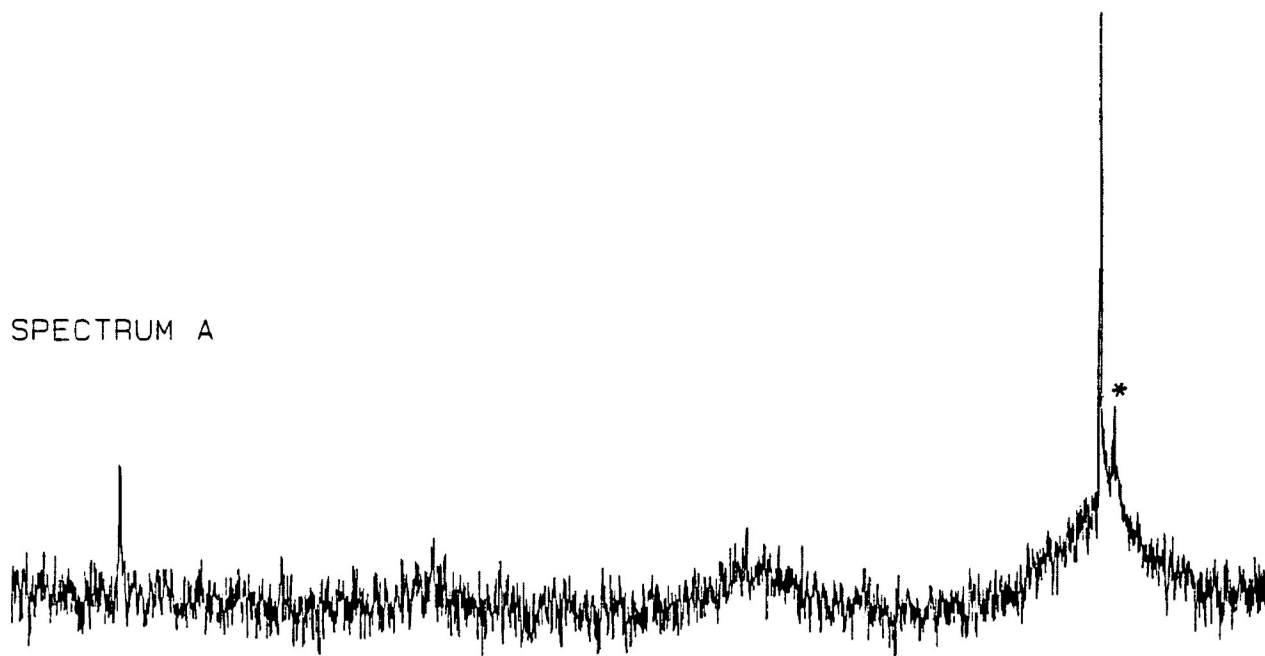


Figure 3 – 7b. Expansion of Figure 3 – 7a (included spectra labelled: $\text{OH}^-:\text{Si}^{\text{IV}} = 0.33:1$). Note resonances *ca.* 0.23 (A), 0.35 (B), 0.46 (C), 0.70 (D) ppm down-frequency of Q_8^3 resonance. Resonances indicated with asterisks are yet unidentified. Spectra are not offset so the shift of the Q_8^3 resonance can be observed. (0.5 Hz artificial line broadening)

SPECTRUM A



SPECTRUM B

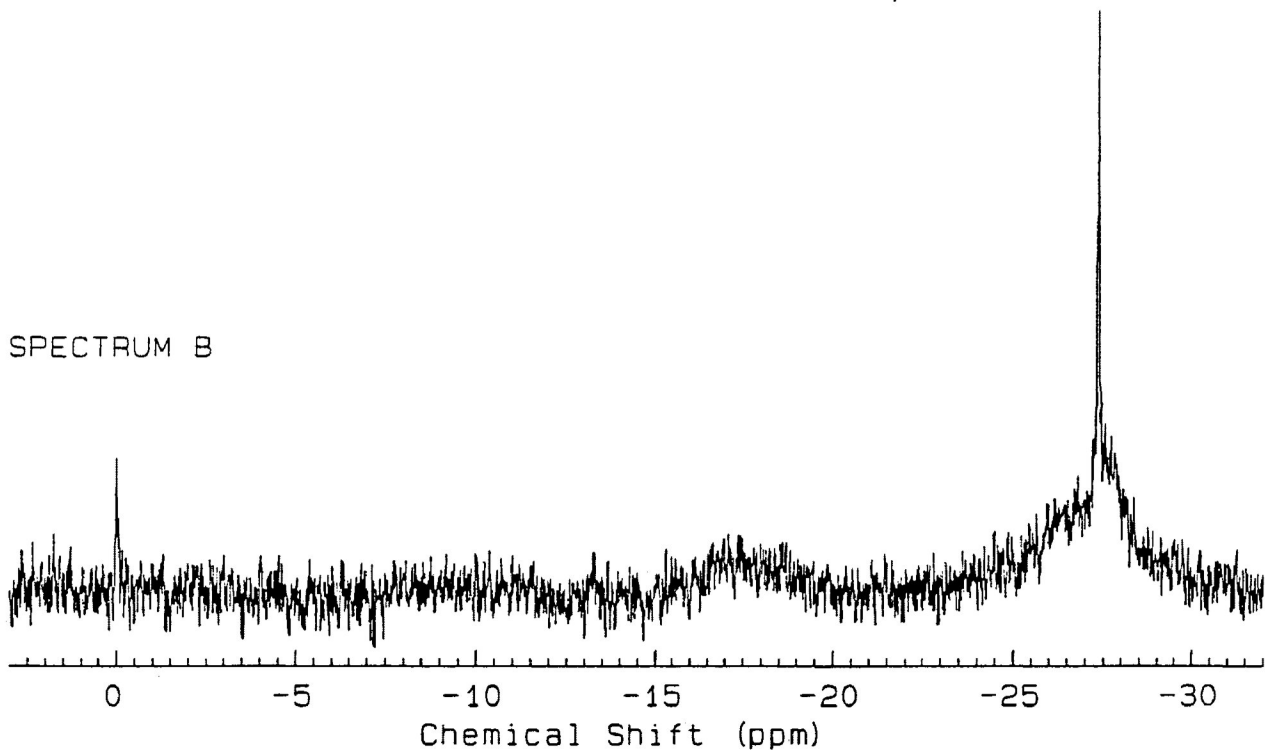


Figure 3-8. ^{29}Si NMR of solutions containing $0.95 \text{ mol kg}^{-1} \text{ SiO}_2$ (95% isotopically enriched ^{29}Si), $0.95 \text{ mol kg}^{-1} \text{ TMAOH}$ and $0.35 \text{ mol kg}^{-1} \text{ HCl}$ at 296.1 K. Spectrum A is at normal atmospheric pressure whereas B is at 27.6 MPa. Down-frequency resonances (indicated with asterisk) are not apparent at elevated pressure. (0.5 Hz artificial line broadening)

also observed at $\text{OH}^-:\text{Si}^{\text{IV}} < 0.8:1$ at least two additional resonances at approximately 0.46 and 0.70 ppm down-frequency of the Q_8^3 resonance (Figure 3-7b).

The ^{29}Si NMR spectra of a solution containing 95% isotopically enriched ^{29}Si was acquired using the high pressure apparatus described in Section 2.3 at 27.6 MPa and at atmospheric pressure (Figure 3-8). In the spectrum acquired at atmospheric pressure, at least one of the down-frequency resonances described in the above study is observed. In the spectrum acquired at 27.6 MPa however, it appears that the down-frequency resonances decreased in relative intensity. Unfortunately, this was the only spectrum acquired with any sample at high pressure as the Vespel pressure jacket ruptured during a subsequent attempt at a higher pressure. It should therefore be noted that these findings are only preliminary and have not been confirmed.

The resonances which occurred at *ca.* 0.23 and 0.35 ppm down-frequency of Q_8^3 resonance were also observed in TEA, TPA and TBA silicate solutions ($\text{OH}^-:\text{Si}^{\text{IV}} < 1:1$) which contained organic solutes (Figure 3-9a). The chemical shifts were slightly different, however, at *ca.* 0.25 and *ca.* 0.38 ppm down-frequency of Q_8^3 resonance (possibly due to solvent effects). In a solution containing 95% isotopically enriched ^{29}Si the resonances at *ca.* 0.25 and *ca.* 0.38 ppm down-frequency of the Q_8^3 resonance (Figure 3-9b) both appear to be singlets and therefore correspond to symmetrical silicate oligomers.

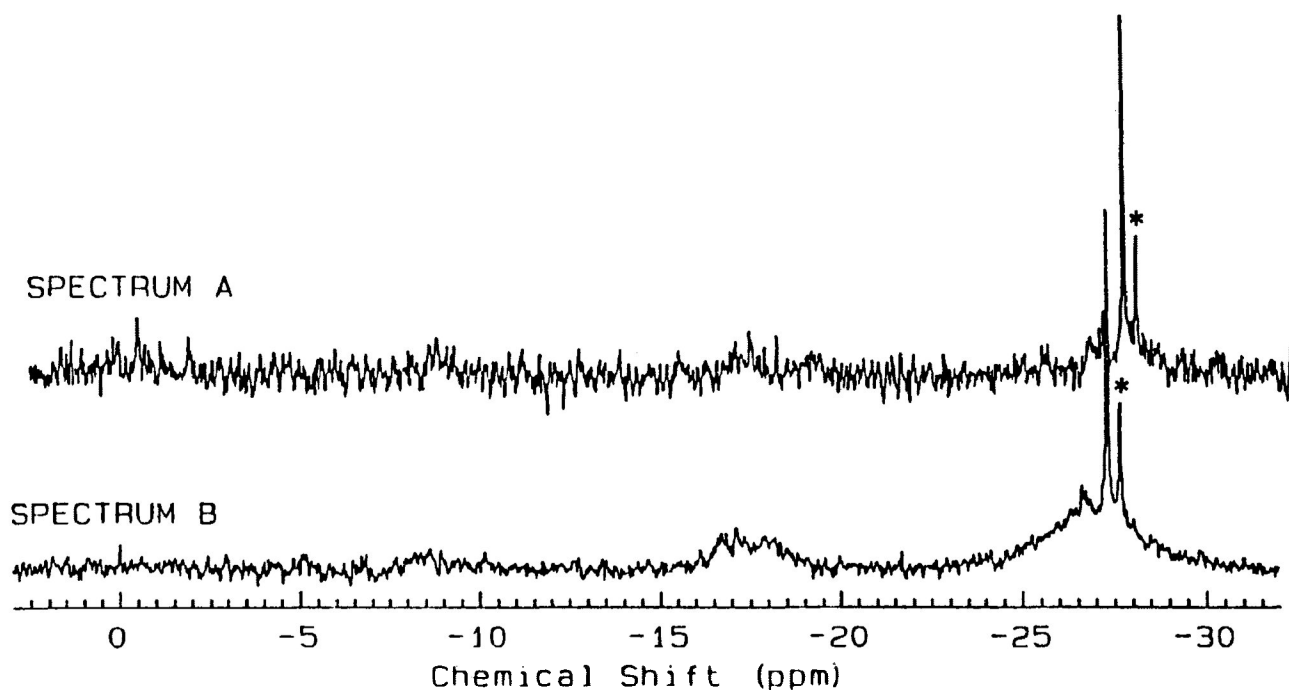


Figure 3 – 9a. ^{29}Si NMR at 296.1 K of solutions containing: 0.34 mol kg^{-1} SiO_2 , 0.17 mol kg^{-1} TPAOH and 57wt% DMSO (Spectrum A); 1.4 mol kg^{-1} SiO_2 , 0.6 mol kg^{-1} TBAOH and 40wt% DMSO (Spectrum B). Note prevalence of resonance *ca.* 0.25 ppm down-frequency (indicated with asterisk) from Q_8^3 resonance. Spectrum A is offset 0.1 ppm for clarity.

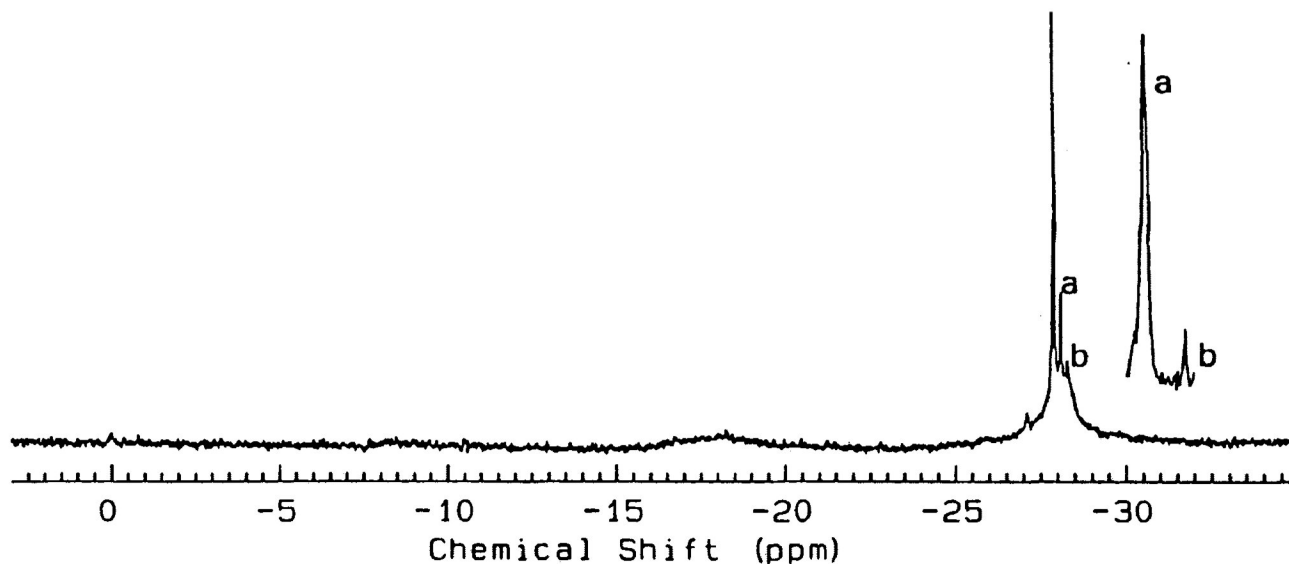


Figure 3 – 9b. ^{29}Si NMR of solution containing 1.9 mol kg^{-1} (95% isotopically enriched ^{29}Si) SiO_2 , 1.2 mol kg^{-1} TBAOH and 35wt% DMSO at 317.1 K. Note the two down-frequency resonances (a and b; 0.25 and 0.38 ppm down-frequency respectively) appear to be singlets. (0.2 Hz artificial line broadening)

3.2. Silicate Kinetics

3.2.1. Analysis of Previous Studies

In alkali-metal silicate solutions, the intermolecular Si-Si exchange rate decreases as alkalinity (*i.e.*, $\text{OH}^-:\text{Si}^{\text{IV}}$ ratio) is increased and at $\text{OH}^-:\text{Si}^{\text{IV}} = 1:1$ is essentially the same for all Si centres (at higher alkalinity, the reactivity of silicate centres varies with the respective pKa values).^[29] Magnetization transfer experiments^[64] have revealed that in TMA silicate solutions Si-Si exchange involving the favoured Q_8^3 and Q_6^3 oligomers is slower than for other silicate oligomers. Knight *et al.*^[56] (employing their boil-freeze-thaw method) observed that Q_6^3 forms faster than Q_8^3 but subsequently decreases in concentration (*e.g.* Figure 3-10 and 3-11). Hasegawa *et al.*^[84] have suggested that because Q_6^3 is always present during the formation of Q_8^3 , Q_6^3 may be an intermediate. In a preliminary investigation, Pole^[54] (employing the boil-freeze-thaw method) observed that the rate of Q_8^3 formation decreased as alkalinity was increased. He also observed at least three transient resonances during the formation of Q_8^3 .

Knight *et al.*^[23,85] reported that germanium could be substituted for one and two Si centres in Q_6^3 and Q_8^3 but only if the solution was freshly prepared or boiled. If the solution was at equilibrium there was no evidence in the ^{29}Si NMR spectrum for germanium substitution. Other investigators^[72,86-89] have substituted aluminium, gallium and boron into TAA silicate oligomers but only aluminium and germanium have been successfully substituted into Q_8^3 .

3.2.2. Method of Initial Rates

Aqueous silicate solutions contain a complex mixture of mutually exchanging oligomers. Each individual oligomer is involved in several exchange

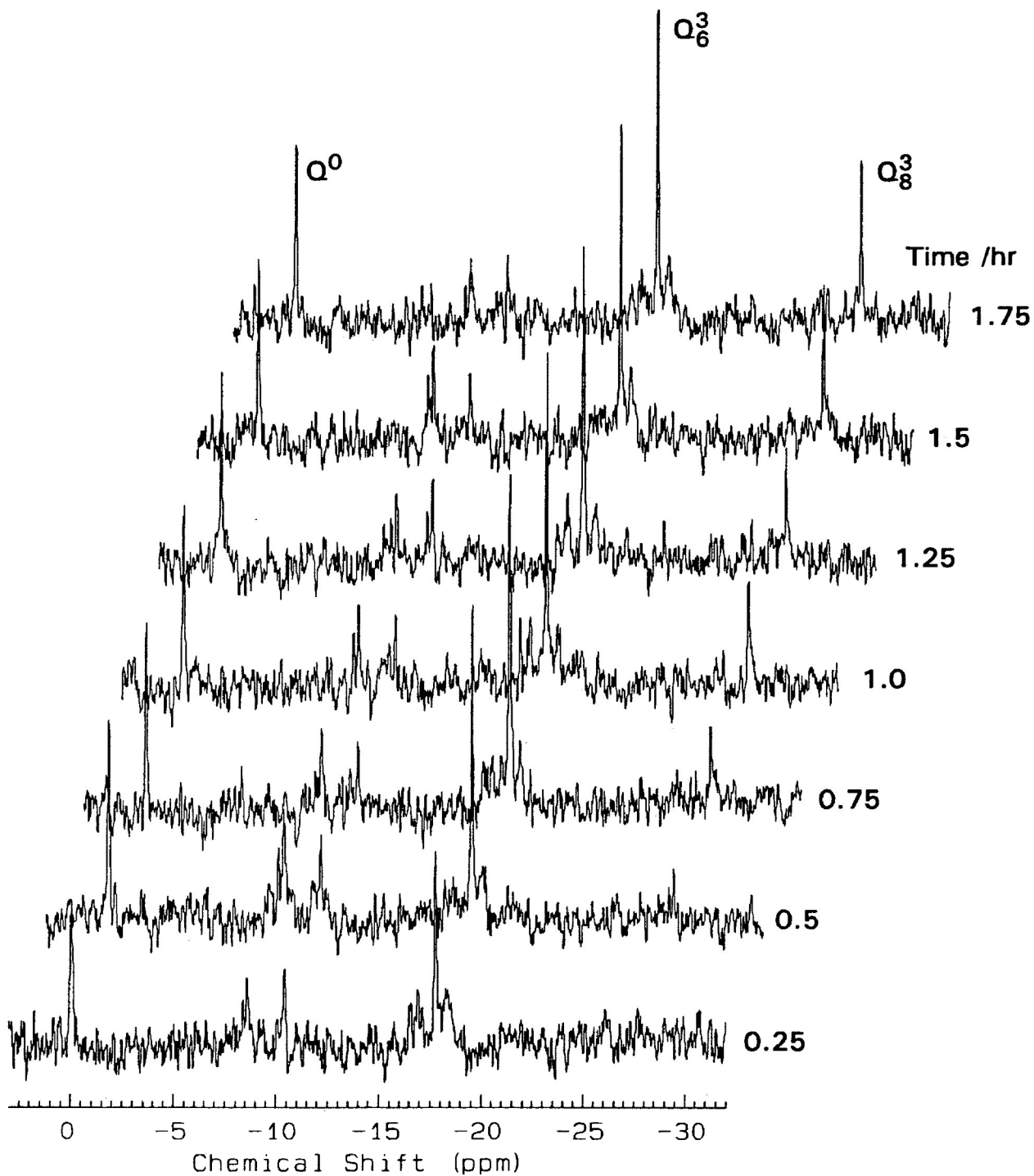


Figure 3 – 10. Time dependence of ^{29}Si NMR spectra, acquired at 296.1 K over 0.25 h intervals, for a solution containing $1.0 \text{ mol kg}^{-1} \text{ SiO}_2$, $1.4 \text{ mol kg}^{-1} \text{ TMAOH}$ and $0.6 \text{ mol kg}^{-1} \text{ TMACl}$ following equilibrium perturbation by the "boil-freeze-thaw" procedure. The Q_8^3 resonance is not apparent 0.25 hours after thawing of the sample.

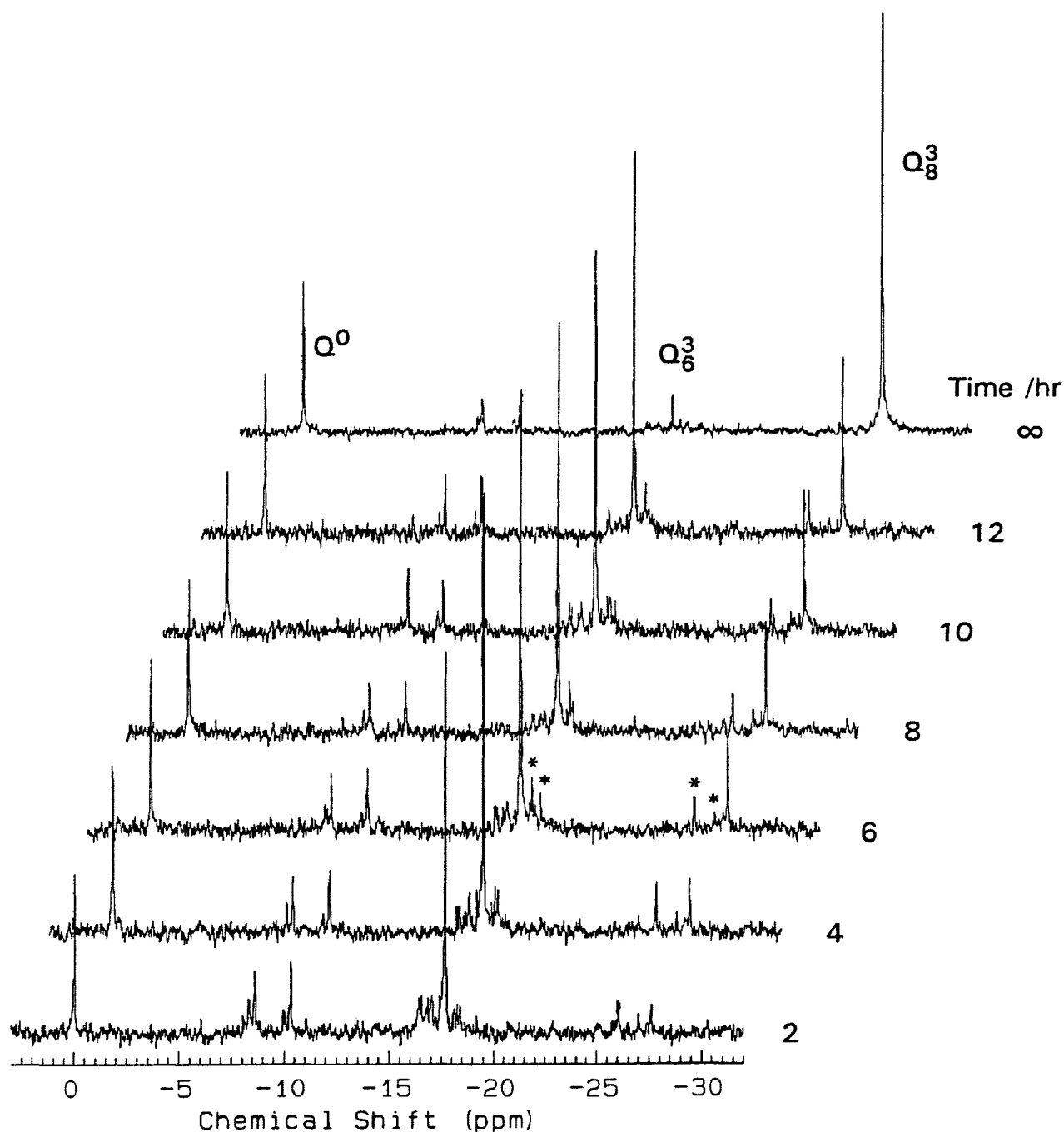


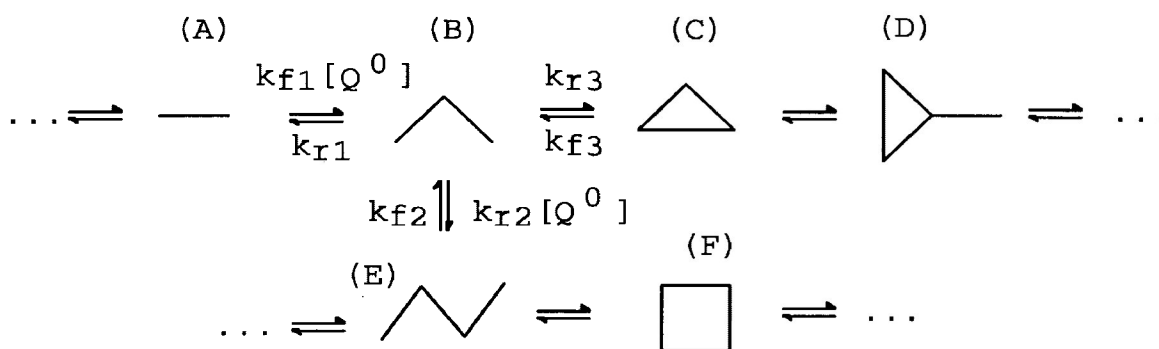
Figure 3 – 11. Time dependence of ^{29}Si NMR spectra for a solution containing $1.0 \text{ mol kg}^{-1} \text{ SiO}_2$, $1.4 \text{ mol kg}^{-1} \text{ TMAOH}$ and $0.6 \text{ mol kg}^{-1} \text{ TMACl}$ at 287 K following equilibrium perturbation by the boil-freeze-thaw procedure. The intensity of most signals decreases monotonically while that of the Q_8^3 increases. Note that the relative intensity of some peaks increases initially but then decreases (e.g. the Q_6^3 resonance and resonances marked with asterisk).

reactions (e.g. Reaction 3-1) such that the net reaction rate is given by:

$$d[x]/dt = \sum (\text{forward rates, } R_f) - \sum (\text{reverse rates, } R_r)$$

For example, the net rate for the linear trimer (species B) as shown in Reaction 3-1 would be:

$$d[B]/dt = k_{f1}[A][Q^0] + k_{f2}[E] + k_{f3}[C] - k_{r1}[B] - k_{r2}[B][Q^0] - k_{r3}[B]$$



Reaction 3-1. Possible reaction scheme for some silicate oligomers. Note that there are *at least* three different exchange reactions involving the linear trimer (species B).

If the exchange system is at equilibrium, $d[x]/dt = 0$ ($\sum R_f = \sum R_r$). Immediately following execution of the boil-freeze-thaw procedure (*i.e.*, @ $t=0$), however, the distribution of silicate oligomers is not at equilibrium; in particular, Q_8^3 is virtually absent^[34,90] (Figure 3-10). The initial rate of Q_8^3 dissociation ($R_{r(t=0)}$) therefore is nearly zero and, as such, the *net* rate of Q_8^3 formation ($(d[Q_8^3]/dt)_{t=0}$) is simply $\sum R_f$. Investigating the initial rates of processes also avoids complications arising from e.g. product inhibition, auto catalysis and subsequent reactions.^[91]

3.2.3. Effect of Pressure on Silicate Kinetics

In principle, rate constants can be measured as a function of pressure in order to provide the volume of activation ΔV^\ddagger (Equation 3-1).^[91-96] For the reaction $A + B \rightleftharpoons [A\dots B]^\ddagger \rightarrow AB$, reaction volume $\Delta \bar{V}$ and activation volume ΔV^\ddagger would be defined by Equations 3-2 and 3-3, respectively. Here \bar{V} denotes partial molar volume.

$$\left[\frac{\partial \ln k}{\partial P} \right]_T = - \frac{\Delta V^\ddagger}{RT} \quad (3-1)$$

$$\Delta \bar{V} = \bar{V}_{AB} - (\bar{V}_A + \bar{V}_B) \quad (3-2)$$

$$\Delta V^\ddagger = \bar{V}^\ddagger - (\bar{V}_A + \bar{V}_B) \quad (3-3)$$

The volume of activation is indicative of the volume profile of a reaction. If the reaction rate increases when the pressure is increased then ΔV^\ddagger is negative. This can be useful *e.g.* in distinguishing between concerted and two-step processes. Bond formation usually contributes a positive effect to ΔV^\ddagger whereas bond cleavage contributes a negative influence. In polar solvents the change in the degree of ionization from the reactants to the activated complex contributes a negative influence due to an increase in local solvent density; this phenomenon is called electrostriction.

3.2.4. Kinetics of TMA Silicate Solutions

Selective inversion recovery and selective saturation experiments were performed on TMA silicate solutions (1:1 and 2:1 $\text{OH}^-:\text{Si}^{\text{IV}}$, and 1.0 and 3.0 mol kg^{-1} SiO_2). These methods require precise knowledge of T_1 relaxation rates which, due to low concentrations of some oligomers, was difficult to

determine. As well, at ambient temperatures Si-Si exchange involving Q_8^3 and Q_6^3 was observed to be slow relative to the rate of T_1 relaxation. Selective inversion recovery and selective saturation experiments can only be used to determine exchange rates on the order of the T_1 relaxation rate. Unfortunately, increasing the temperature, to increase the exchange rate, decreased spectral resolution owing to the equilibrium shift away from Q_8^3 and Q_6^3 . Therefore, both methods proved unsatisfactory for quantifying the rate of Q_8^3 formation or dissociation. Nevertheless, selective saturation experiments were instrumental in determining that the monomer is slowly exchanging with Q_8^3 and Q_6^3 , and rapidly exchanging with all other oligomers (*i.e.*, on the order of the rate calculated for alkali-metal silicate solutions^[29]). The boil-freeze-thaw procedure is well suited for analyzing of the slow exchange kinetics involving Q_8^3 and Q_6^3 oligomers at ambient temperature (*e.g.* Figure 2-2).

The boil-freeze-thaw procedure was employed at 296.1 K to obtain $(d[Q_8^3]/dt)_{t=0}$ for TMA silicate solutions ($1.0 \text{ mol kg}^{-1} \text{ SiO}_2$) at various $\text{OH}^-:\text{Si}^{\text{IV}}$ ratios (see Table III-V). The kinetics were too fast to monitor at $\text{OH}^-:\text{Si}^{\text{IV}} = 1:1$ and at $\text{OH}^-:\text{Si}^{\text{IV}} = 2:1$ crystals formed (presumably solid TMA-cubic octamer^[45]). Figure 3-12 shows that, within these experimental limits, $(d[Q_8^3]/dt)_{t=0}$ decreases as alkalinity is increased at constant SiO_2 and TMA^+ ion concentrations. The initial pH was determined using equivalent, non-deuterated solutions immediately following execution of the boil-freeze-thaw procedure (see Table III-V at end of chapter).

Addition of TMA^+ ions had a comparatively small effect on $(d[Q_8^3]/dt)_{t=0}$ at constant SiO_2 and $\text{OH}^-:\text{Si}^{\text{IV}}$ ratio (see Table III-VI at end of chapter and Figure 3-13). Addition of up to 1.7 mol kg^{-1} TMACl did not significantly alter

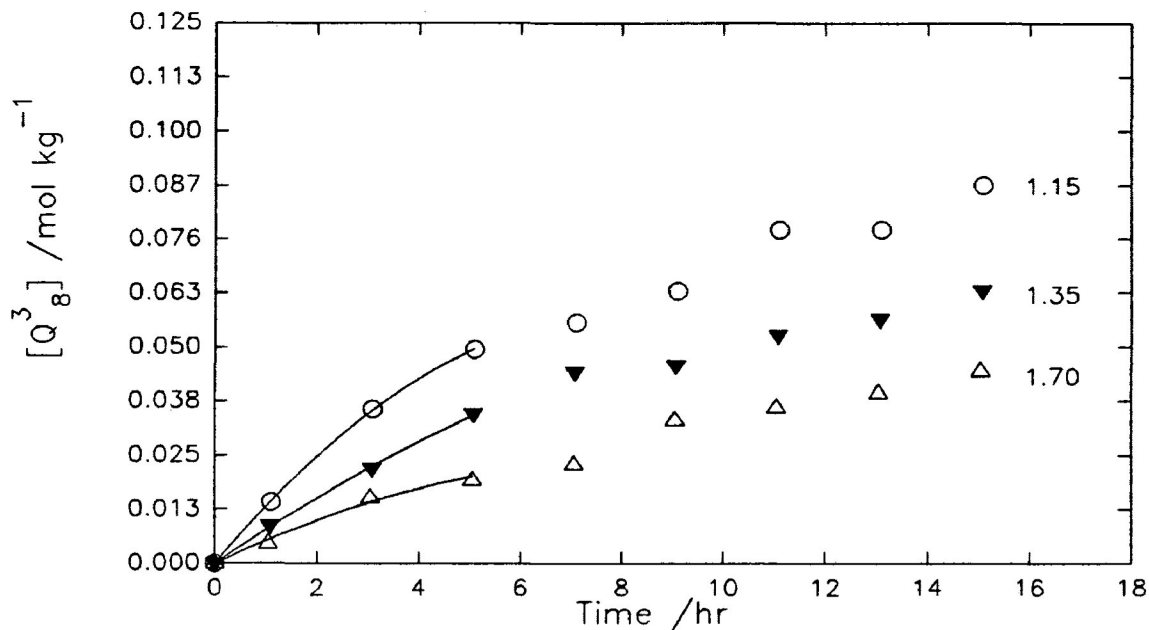


Figure 3-12. Evolution of Q_g^3 at 296.1 K following the boil-freeze-thaw procedure. Experimental data and polynomial curve fit^[99] of the first four data points are shown. Samples contain $1.0 \text{ mol kg}^{-1} \text{ SiO}_2$. $[\text{TMAOH}]$ is indicated on figure. The $[\text{TMA}^+]$ was increased to 2.0 mol kg^{-1} in each case by the addition of TMACl. Not all data sets are depicted in this figure.

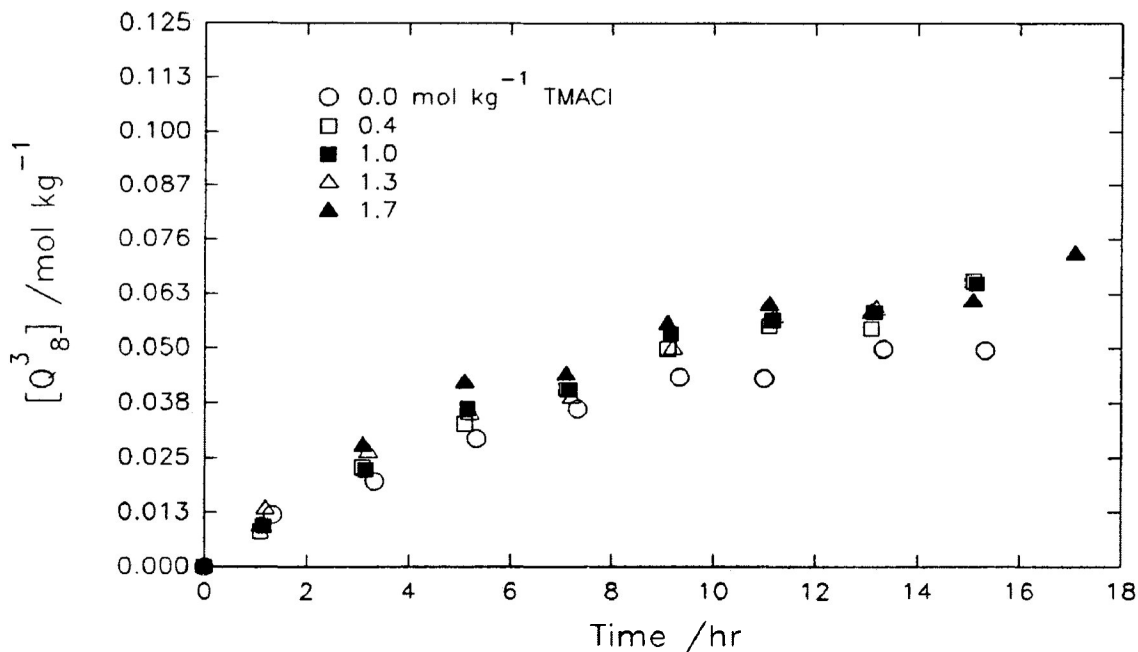


Figure 3-13. Evolution of Q_g^3 at 296.1 K following the boil-freeze-thaw procedure. Samples contain $1.0 \text{ mol kg}^{-1} \text{ SiO}_2$ and $1.4 \text{ mol kg}^{-1} \text{ TMAOH}$. The $[\text{TMA}^+]$ was increased by addition of TMACl. Concentration of added TMACl is shown in figure. Not all data sets are depicted in figure.

the initial pH of samples (changes were within 0.010 pH units).

Increasing the concentration of SiO_2 at constant TMAOH concentration decreases the resultant $\text{OH}^-:\text{Si}^{\text{IV}}$ ratio and, thereby, pH. The resulting increase in $(d[\text{Q}_8^3]/dt)_{t=0}$ (see Table III-VII at end of chapter and, Figures 3-14a and b) therefore arises from the combined influence of both parameters, $[\text{SiO}_2]$ and $[\text{H}^+]$.

For comparison, the boil-freeze-thaw procedure was employed at 296 K for sodium silicate solutions (1.0 and 2.0 mol kg^{-1} NaOH and 1.0 mol kg^{-1} SiO_2). An equilibrium distribution of oligomers was observed by fifteen minutes after thawing.

3.2.5. Transient Species in TMA Silicate Solutions

In accordance with previous reports,^[54] three resonances (-26.2, -27.2 and -27.7 ppm) were frequently observed within the first several hours following the boil-freeze-thaw procedure but not in the final *equilibrium* spectra. We observed at least three additional resonances (-16.4, -19.0 and -27.3 ppm) which were not previously reported (Figure 3-11 and Figure 3-15a). Such *transient* resonances were most pronounced in experiments performed at <290 K and for samples with $\text{OH}^-:\text{Si}^{\text{IV}} = 1.4:1$ (1.0 mol kg^{-1} SiO_2) and added TMACl (>1.0 mol kg^{-1}). Splitting patterns obtained from a sample prepared with 95% ^{29}Si isotopically enriched silica enabled us to assign some of them (Figure 3-15b). In accordance with data of Harris *et al.*^[19-22] the quartet resonance at -26.2 ppm and the triplet at -16.4 ppm correspond to the doubly bridged four ring oligomer (see Table I-I). These resonances both have a coupling constant of 3.2 Hz and the fitted peaks have areas in a 2:1 ($\text{Q}^3:\text{Q}^2$) ratio. The multiplet at -27.7 ppm and the triplet at -18.75 ppm are assigned to

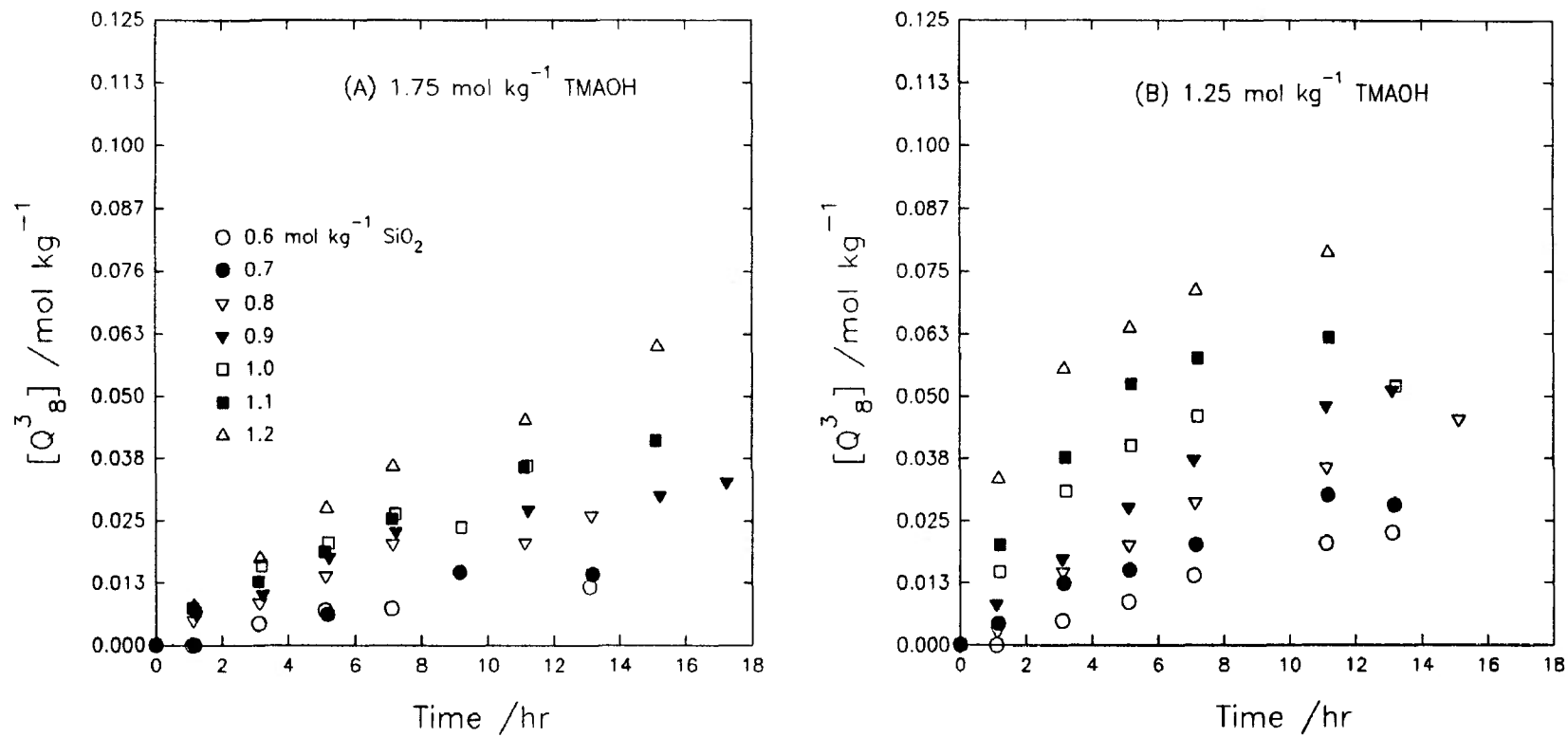


Figure 3– 14. Evolution of Q_8^3 at 296.1 K following the boil-freeze-thaw procedure. Samples contain (A) 1.75 mol kg⁻¹ TMAOH or (B) 1.25 mol kg⁻¹ TMAOH and various SiO₂ concentrations as indicated.

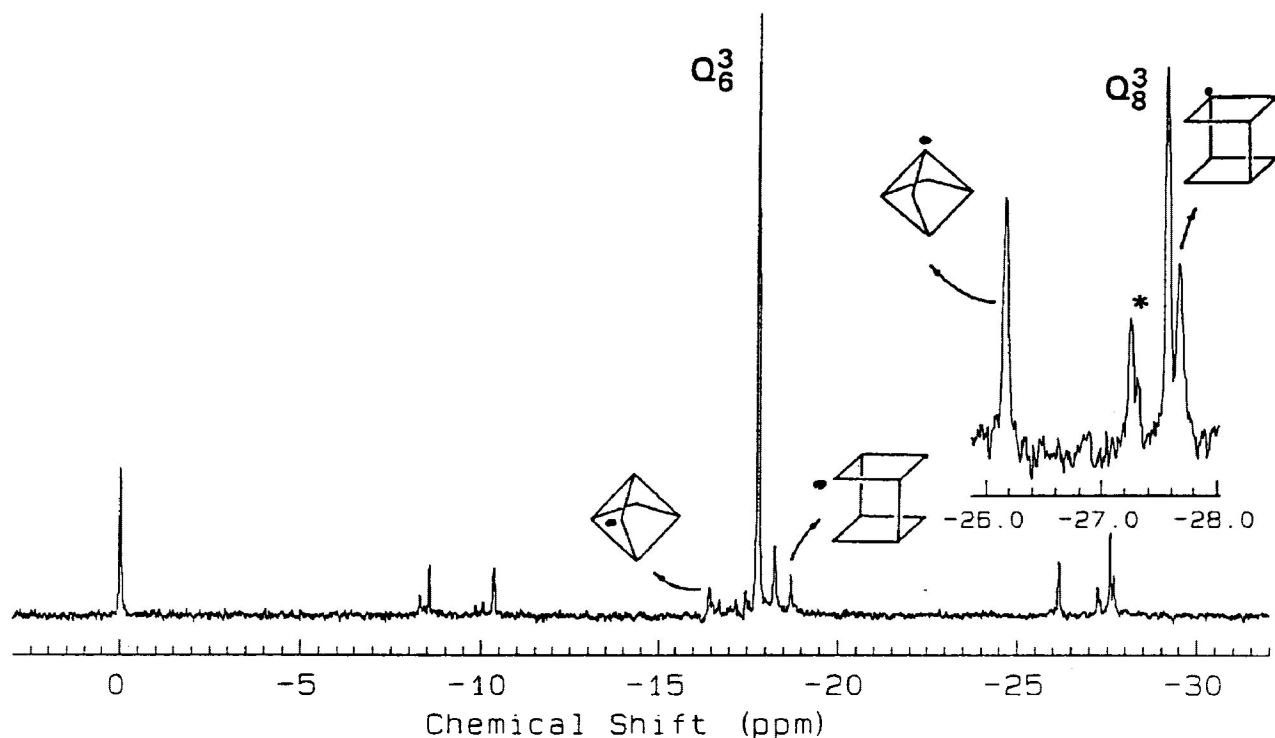


Figure 3-15a. ^{29}Si NMR spectrum of a solution containing $1.0 \text{ mol kg}^{-1} \text{ SiO}_2$, $1.4 \text{ mol kg}^{-1} \text{ TMAOH}$ and $1.7 \text{ mol kg}^{-1} \text{ TMACI}$ at 280.0 K . The spectrum was acquired over 10 hours following the boil-freeze-thaw procedure. Transient resonances and corresponding structures are shown. The resonances indicated with an asterisk are yet unidentified. (0.5 Hz artificial line broadening)

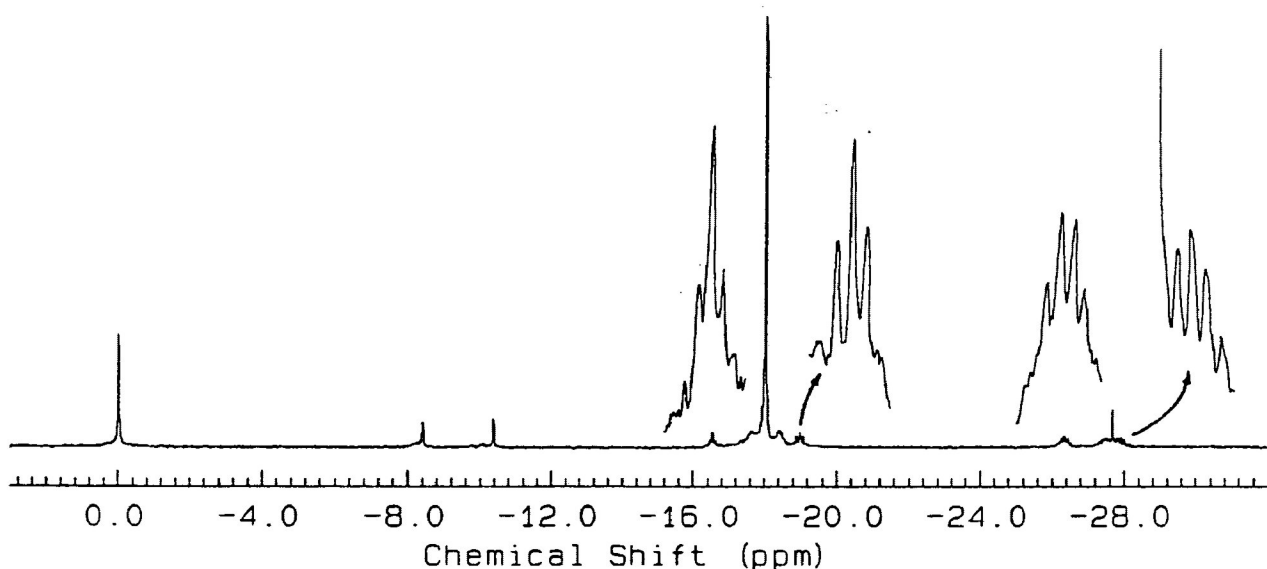


Figure 3-15b. ^{29}Si NMR spectrum at 273.8 K of the equivalent solution that is 95% isotopically enriched in ^{29}Si . The coupling constant of resonances at -16.4 and -26.2 ppm is ca. 3.2 Hz and at -19.0 and -27.7 ppm is ca. 4.0 Hz . (0.3 Hz artificial line broadening).

tricyclic octamer (see Table I-I). Homonuclear decoupling experiments yielded confirmation of coupling between these latter two resonances. These two resonances have a coupling constant of 4.0 Hz and the fitted peaks have equal area.

The resonances clustered at *ca.* -27.3 ppm remain unassigned. Based on chemical shifts, possible structures corresponding to these resonances include: tricyclic hexamer (2); pentacyclic heptamer; pentacyclic nonamer; singly and doubly bridged cyclic tetramer; hexacyclic octamer; tricyclic octamer (1 and 2); bicyclic hexamer; and substituted cyclic tetramer (see Table I-I). Homonuclear decoupling experiments (*i.e.*, using ²⁹Si enriched samples) were ineffective at correlating any of the corresponding multiplets to other resonances.

3.2.6. Transient Species in Other TAA Silicate Solutions

Silicate solutions containing TAA⁺ ions other than TMA⁺ also yielded transient resonances (*i.e.*, resonances which increase, then decrease in intensity following the boil-freeze-thaw procedure and are not observed at equilibrium). For one TBA silicate sample, at least six transient resonances were observed in the range of -25 to -27 ppm and possibly another four in the range of -15.5 to -18 ppm (Figures 3-16a and b). An equivalent ²⁹Si enriched sample yielded singlets for two of these transient resonances at -16.9 ppm and -26.5 ppm indicating that they correspond to magnetically symmetrical oligomers (Figure 3-16c). The -26.5 ppm resonance likely corresponds to the tetrahedral tetramer species Q₄³.^[24] However, the resonance could, although less likely, correspond to double six ring^[3] (this oligomer has not been proven to exist in solution). The singlet resonance at -16.9 probably corresponds to

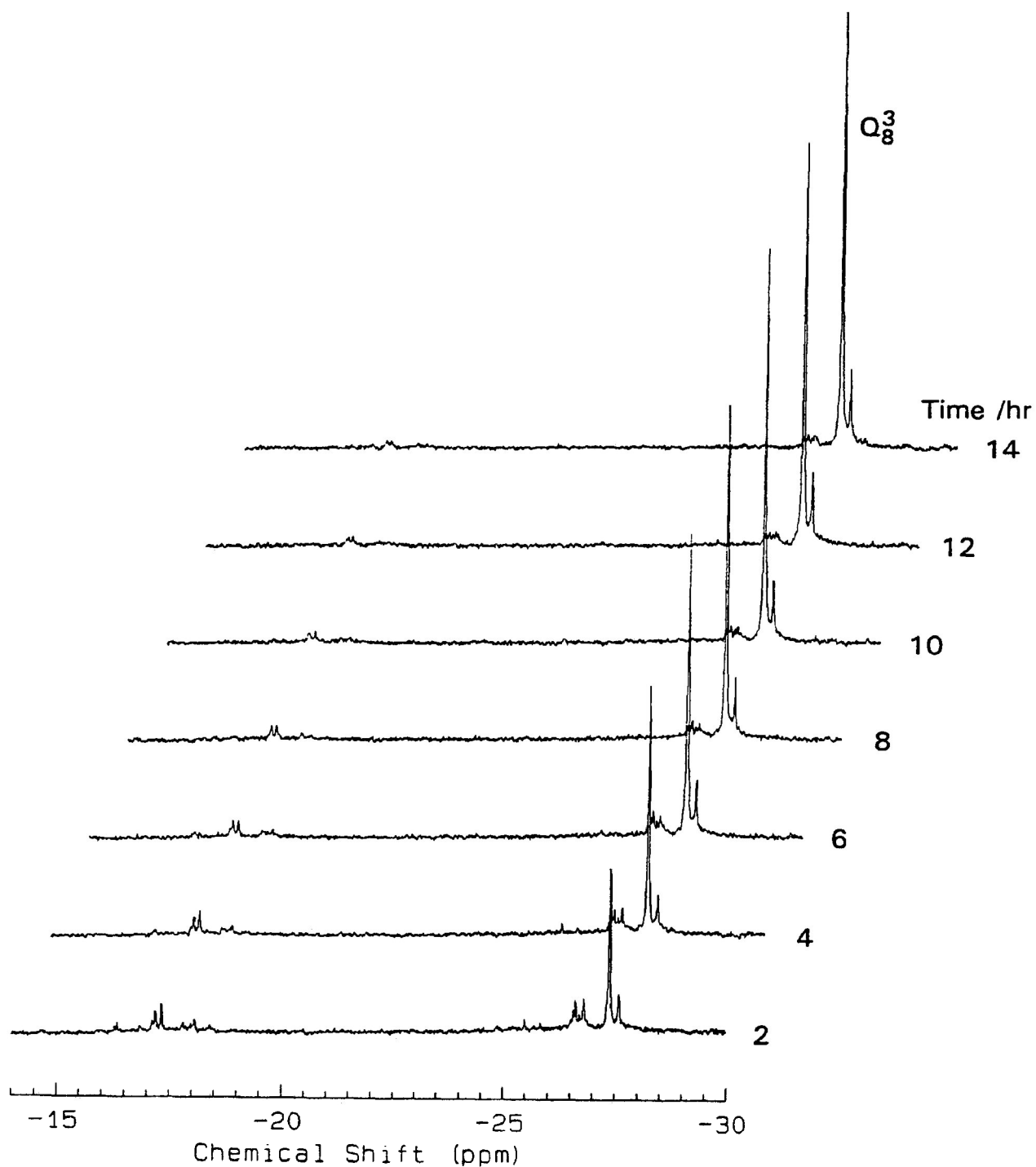


Figure 3 – 16a. Time dependence using ^{29}Si NMR of a solution containing $1.5 \text{ mol kg}^{-1} \text{ SiO}_2$, $0.88 \text{ mol kg}^{-1} \text{ TBAOH}$ and 30wt% DMSO at 276.8 K following equilibrium perturbation by the boil-freeze-thaw procedure. Note the relative intensity of most resonances decreases whereas the Q_8^3 resonance and down-frequency resonance increase.

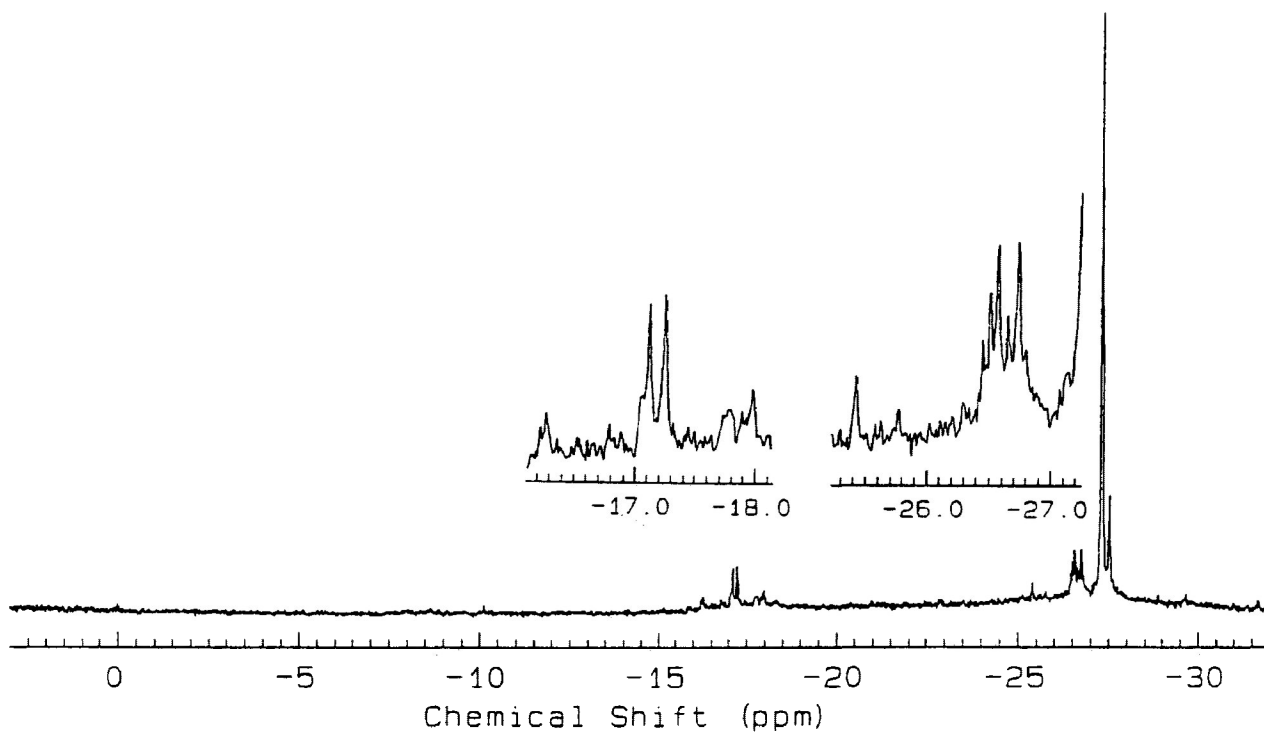


Figure 3 – 16b. ^{29}Si NMR spectrum at 276.8 K of a solution containing 1.5 mol kg^{-1} SiO_2 , 0.88 mol kg^{-1} TBAOH and 30wt% DMSO. The spectrum was acquired over 3 hours following the boil-freeze-thaw procedure.

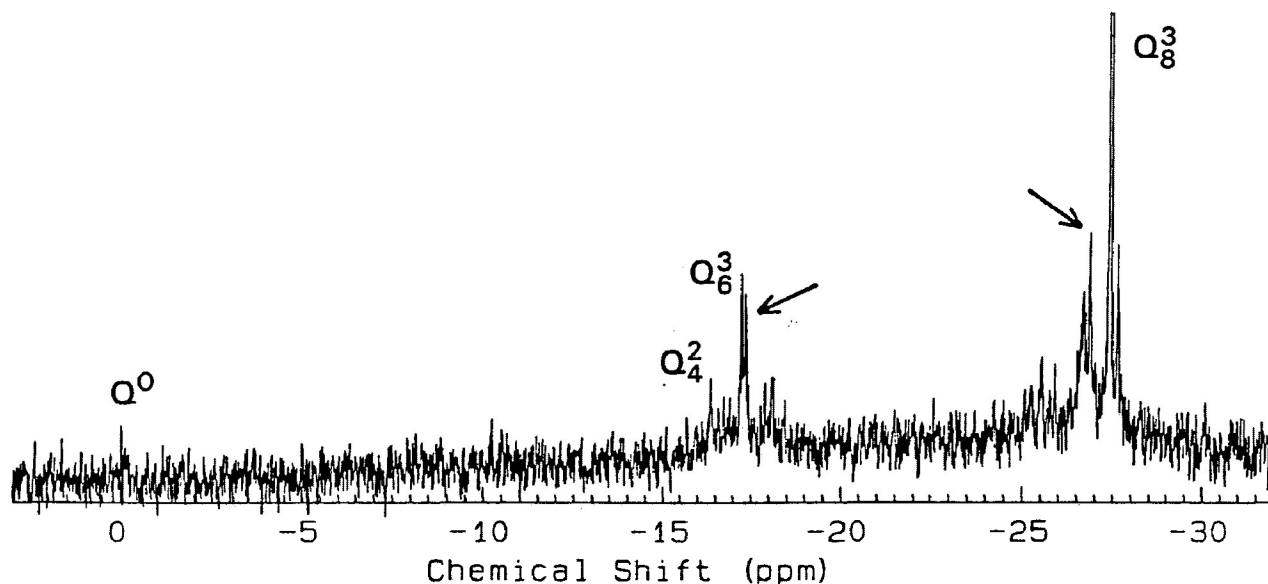


Figure 3 – 16c. ^{29}Si NMR spectrum of at 276.8 K of the equivalent solution that is 95% isotopically enriched in ^{29}Si . The newly observed singlet resonances at -16.9 and -26.5 ppm are indicated with arrows. The Q_8^3 resonance is 50% of actual height.

a protonated Q_6^3 structure (see Section 4.3). It is also possible that this resonance is occurring from a double five^[24] ring structure (which has been crystallized from TBA silicate solutions^[80]) or previously unreported single five or six ring structures.

An unusually large transient resonance, at -27.5 ppm was observed for a solution containing 2.0 mol kg⁻¹ SiO₂, 1.2 mol kg⁻¹ TBAOH and 40 wt% DMSO (Figure 3-17). This resonance was not observed at T > 280 K and as determined from an equivalent ²⁹Si enriched sample does not correspond to a symmetrical oligomer. Based on the intensity and chemical shift of this resonance and, the intensity and chemical shift of other resonances in the spectrum, the only known oligomer which possibly could correspond to this resonance is the pentacyclic nonamer (Table I-I). Resonances at -18.3 ppm and the cluster at ca.-16.5 ppm would also be assigned to the pentacyclic nonamer (resonances are slightly shifted from those in Table I-I).

3.2.7. Effect of Na⁺ Ions on TMA Silicate Solutions

Upon addition of sodium chloride (1.75 mol kg⁻¹) to pre-equilibrated TMA silicate solutions all ²⁹Si resonance immediately shifted up-frequency ca. 0.7 ppm. However, over a period of four hours, the Q_6^3 resonance slowly shifted back down-frequency. The concentration of Q_6^3 monotonically decreased within four hours after the NaCl addition (Figure 3-18). Subsequently, the distribution of silicate oligomers changed only slightly. The Q_6^3 resonance also shifted back down-frequency. However, the down-frequency shift was only ca. 0.20 ppm and occurred over a twenty minute time period.

3.2.8. Germanosilicates

Knight *et al.*^[23,85] reported that germanium could be substituted into Q_6^3

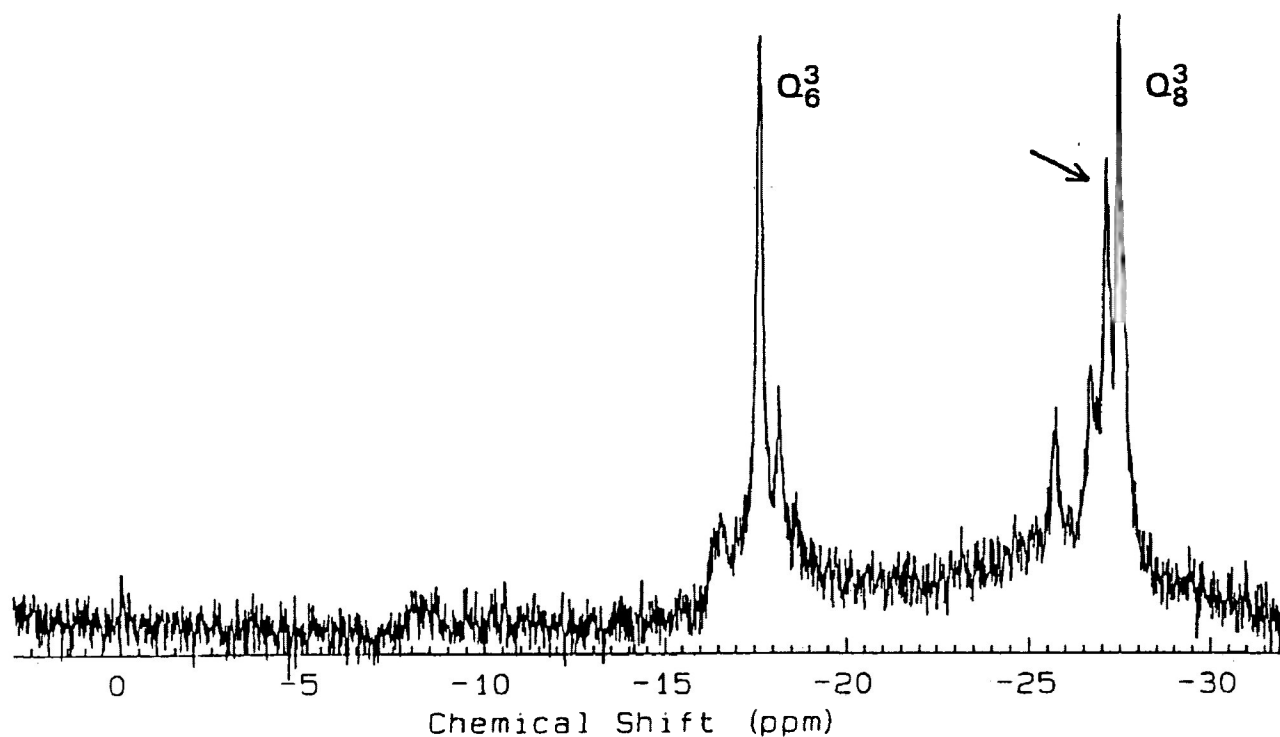


Figure 3-17. ^{29}Si NMR spectrum of a solution containing 2.0 mol kg^{-1} SiO_2 , 1.2 mol kg^{-1} TBAOH and 40wt% DMSO at 276.8 K. The spectrum was acquired over 4 hours following the boil-freeze-thaw procedure. The newly observed transient resonance at -27.5 ppm is indicated with an arrow.

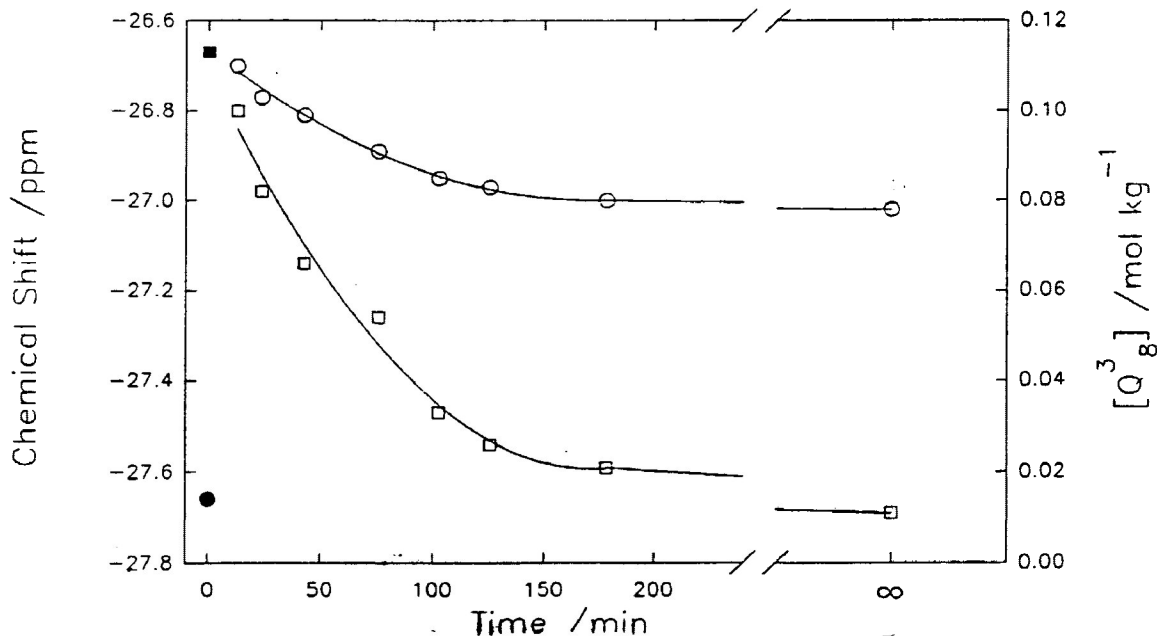


Figure 3-18. Chemical shift (O; externally referenced) and concentration (\square) of Q_8^3 as a function of time following addition of 1.74 mol kg^{-1} NaCl to a sample containing 1.0 mol kg^{-1} SiO_2 , 1.4 mol kg^{-1} TMAOH and 0.6 mol kg^{-1} TMAOI at 300 K. Closed symbol represents conditions prior to NaCl addition.

and Q_6^3 . We employed the boil-freeze-thaw procedure on a similar sample and observed the same ^{29}Si NMR line-splitting pattern for the Ge-substituted Q_8^3 as they described (Figure 3-19). We also added GeO_2 to a solution claimed to contain mostly double five ring;^[80] following the boil-freeze-thaw procedure, we observed line-splitting patterns similar to that shown in Figure 3-19. However, resonances corresponding to the Ge-substituted oligomer were broad. Attempts were also made to substitute germanium into the transient species mentioned in Section 3.2.5 and 3.2.6. No additional resonances were ever observed to indicate germanium substitution into these species. However, significant kinetic broadening was observed for all resonances other than those of Q_6^3 and Q_8^3 (Ge-substituted and non-substituted). Despite numerous attempts (including novel pulse sequences for low-frequency nuclei^[97]) the large quadrupolar moment of ^{73}Ge prevented detection of corresponding ^{73}Ge resonances.

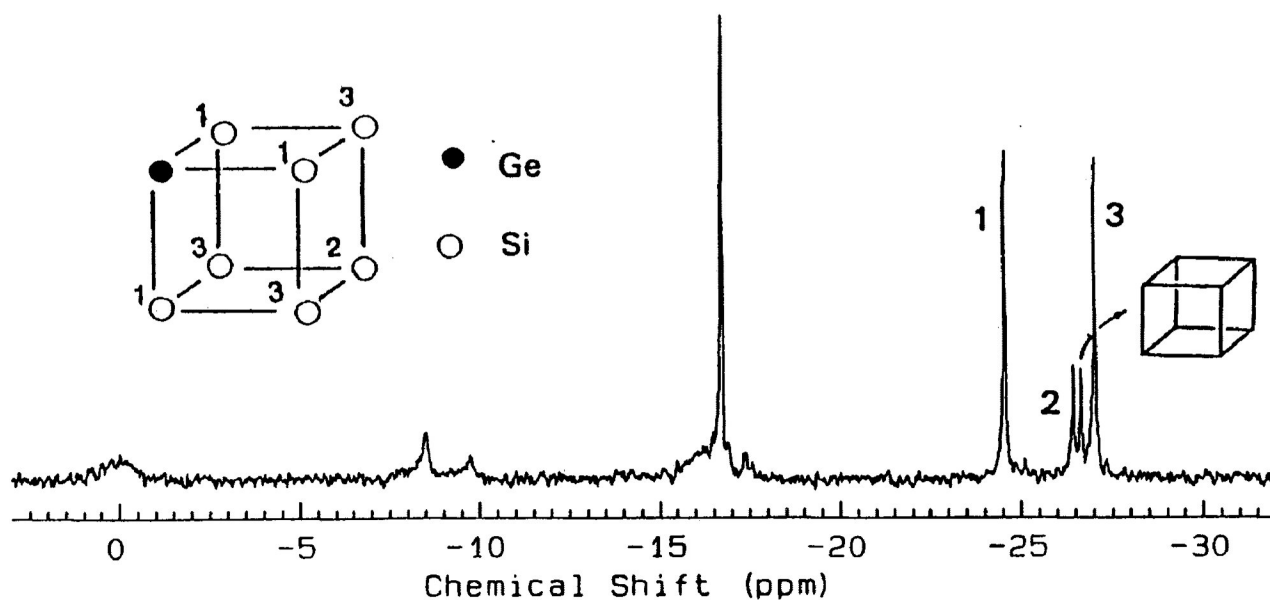


Figure 3-19. ^{29}Si NMR spectrum of a solution containing $0.55 \text{ mol kg}^{-1} \text{ SiO}_2$, $0.25 \text{ mol kg}^{-1} \text{ GeO}_2$, $1.1 \text{ mol kg}^{-1} \text{ TMAOH}$ and 18 wt% methanol at 285.0 K. The spectrum was acquired over 12 hours following the boil-freeze-thaw procedure. The resonances occurring at -24.2, -26.0 and -26.7 ppm correspond to the Ge substituted Q_8^3 .

3.3. Analysis of Kinetic Data

Regardless of silica, TMA⁺ or hydrogen ion concentration of each sample, Q₈³ was not detectable within the first few minutes following perturbation of equilibrium (see Section 3.2.4). This is important since determining the initial net rate of Q₈³ formation [(d[Q₈³]/dt)_{t=0}] depends on the concentration of Q₈³ being equal to or very near zero at t=0 (*i.e.*, R_{r (t=0)} ≈ 0).

The initial rate of Q₈³ formation was determined by fitting the first four data points in Figure 3-12, 3-13 and 3-14 to the second order polynomial [Q₈³] = a + bt + ct².^[98,99] Since there is no detectable Q₈³ at t=0, the constraint of a=0 was used. The initial rate, b, was extracted by taking the derivative of the fitted curve and setting t=0. Tables III-V, III-VI and III-VII contain (d[Q₈³]/dt)_{t=0} calculated in this way for each sample.

The initial reaction rate (d[Q₈³]/dt)_{t=0} was assumed to be dependent on the initial H⁺, Si^{IV} (dissolved SiO₂), and TMA⁺ ion concentrations as in Equation 3-4:

$$(d[Q_8^3]/dt)_{t=0} = k_{f0} [H^+]_0^a [Si^{IV}]_0^b [TMA^+]_0^c \quad (3-4)$$

where k_{f0} is the initial forward rate constant and a,b,c are reaction orders. The [Si^{IV}]₀ refers to the total dissolved silica concentration exclusive of Q₈³ and Q₆³ concentrations (see Section 4.4).

The dependence of (d[Q₈³]/dt)_{t=0} on [H⁺]₀ is determined from Figure 3-20. For the corresponding solutions, [Si^{IV}]₀^b and [TMA⁺]₀^c are constant and can be incorporated into a pseudo rate constant, k'_{f0}. Thus Equation 3-4 simplifies to:

$$(d[Q_8^3]/dt)_{t=0} = k'_{f0} [H^+]_0^a \quad (3-5)$$

The correlation of the data in Figure 3-20 is relatively linear over the pH range 13.23 to 13.57 yielding $a = 1.64 \pm 0.14$. The slight curve in the data is possibly due to small differences in the degree of silicate protonation over the pH range. Therefore the order, a , is slightly dependant on alkalinity. The change in slope above pH 13.6 probably indicates a substantial change in the degree of silicate protonation.

The dependence of $(d[Q_8^3]/dt)_{t=0}$ on $[TMA^+]_0$ was then determined from Figure 3-21. For the corresponding solutions, both $[H^+]_0$ and $[Si^{IV}]_0$ were constant. Therefore, $[H^+]_0$ and $[Si^{IV}]_0$ can be incorporated into a pseudo rate constant, k''_{f0} as in Equation 3-6. The order c was determined to be 0.362 ± 0.076 .

$$(d[Q_8^3]/dt)_{t=0} = k''_{f0} [TMA^+]_0^c \quad (3-6)$$

The effect of the initial Si^{IV} concentration on $(d[Q_8^3]/dt)_{t=0}$ (Figure 3-14) is calculated next. The initial pH and TMA^+ ion concentrations of each solution are known (Table III-VII). Equation 3-4 is rearranged and the log of each side taken:

$$\log((d[Q_8^3]/dt)_{t=0}) + 1.64 * \log[H^+]_0 - 0.362 * \log[TMA^+]_0 = \log(k_{f0}) + b * \log[Si^{IV}]_0$$

The order b is determined from the average of the slopes in Figure 3-22 to be 0.82 ± 0.25 for the pH range 13.23 to 13.57.

Equation 3-4 can now be quantified to:

$$(d[Q_8^3]/dt)_{t=0} = k_{f0} [H^+]^{1.64 \pm 0.14} [Si^{IV}]^{0.82 \pm 0.25} [TMA^+]^{0.362 \pm 0.076} \quad (3-7)$$

where, at 296.1 K, $\log(k_{f0}) = 19.89 \pm 0.35$ ($k_{f0} = 7.94 \times 10^{19} \text{ hr}^{-1}$ or

$2.21 \times 10^{16} \text{ s}^{-1}$) as determined from the average y-axis intercept of Figure 3-22.

Although general application of Equation 3-7 appears quite limited due to the narrow pH constraints (13.23 to 13.57), in fact, it applies to a wide range of solutions owing to the inherent buffering tendency of aqueous silicates. In the derivation of Equation 3-7 it was assumed that $R_r(Q_8^3) \approx 0$ for the first few hours of reaction. Since $R_r(Q_8^3)$ is most likely a function of $[Q_8^3]$, this assumption (particularly for solutions with low $\text{OH}^-:\text{Si}^{\text{IV}}$ ratio) may not be entirely accurate. Therefore, Equation 3-7 is only a best approximation of the true rate equation. Nonetheless, it does provide valuable insight into the kinetic role of various solution species in the formation of TMA associated Q_8^3 .

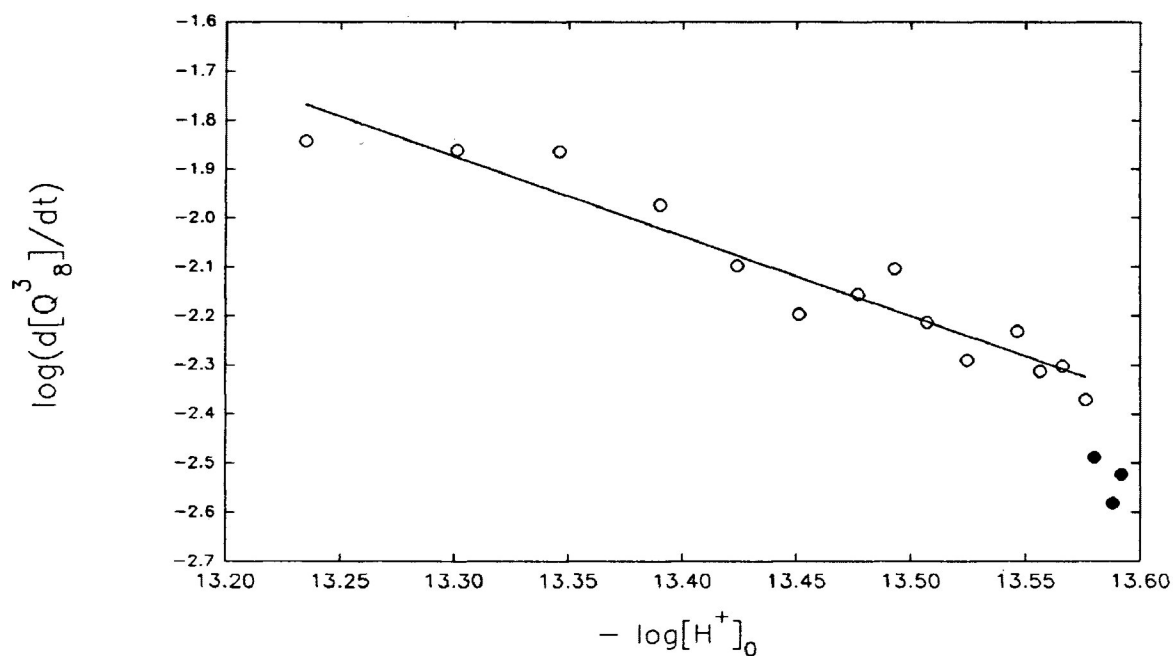


Figure 3 – 20. The dependence of the initial rate of Q_8^3 formation on initial $[H^+]$ for samples represented in Table IV – I. The slope of the line excluding points at $pH > 13.57$ is -1.64 ± 0.14 .

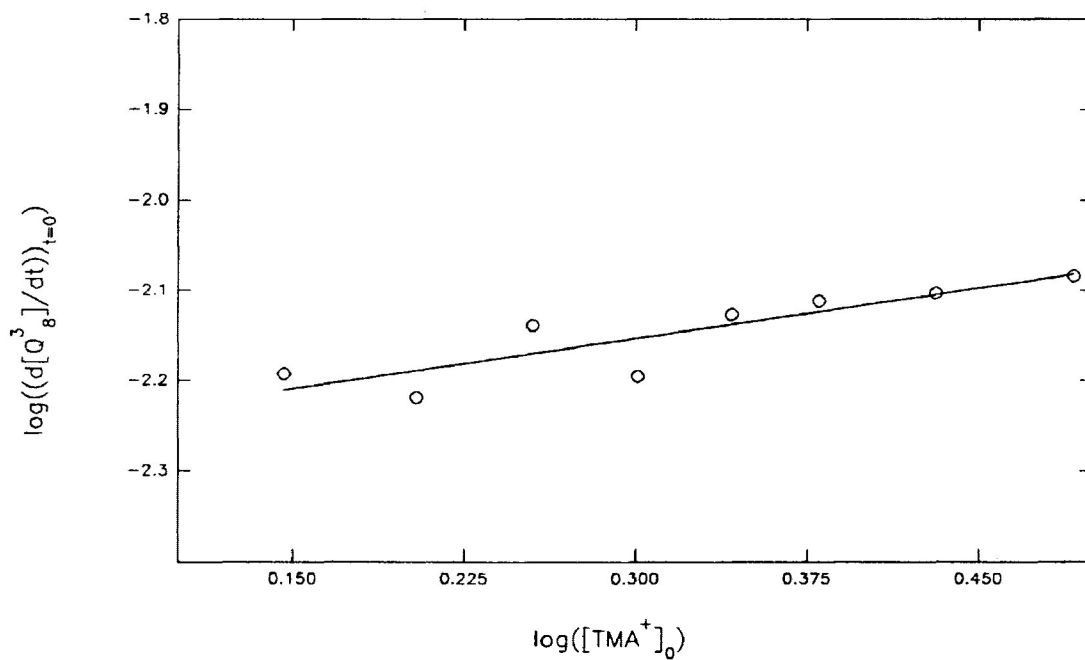


Figure 3 – 21. The dependence of the initial rate of Q_8^3 formation on the net $[TMA^+]$ for the samples represented in Table IV – III. The slope of the fitted line is 0.362 ± 0.076 .

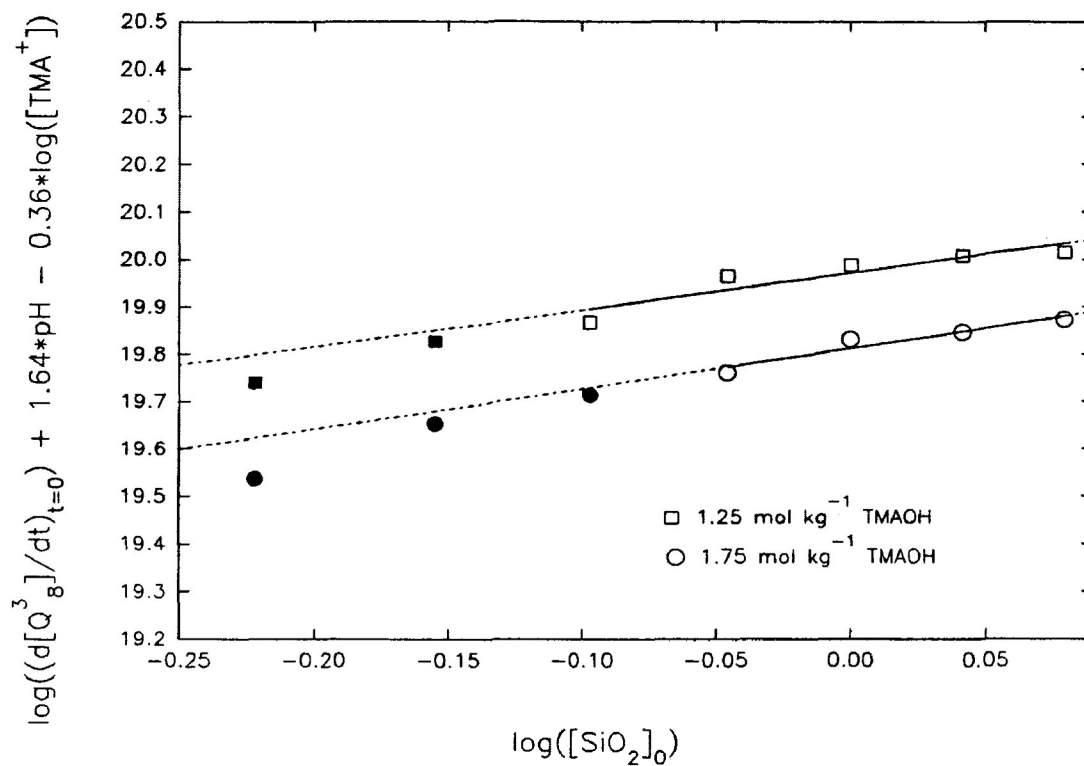


Figure 3 – 22. The dependence of $(d[Q_g^3]/dt)_{t=0} * [H^+]^{1.64} * [TMA^+]^{0.36}$ on $[SiO_2]_0$ for samples represented in Table IV – III and Figure 3 – 14. The solid line and open symbol covers the pH range between 13.23 to 13.57. Average slope of the lines is 0.82 ± 0.25 with an average y – axis intercept of 19.89 ± 0.22 .

Table III-V. Initial rate of Q_8^3 formation at 296.1 K and initial pH at 298 K for samples containing $1.0 \text{ mol kg}^{-1} \text{ SiO}_2$, $2.0 \text{ mol kg}^{-1} \text{ TMA}^+$ ions and various $\text{OH}:\text{Si}^{\text{IV}}$ ratios.

$\text{OH}:\text{Si}^{\text{IV}}$ ratio	$(d[Q_8^3]/dt)_{t=0}$ $/10^{-3} \text{ mol kg}^{-1} \text{ hr}^{-1}$	initial pH (± 0.010)
1:1	0.10 (estimate)	12.906
1.15:1	14.375 ± 0.12	13.235
1.2:1	$13.750 \pm .12$	13.301
1.25:1	13.625 ± 1.00	13.346
1.3:1	10.625 ± 0.7	13.390
1.35:1	8.000 ± 0.19	13.424
1.4:1	6.375 ± 1.80	13.451
1.45:1	7.000 ± 0.46	13.477
1.5:1	7.875 ± 0.94	13.493
1.55:1	6.125 ± 0.80	13.507
1.6:1	5.125 ± 0.84	13.525
1.7:1	5.875 ± 0.48	13.545
1.75:1	4.875 ± 0.66	13.556
1.8:1	5.000 ± 0.44	13.566
1.85:1	4.250 ± 0.53	13.576
1.9:1	3.250 ± 0.80	13.580
1.95:1	2.625 ± 0.81	13.588
2:1	3.000 ± 0.14	13.592

Table III-VI. Initial rate of Q_8^3 formation at 296.1 K for samples containing 1.4 mol kg⁻¹ TMAOH, 1.0 mol kg⁻¹ SiO₂ and various concentrations (0.0 to 1.7 mol kg⁻¹) of added TMACl. For all samples, initial pH was 13.451 ± 0.010.

[TMACl] /mol kg ⁻¹	(d[Q ₈ ³]/dt) _{t=0} /10 ⁻³ mol kg ⁻¹ hr ⁻¹
0.0	6.42 ± 0.40
0.2	6.04 ± 0.61
0.4	7.26 ± 0.55
0.6	6.37 ± 1.80
0.8	7.47 ± 1.04
1.0	7.74 ± 0.42
1.3	7.89 ± 0.75
1.7	8.25 ± 0.84

Table III-VII. Initial rate of Q_8^3 formation at 296.1 K and initial pH at 298 K for samples containing 1.25 and 1.75 mol kg⁻¹ TMAOH and various SiO₂ concentrations (0.6 to 1.2 mol kg⁻¹)

[SiO ₂] /mol kg ⁻¹	[TMAOH] /mol kg ⁻¹	(d[Q ₈ ³]/dt) _{t=0} /10 ⁻³ mol kg ⁻¹ hr ⁻¹	initial pH (±0.010)
0.6	1.25	1.500 ± 1.10	13.773
0.7	1.25	3.091 ± 0.50	13.624
0.8	1.25	4.732 ± 0.74	13.578
0.9	1.25	7.875 ± 0.55	13.477
1.0	1.25	13.625 ± 1.0	13.346
1.1	1.25	19.250 ± 2.1	13.268
1.2	1.25	26.275 ± 5.1	13.189
0.6	1.75	0.625 ± 0.12	13.936
0.7	1.75	1.102 ± 0.70	13.841
0.8	1.75	1.734 ± 0.52	13.758
0.9	1.75	3.768 ± 0.69	13.581
1.0	1.75	4.875 ± 0.66	13.556
1.1	1.75	6.625 ± 1.75	13.483
1.2	1.75	8.625 ± 2.5	13.430

Chapter IV. Discussion

4.1. Current Theories of Q_8^3 Stabilization

Aqueous silicate solutions which contain no organic solutes and are prepared with alkali-metal^[27-29] or long carbon chain tetraalkylammonium^[21] cations contain low concentrations of Q_8^3 . Short chain tetraalkylammonium cations (particularly TMA^+ cations) can favour Q_8^3 so that, under certain solution conditions, it is the only detectible oligomer.^[21] Clearly short chain TAA^+ ions play an important role in stabilizing Q_8^3 .

Hendricks *et al.*^[32] indicated that since the large size of TAA^+ ions precludes cation-anion pairing, TAA^+ ions have an indirect influence on Q_8^3 (see Section 1.2.5). When the size of TAA^+ ions is increased, water structuring increases; this would result in polymerization of silicate oligomers. However, by increasing the size of silicate oligomers, TAA^+ ions are forced closer together. Such "ion-crowding" produces an "electrostatic stress" which can only be relieved by a decrease in the size of silicate oligomers. It is the unique size of TMA^+ ions which induces enough water structuring – without producing significant "electrostatic stress" – to favour formation of Q_8^3 . There is no direct association between TMA^+ ions and Q_8^3 .

A second theory states that hydrated TMA^+ ions aid in arranging silicate species, thereby facilitating the formation of Q_8^3 (see Section 1.2.5).^[3,66] In solid^[42] and gaseous^[39-41] phases of hydrated $TMAOH$, the TMA^+ ions are enclosed in a polyhedral framework of hydrogen-bonded water molecules and hydroxide ions. It seems likely that in solution a similar polyhedral framework would also surround TMA^+ ions.^[47] Non-framework water molecules and hydroxide ions (*i.e.*, those that are not directly surrounding TMA^+ ions) would

most certainly exchange with framework water molecules and hydroxide ions. Since orthosilicate anions are of similar size and chemistry to that of water^[49] it is likely that they also exchange with the framework water molecules. Held in close proximity, the orthosilicate ions would readily condense into small oligomers which, owing to electrostatic attraction, would be associated with several TMA⁺ ions. Ultimately, cage-like oligomers would be formed with hydrated TMA⁺ ions surrounding them. Within a crystalline TMA silicate lattice, Q₈³ is associated with eight hydrated TMA⁺ ions; six are in close, octahedral association and the remaining two (for charge balance) reside outside this immediate shell.^[43] It has been proposed that in solution, a similar cluster is formed.^[3,50]

4.2. Evidence for a Direct Association Between Q₈³ and TMA Ions

For alkali-metal silicate solutions, when alkalinity is increased, *all* ²⁹Si resonances shift up-frequency.^[19,27] For TMA silicate solutions, Q₈³ and Q₆³ resonances shift down-frequency, whereas all other resonances shift up-frequency as alkalinity is increased (including Q³ resonances which shift only slightly up-frequency; Table III-I). The overall shift to higher frequencies is primarily due to deprotonation equilibria.^[27,28] At OH⁻:Si^{IV} ≥ 1:1, most Q³ centres are fully deprotonated. Therefore, increasing the OH⁻:Si^{IV} ratio should have little effect on Q³ chemical shifts, as was observed for all dominant Q³ resonances except those corresponding to Q₈³ and Q₆³. When the cation is changed from TMA⁺ to ETMA⁺, there is an up-frequency shift (relative to the monomer) of Q₈³ and Q₆³ resonances only. All other resonances, including Q³ resonances, are unaffected. This can be seen in Figure 1-2 (also note Figure 1 of reference 32). Therefore, Q₈³ and Q₆³ oligomers must have a unique

solution environment – quite unlike that of other silicate oligomers – in systems containing quaternary ammonium ions (especially TMA⁺ ions).

The cubic octamer is the only detectible oligomer in TMA silicate solutions which contain 90 wt% methanol (or DMSO). If a similar sample is prepared with NaOH instead of TMAOH, a gel forms (*i.e.*, all silicate oligomers are virtually insoluble; see Section 3.1.2). Silicate polyanions would not normally be expected to occur in solvent mixtures with low dielectric strengths. Hendricks *et al.*^[51] have suggested that the increased concentration of Q₈³ in TMA silicates containing organic solutes is due to "mass action equilibration" (*i.e.*, if the water in Equations 1.4 to 1.6 is replaced with organic molecules the equilibrium will shift to more polymerized oligomers) and to a reduction in the chemical potential of water (caused by hydrophobic water structuring by the organic solute). It appears however that this theory would only explain a general polymerizing effect (as observed with alkali-metal silicate solutions^[30]) not an effect which would favour one specific oligomer. It seems more likely that hydrated TAA⁺ ions act as a "mediator" between the methanol and specific silicate anions, *i.e.*, Q₈³.

In TMA silicate solutions the rate of Si-Si exchange between Q₈³ or Q₆³ and other silicate oligomers is significantly slower than exchange between all other silicate oligomers (Section 3.2.4). Upon addition of germanium, resonances corresponding to Q₈³, Q₆³ and their Ge-substituted analogues remain relatively sharp whereas all other silicate resonances – including other Q³ resonances – are broadened (Figure 3-19) due to rapid Si-Si exchange between silicate and germano-silicate spin sites. It would appear, therefore, that TMA⁺ ions impart special stability to Q₈³ and Q₆³ anions (and their Ge-

substituted analogues).

All resonances, except those of Q_8^3 and Q_6^3 , were significantly broadened by addition of 10^{-5} mol kg^{-1} Mn(II) (Table III-III and Figure 3-2). The Q_6^3 and Q_8^3 resonances were broadened, but not to the extent of other Q^3 resonances. The concentration of $MnCl_2$ is too low to induce exchange broadening of this magnitude. Therefore, Q_6^3 and Q_8^3 must somehow be shielded from interaction with Mn(II) ions.

We and other researchers^[50] have examined attenuated total reflection (ATR) infrared spectra of TMA silicates (Section 3.1.2). Groenen *et al.* suggest that, since the solution and crystalline phases of Q_8^3 have almost identical ATR infrared spectra, the structure of the immediate environment around the solution phase Q_8^3 is probably very similar to that in crystalline TMA silicates.^[50]

It is evident from the enhanced solubility of Q_8^3 in methanolic solutions and the chemical shift data that hydrated TMA^+ (and certain other hydrated TAA^+) ions directly associate with Q_8^3 and Q_6^3 . These hydrated TMA^+ ions evidently provide a protective shell that impedes Si-Si chemical exchange and paramagnetic relaxation. Therefore, the water structuring/ion crowding theory proposed by Hendricks *et al.*^[32] appears to be inconsistent with the results. As well, the theory whereby TMA^+ ions surround cage-like silicate oligomers does not attempt to explain the nature of the $TMA^+-Q_8^3$ association. Groenen *et al.*^[50] have described TMA^+ -associated Q_8^3 as a $Q_8^3/TMA^+/H_2O$ cluster. We have also adopted this nomenclature.

4.3. Nature of the Solution Phase Q_8^3 (and Q_6^3)/TMA⁺/H₂O Cluster

Increasing the TMA⁺ ion concentration has little effect on the chemical shift of Q_8^3 and Q_6^3 resonances (Section 3.1.2). Therefore, such TMA⁺ stabilized polyanions must contain a specific number of TMA⁺ ions beyond which none can associate, even weakly. Increasing the alkalinity, however, causes a unique down-frequency shift of the Q_8^3 and Q_6^3 resonances (Section 3.1.2 and Figure 3-7b) unrelated to silicate protonation equilibria. This may indicate formation of an electric double layer – OH⁻...TMA⁺... Q_8^3 – about the Q_8^3 and Q_6^3 polyanions.

The concentration of Q_8^3 /TMA⁺/H₂O and Q_6^3 /TMA⁺/H₂O clusters is dependant on TMA⁺ ion concentration but not on the alkalinity at OH⁻:Si^{IV} ≥ 1:1 (Figure 3-1a and 3-1b), *i.e.*, unlike the concentrations of all other silicate oligomers which *are* pH dependent.^[27-29] Hydrated TMA⁺ ions are the limiting reagent in the formation of the clusters. However as the OH⁻:Si^{IV} ratio is decreased from 1:1, the concentration of Q_8^3 /TMA⁺/H₂O clusters decreases (Figure 3-7a). Under these low alkalinity conditions, some of the terminal Si-O⁻ groups become protonated thereby weakening the electrostatic attraction between Q_8^3 and hydrated TMA⁺ ions. Indeed, at OH⁻:Si^{IV} ≤ 0.3:1 the Q_8^3 resonance is not observed.

At OH⁻:Si^{IV} ratios from 0.3:1 to 1:1 at least four resonances occur at (more or less) regular intervals down-frequency of the Q_8^3 resonance (Figure 3-7b). At least two of the four species are symmetrical (Figure 3-9b). The first two down-frequency resonances have previously been attributed to double five and double six ring structures.^[4,78,79] However, it seems unlikely that resonances corresponding to larger double six ring structures (which, in any

case, only could account for two of the four resonances) would occur at regular intervals; the double five ring resonance has been predicted to occur well up-frequency of the Q_8^3 resonance.^[24] As well, following boil-freeze-thaw perturbation, the intensity ratio of the Q_8^3 resonance to the first down-frequency side peak remains constant whereas the intensity of all other resonances decreases (Figure 3-16a). If the down-frequency side peak corresponded to larger, less rigid^[24] double ring structures^[78,79] it would not be expected to evolve at the same rate as Q_8^3 . Therefore, it seems most likely that these resonances correspond to various protonated states of the $Q_8^3/TMA^+/H_2O$ cluster. Indeed, as the degree of protonation of a silicate oligomer increases the corresponding resonance(s) is expected to shift down-frequency.^[24] The protons would reside inside the hydrated TMA shell and would be exchanging between silicate centres very rapidly (*i.e.*, on the NMR time scale). By analogy it is probable that the newly observed singlet resonance at -16.9 ppm (Figure 3-16b) corresponds to a protonated $Q_8^3/TMA^+/H_2O$ cluster.

In the one experiment that was performed at elevated pressure, the resonances down-frequency of Q_8^3 decreased in intensity. This might be the result of accelerated Si-Si exchange between the protonated and unprotonated $Q_8^3/TMA^+/H_2O$ clusters (*i.e.*, kinetic broadening). However, there is insufficient data to state this implicitly.

The concentration of $Q_8^3/TMA^+/H_2O$ decreases and its resonance shifts up-frequency as X_{TEA^+} or X_{TBA^+} is increased (Section 3.1.3. and Figures 3-3b and 3-4b). These TAA⁺ ions do not favour Q_8^3 (at this concentration^[100]) probably because their large size (*i.e.*, small charge/radius ratio) hinders significant electrostatic association with silicate oligomers. The limiting mole

fraction (Table III-IV) is therefore indicative of the minimum concentration of TMA⁺ ions required to stabilize Q₈³/TMA/H₂O. The up-frequency shift of Q₈³/TMA⁺/H₂O resonance (Figure 3-3b) as X_{TEA⁺} is increased is possibly caused by hydrated TEA⁺ ions exchanging with hydrated TMA⁺ ions (which are surrounding Q₈³) and "relaxing" the TMA shell (*i.e.*, the shell becoming less dense).

The stability of Q₈³/TMA⁺/H₂O clusters was examined by adding alkali-metal cations to TMA silicate solutions (Figure 3-3a and 3-4a). Previously, Keijsper and Post^[64] observed that the rate of Si-Si exchange, at equilibrium, from other silicate oligomers to Q₈³ is unaffected by addition of NaCl. Since Na⁺ ions decrease the concentration of Q₈³/TMA⁺/H₂O clusters (Figure 3-3a, 3-4a, 3-5 and 3-6), Na⁺ ions therefore must increase the rate of Q₈³/TMA⁺/H₂O dissociation. The limiting mole fraction for Na⁺ and Cs⁺ ions is smaller than for TBA⁺ and TEA⁺. Alkali-metal cations have a larger charge/radius ratio than TAA⁺ ions and thus probably have a stronger electrostatic attraction for Q₈³. Therefore, associated TMA⁺ ions are displaced and the Q₈³/TMA⁺/H₂O clusters are destabilized.

Investigators^[36,55] had previously suggested that since the Q₈³ resonance shifts up-frequency as the Q₈³ concentration decreases, the chemical shift of the Q₈³ resonance is related to Q₈³ stability. However, immediately following addition of solid NaCl to TMA silicate solutions, the Q₈³ resonance shifts up-frequency 0.7 ppm (*i.e.*, towards the chemical shift for Q₈³ in the absence of TMA⁺ ions) and then slowly shifts back down-frequency as the concentration of Q₈³/TMA⁺/H₂O decreases (Figure 3-18). For a Na silicate solution, the Q₈³ resonance is at *ca.* -26 ppm relative to the monomer. When the NaCl is

added, Na^+ ions immediately associate with the $\text{Q}_8^3/\text{TMA}^+/\text{H}_2\text{O}$ cluster causing the up-frequency shift. The association/dissociation of Na^+ ions with the cluster must be rapid on the NMR time scale in order for there to be a single, sharp Q_8^3 resonance. Over the next four hours, Na^+ ions dissociate Q_8^3 clusters into other oligomers which, in turn, "ion pair"^[31] with an increasing fraction of the added Na^+ ions. Consequently there are fewer Na^+ ions available to associate with the $\text{Q}_8^3/\text{TMA}^+/\text{H}_2\text{O}$ clusters and the time-averaged Q_8^3 resonance gradually moves back down-frequency.

4.4. Mechanism of $\text{Q}_8^3/\text{TMA}^+/\text{H}_2\text{O}$ Cluster Formation

In TMA silicate solutions the Si-Si exchange rate between $\text{Q}_8^3/\text{TMA}^+/\text{H}_2\text{O}$ or $\text{Q}_6^3/\text{TMA}^+/\text{H}_2\text{O}$ and other silicate oligomers is relatively slow compared to the exchange rate between all other silicate oligomers (Section 2.3.4). We studied the initial rate of $\text{Q}_8^3/\text{TMA}^+/\text{H}_2\text{O}$ formation $(d[\text{Q}_8^3]/dt)_{t=0}$ using the boil-freeze-thaw procedure (Section 2.3.4).

Immediately after the sample has been thawed, the Q_8^3 and Q_6^3 resonances are not observed and, instead, there is a wide distribution of silicate oligomers^[34] (Figure 3-10). Addition of large amounts of NaCl to TMA silicate solutions reportedly^[64] has no effect on the Si-Si exchange rate between small silicate oligomers which is similar to that of Na silicate solution systems (see Section 3.2.4).^[29] Accordingly, when boil-freeze-thaw experiments were performed on TMA silicate and sodium silicate solutions, there was a similar distribution of oligomers within the first few minutes after thawing (see Section 3.2.4). Therefore, the Si-Si exchange rate of small oligomers is relatively independent of the concomitant cation.

Clearly, the $\text{Q}_8^3/\text{TMA}^+/\text{H}_2\text{O}$ cluster cannot form from smaller oligomers and

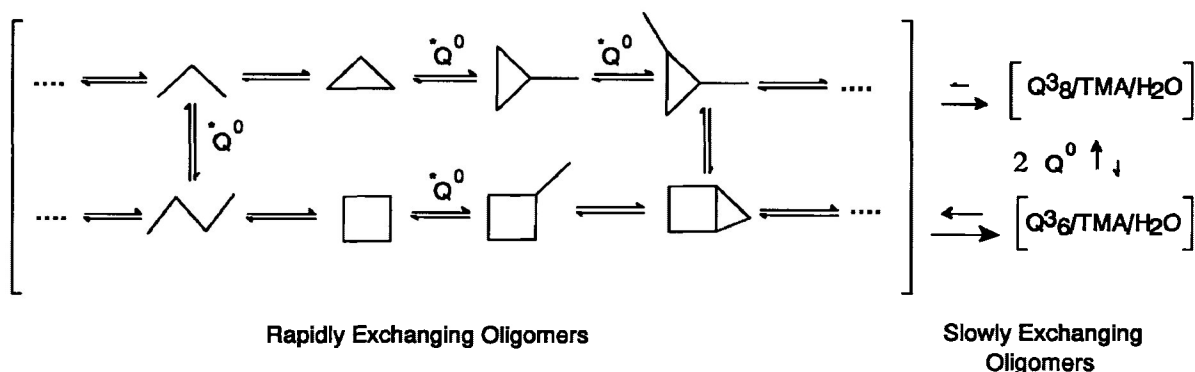
"free" TMA^+ ions (*i.e.*, TMA^+ ions which are not associated with cluster structures) in a single elementary step. It has been suggested^[54] that Q_6^3 is a major intermediate in the formation of Q_8^3 because it is a stable oligomer and only requires two additional monomer units to yield Q_8^3 . However, if $\text{Q}_6^3/\text{TMA}^+/\text{H}_2\text{O}$ cluster is indeed a major precursor, the greatest rate of $\text{Q}_8^3/\text{TMA}^+/\text{H}_2\text{O}$ cluster formation would occur at or after the $\text{Q}_6^3/\text{TMA}^+/\text{H}_2\text{O}$ cluster has reached its maximum concentration. In all our experiments, the $\text{Q}_6^3/\text{TMA}^+/\text{H}_2\text{O}$ concentration was greatest two to six hours after boil-freeze-thaw perturbation, whereas, the fastest rate of $\text{Q}_8^3/\text{TMA}^+/\text{H}_2\text{O}$ formation was at $t=0$ (*i.e.*, when there was negligible $\text{Q}_6^3/\text{TMA}^+/\text{H}_2\text{O}$ and $\text{Q}_8^3/\text{TMA}^+/\text{H}_2\text{O}$).

It seems unlikely that hydrated TMA^+ ions would yield only the $\text{Q}_6^3/\text{TMA}^+/\text{H}_2\text{O}$ and $\text{Q}_8^3/\text{TMA}^+/\text{H}_2\text{O}$ clusters. They would be expected to aggregate about other cage-like oligomers and form analogous hydrophobic shells with other oligomers. However, other oligomers probably lack the appropriate size, geometry and/or electrostatic attraction for the shell to be sufficiently compact to yield maximum stability. The transient species described in Section 3.2.5 (*i.e.*, bridged cyclic tetramer and tricyclic octamer) probably owe their moderately enhanced stability (relative to Q_8^3 and Q_6^3) to being relatively rigid and having nearly spherical symmetry.

The rate of $\text{Q}_8^3/\text{TMA}^+/\text{H}_2\text{O}$ cluster formation is dependant on $[\text{H}^+]^{1.64 \pm 0.14}$ in the pH range of 13.23 to 13.57 (Section 3.2.4 and 3.3). This is consistent with the mechanism proposed by Kinrade and Swaddle^[29] whereby polymerization is mediated by formation of a neutral silicate centre (see Section 1.2.4). The rather high reaction order with respect to $[\text{H}^+]$ is indicative of the degree of deprotonation of silicate centres at these elevated pH levels.

Since the rate of $Q_8^3/TMA^+/H_2O$ cluster formation is approximately first order with respect to the initial Si^{IV} concentration ($[Si^{IV}]^{0.82 \pm 0.25}$), it is apparent that only one silicon centre is involved in this rate determining "activation" step.

That the rate of $Q_8^3/TMA^+/H_2O$ cluster formation also depends on the TMA^+ ion concentration (order = 0.36 ± 0.08) would suggest it is protonation of cage-like polyanions having partial (or expanded) TMA shells that is rate determining. The protective environment of these species might help in maintaining the activated site long enough to attract nearby silicate anions (note the stability of the protonated Q_8^3 and Q_6^3 clusters). The $Q_8^3/TMA^+/H_2O$ cluster, once formed, has optimum protection from its hydrophobic hydration shell and thus is favoured by the equilibrium system given sufficient TMA^+ concentrations. The $Q_8^3/TMA^+/H_2O$ cluster has somewhat lower stability, and yet it is too stable to be an important direct precursor in the formation of $Q_8^3/TMA^+/H_2O$ clusters. The general mechanism can be seen in Reactions 4-1.



Reaction 4-1. Reaction scheme depicting the various Si-Si exchange rates between oligomers in a TMA silicate solution.

4.5. Implications to the Mechanism of Zeolite Synthesis

Two theories have been proposed for zeolite synthesis (Section 1.3.2). In the secondary building unit (SBU) theory, large ring or cage aluminosilicate species (similar to those in zeolite frameworks) exist in solution. These species could provide both the nucleation point and, by their sequential condensation, the mode of growth. For the cation templating theory, the zeolite framework is dictated by the size and shape of a hydrated cation. Zeolite synthesis could be initiated by the exchange of water molecules (around the hydrated cation) for aluminate or silicate anions. The anions would be held in position for sufficient time to form siloxy or alumino-siloxy linkages which could ultimately result in nucleation and growth of a zeolite.

The reported existence of soluble double five and double six ring oligomers has been used to promote the feasibility of the SBU theory. However, for a solution claimed to contain mostly double five ring^[80] we have shown (by Ge substitution; Section 3.2.8) that the solution actually contains Q_8^3 . As well, for solutions with $OH^-:Si^{IV} \leq 1:1$ two resonances down-frequency of Q_8^3 were previously attributed to double five and double six ring structures.^[4,78,79] We have shown that these resonances and possibly others are simply due to protonated states of Q_8^3 (Section 4.3).

We have shown that in solution, hydrated TAA^+ (particularly TMA^+) ions directly associate with certain silicate oligomers (Section 4.2). Our results therefore support the cation templating theory.

4.6. Conclusions

We have demonstrated that hydrated TAA⁺ (particularly TMA⁺) ions directly associate with certain silicate oligomers (*i.e.*, Q₈³ and Q₆³). TMA⁺ ions form a protective shell around these oligomers (possibly similar to the solid state Q₈³(and Q₆³)/TMA⁺/H₂O clusters) which stabilizes these oligomers by impeding Si-Si exchange and restricting interaction with paramagnetic ions. As well, the shell of hydrated TAA⁺ ions acts as a "mediator" between organic solutes and Q₈³ thus increasing the concentration of Q₈³ in solutions containing organic solutes.

For TMA silicate solutions, we have determined that the initial rate of Q₈³ formation is proportional to [H⁺]^{1.64}, [Si^{IV}]^{0.82} and [TMA]^{0.36} for the pH range of 13.23 to 13.57. Possibly, the rate determining step is protonation of cage-like oligomers having partial a TMA shell. As well, the Si-Si exchange rate of small silicate oligomers is similar to that determined for Na silicate solutions systems.

The unique down-frequency shift of Q₈³ and Q₆³ resonances as alkalinity is increased is possibly due to an electric double layer – OH⁻...TMA⁺...Q₈³ – about the Q₈³ and Q₆³ polyanions.

At OH⁻:Si^{IV} ≥ 1:1, TMA⁺ ions are the limiting reagent in the formation of Q₈³. However, at OH⁻:Si^{IV} < 1:1 the electrostatic attraction between TMA⁺ ions and Q₈³ is weakened and thus the concentration of Q₈³ cluster decreases. The shell is still electrostatically strong enough to stabilize protonated Q₈³ clusters. At least four resonances down-frequency of the Q₈³ resonance most likely correspond protonated Q₈³ clusters.

Transient resonances (observed following the boil-freeze-thaw procedure

for TMA silicate solutions) at -26.2 and -16.4 ppm have been attributed to the doubly bridged four ring oligomer, as well, resonances at -27.7 and -18.75 ppm assigned to the tricyclic octamer (Figure 3-15). For a TBA silicate solution, two transient singlet resonances at -16.9 and -26.5 ppm (Figure 3-16c) most likely correspond to a protonated Q_8^3 cluster and the tetrahedral tetramer, respectively.

Alkali-metal cations increase the rate of Q_8^3 dissociation but have little effect on the rate of Q_8^3 formation. Therefore, alkali-metal cations displace TMA^+ ions which are surrounding Q_8^3 and destabilize the $Q_8^3/TMA^+/H_2O$ cluster. As well, we have shown that the chemical shift of the Q_8^3 resonance is not related to its stability (Section 3.1.2).

Chapter V. Future Studies

5.1. Kinetics of Q_8^3 Formation

The boil-freeze-thaw procedure employed at various temperatures can be used to investigate ΔS^\ddagger , ΔH^\ddagger and ΔG^\ddagger of formation of Q_8^3 for TMA silicate solutions. The pH of equivalent non-deuterated solutions must be measured for each temperature. Solutions used must be carefully chosen so that the rate of Q_8^3 formation can be easily monitored.

TAA silicate solutions containing organic solutes favour Q_8^3 . The boil-freeze-thaw procedure can also be employed to investigate the Si-Si exchange kinetics of oligomers which exist in these solutions. Such kinetic studies are vital to the understanding of the structure directing roles of cations in solution and zeolite synthesis mixtures.

5.2. Metal Substitution in Silicate Oligomers

Metals such as Ni, W, Cr, Fe, Ti, Mo, Ga, Ge, Zn, Mg and Co can be incorporated into the framework of zeolite-like structures.^[58] It is therefore plausible that these metals can also exchange with soluble silicate oligomers. In a preliminary study we examined silicate solutions containing Sn, V, Ga, Pb, As, P, Zn and Ti. So far we have observed new ^{29}Si resonances for solutions containing Sn^{IV} ions. Tin-117 resonances can be easily observed since the nucleus is dipolar and relatively NMR sensitive. Therefore we can conduct a comprehensive speciation/kinetic study by ^{29}Si and ^{117}Sn NMR. Resonances of other nuclei such as ^{207}Pb and ^{31}P are readily observable since the nuclei are dipolar as well. Therefore ^{207}Pb or ^{31}P NMR can also be used to help investigate new silicate oligomers.

5.3. Identification of Silicate Anions

Metal substitution into silicate oligomers can aid in the identification of silicate species^[23,85] (*i.e.*, by observing the line-splitting patterns in ²⁹Si spectra). Unassigned transient resonances described in Section 3.2.5 and 3.2.6 could possibly be identified by substituting Ge into the oligomer and observing the line-splitting pattern in the ²⁹Si NMR spectra. In a preliminary investigation the resonance attributed to the tetrahedral tetramer^[24] could not be confirmed by metal substitution because rapid Si-Si exchange and low solubility of Ge^{IV} in Na silicate solutions precluded observation any new resonances.

5.4. Investigation of Protonated Q₈³ Clusters

We have demonstrated that there are at least four resonances down-frequency of the Q₈³ resonance in solutions with OH⁻:Si^{IV} ≤ 1:1. At least two of these resonances are singlets. Using ²⁹Si isotopically enriched silica, it could be possible to show that the other two are also singlets. We have also shown that by using TAA⁺ (other than TMA⁺) ions and organic solutes the first down-frequency resonance can be enhanced. Since Ge readily substitutes into Q₈³, Ge should also readily substitute into protonated states of Q₈³. However, at OH⁻:Si^{IV} ≤ 1:1 the Si-Si exchange is rapid between Q₈³ and other oligomers. Therefore, low temperatures and high SiO₂ concentrations must be used to investigate these particular Ge-substituted analogues.

References:

1. Cotton, F.A.; Wilkinson, G. *Advanced Inorganic Chemistry*, 5thed.; Wiley: Toronto; **1988**.
2. Sjöberg, S.; Öhman, L.; Ingri, N. *Acta Chem. Scand., Ser. A* **1985**, 39, 93.
3. McCormick, A.V.; Bell, A.T. *Cat. Rev. Sci. Eng.* **1989**, 31, 97.
4. Bell, A.T. in *Zeolite Synthesis*, ACS Symp. Ser. 398; ACS: Washington; **1989**, pp. 66-82.
5. Knight, C.T.G. *J. Chem. Soc., Dalton Trans.* **1988**, 1457.
6. Engelhardt, G.; *et al.* *Z. Chem.* **1974**, 14, 109.
7. Lentz, C.W. *Inorg. Chem.* **1964**, 3, 574.
8. Dent-Glasser, L.S.; Sharman, S.K. *Br. Polym. J.* **1974**, 6, 283.
9. Hoebbel, D.; Garzo, G.; Engelhardt, G.; Jancke, H.; Franck, P.; Wieker, W. *Z. Anorg. Allog. Chem.* **1976**, 424, 115.
10. Wieker, W.; Hoebbel, D. *Z. Anorg. Allog. Chem.* **1969**, 365, 139.
11. Thiol, E.; Wieker, W.; Stade, H. *Z. Anorg. Allg. Chem.* **1965**, 340, 261.
12. Iler, R.K. *Coll. Interface Sci.* **1980**, 75, 138.
13. Garzo, G.; Hoebbel, D.; Vargha, A.; Ujszaszi, K. *J. Chem. Soc., Dalton Trans.* **1984**, 1857.
14. Calhoun, H.P.; Masson, C.R. *J. Chem Soc., Dalton Trans.* **1980**, 1282.
15. Garzo, G.; Vargha, A.; Szekely, T.; Hoebbel, D. *J. Chem. Soc., Dalton Trans.* **1980**, 2068.
16. Freund, E. *Bull. Soc. Chim. Fr.* **1973**, (7-8), 2238, 2244.
17. Beard, W.C. *Adv. Chem. Ser.* **1973**, 121, 162.
18. Marinangeli, A.; Morelli, M.A.; Simoni, R.; Bertulazza, A. *Can. J. Spectr.* **1978**, 23, 174.

19. Harris, R.K.; Knight, C.T.G. *J. Chem. Soc., Faraday Trans. 2*. **1983**, *79*, 1525, 1539.
20. Harris, R.K.; Knight, C.T.G. *J. Mol. Struct.* **1982**, *78*, 273.
21. Harris, R.K.; Knight, C.T.G.; Hull, W.G. *J. Am. Chem. Soc.* **1981**, *103*, 1577.
22. Harris, R.K.; Jones, J.; Knight, C.T.G.; Pawson, D. *J. Mol. Struct.* **1980**, *69*, 95.
23. Knight, C.T.G.; Kirkpatrick, R.J.; Oldfield, E. *J. Am. Chem. Soc.* **1986**, *108*, 30.
24. Kinrade, S.D.; Swaddle, T. W. *Inorg. Chem.* **1988**, *27*, 4253.
25. Janes, N.; Oldfield, E. *J. Am. Chem. Soc.* **1986**, *108*, 6769.
26. Marsmann, H. *NMR* **1981**, *17*, 65.
27. Engelhardt, G.; Zeigan, D.; Jancke, H.; Hoebbel, D.; Wieker, W. *Z. Anorg. Allg. Chem.* **1975**, *418*, 17.
28. McCormick, A. V.; Bell, A. T.; Radke, C. J. *Stud. Surf. Sci. Catal.* **1986**, *28*, 247; *Zeolites* **1987**, *7*, 183.
29. Kinrade, S.D.; Swaddle, T.W. *Inorg. Chem.* **1988**, *27*, 4259.
30. Kinrade, S.D.; Maa, K. unpublished results.
31. Kinrade, S.D.; Pole, D.L. *Inorg. Chem.* **1992**, *31*, 4558.
32. Hendricks, W.M.; Bell, A.T.; Radke, C.J. *J. Phys. Chem.* **1991**, *95*, 9513.
33. McCormick, A.V.; Bell, A.T.; Radke, C.J. *J. Chem. Phys.* **1989**, *93*, 1733.
34. Hoebbel, D.; Garzo, G.; Engelhardt, G.; Vargha, A. *Z. Anorg. Allg. Chem.* **1982**, *494*, 31.
35. Hasegawa, J.; Kuroda, K.; Kato, C. *Bull. Chem. Soc. Japan.* **1986**, *59*, 2279.
36. Thouvenot, R.; Hervé, G.; Guth, J.L.; Wey, R. *Nouv. J. Chim.* **1986**, *10*, 479.

37. Schlenkrich, F.; Beil, E.; Rademacher, O.; Scheler, H. *Z. Anorg. Allg. Chem.* **1984**, *511*, 41.
38. Kinrade, S.D.; DelNin, J. unpublished results.
39. Yang, X.; Castleman, A.W. *J. Phys. Chem.* **1990**, *94*, 8500.
40. Wei, S.; Shi, Z.; Castleman, A.W. *J. Phys. Chem.* **1991**, *94*, 3268.
41. Yang, X.; Castleman, A.W. *J. Am. Chem. Soc.* **1989**, *111*, 6845.
42. McMullan, R.K.; Mak, T.C.; Jeffrey, G.A. *J. Chem. Phys.* **1966**, *44*, 2339.
43. Smolin, Yu. I.; Shepelev, Yu. F.; Domes, R.; Hoebel, D.; Wieker, W. *Kristallografiya* **1979**, *24*, 38.
44. Chang, C.D.; Bell, A.T. *Cat. Letters.* **1991**, *8*, 305.
45. Franks, F.; Smith, H.T. *Trans. Faraday Soc.* **1967**, *63*, 2586.
46. Hecht, D.; Tadesse, L.; Walters, L. *J. Am. Chem. Soc.* **1992**, *114*, 4336.
47. van der Berg, J.P.; de Jong-Versloot, P.C.; Keijsper, J.; Post, M.F.M. *Studies in Surface Science and Catalysis*; Elsevier: Amsterdam, **1987**, pp. 85.
48. (a) Ramanathan, P.S.; Krishnan, C.V.; Friedman, H. *J. Solution Chem.* **1972**, *1*, 237. (b) Jolicoeur, C.; Philip, P.R.; Perron, G.; Ledac, P.A.; Desnoyers, J.E. *Can. J. Chem.* **1972**, *50*, 3167.
49. Iler, R.K. *The Chemistry of Silica*; Wiley: New York, **1979**.
50. Groenen, K.J.J.; Emeis, C.A.; van den Berg, J.P.; de Jong-Versloot, P.C. *Zeolites* **1987**, *7*, 474.
51. Hendricks, W.M.; Bell, A.T.; Radke C.J. *J. Phys. Chem.* **1991**, *95*, 9519.
52. Oldfield, E. *J. Chem. Soc., Chem. Commun.* **1986**, 66.
53. Kinrade, S.D.; Whatley, S. unpublished results
54. Pole, D.L. Honours thesis, Lakehead University, Canada, 1991.
55. Engelhardt, G.; Rademacher, O. *J. Mol. Liq.* **1984**, *27*, 125.

56. Knight, C.T.G.; Kirkpatrick, R.J.; Oldfield, E. *J. Chem. Soc., Chem. Comm.* **1986**, 66.
57. Szostak, R. *Molecular Sieves. Principals of Synthesis and Identification*. Van Nostrand Reinhold: New York, **1989**, pp. 40-45.
58. Szostak, R. *Molecular Sieves. Principals of Synthesis and Identification*; Van Nostrand Reinhold: New York, **1989**, pp. 205.
59. Ueda, S.; Kageyama, N.; Koizumi, M. *Proc. of the 6th International Zeolite Conference*; Butterworths: UK, **1983**, pp. 905.
60. Wenqin, P.; Ueda, S.; Koizumi, M. *Proc. of the 7th International Zeolite Conference*; Elsevier: Tokyo, **1986**, pp. 177.
61. Barrer, R.M. *The Hydrothermal Chemistry of Zeolites*; Academic Press: London, **1983**.
62. Dwyer, F.G.; Chu, P. *J. Catal.* **1979**, *50*, 263.
63. Knight, C.T.G. Ph.D. thesis, University of East Anglia, UK. **1982**.
64. Keijsper, J.J.; Post, M.F.M. *Zeolite Synthesis*. (196th National Meeting of the American Chemical Society); ACS: Washington, **1989**, pp. 28.
65. Knight, C.T.G. *Zeolites*. **1990**, *10*, 140.
66. Wijnen, P.; Beelen, T.; DeHaan, J.; van de Ven, L.; van Santen, R. *Colloids and Surfaces*. **1990**, *45*, 255.
67. Flanigen, E.M. in: *Proc. of the 5th International Zeolite Conference*; Rees. L.U.C. ed.; Heyden: London, **1980**, pp. 760.
68. Guth, J.; Caultet, P.; Jacques, P.; Wey, R. *Bull. Soc. Chim. Fr.* **1980**, 1.
69. Engelhardt, G; Fahlke, B.; Mazi, M.; Lippmaa, E. *Zeolites*. **1985**, *5*, 49.
70. Meier, W.M. *Molecular Sieves*; Society of Chemistry and Industry: London, **1968**, pp. 10-27.
71. Haggin, J. *Chem. Eng. News* **1993**, *71*, (Sept. 13), 41.
72. (a) Kinrade, S.D. Ph.D. thesis, University of Calgary, Canada, 1987. (b) Kinrade, S.D.; Swaddle, T.W. *Inorg. Chem.* **1989**, *28*, 1952.

73. DeFretas, A.S.; McMulloch, A.W.; McInnes, A.G. *Can. J. Chem.* **1991**, *69*, 611.
74. *Vespef*[®] *Technical Bulletin A-52349*; E.I. du Pont de Nemours & Co., Wilmington, Delaware.
75. Kel-F[®]; 3M Company, St. Paul, Minnesota.
76. PEEK (polyetheretherketone) components. supplied by Cole-Parmer Company, Niles, Illinois.
77. Ammann, C.; Meier, P.; Merbach, A.E. *J. Magn. Reson.* **1982**, *46*, 319.
78. Groenen, E.J.J.; Kortbeek, A.G.T.G.; Mackay M.; Sudmeijer, O. *Zeolites* **1986**, *6*, 403.
79. Rademacher, O.; Ziemens O.; Scheler, H. *Z. Anorg. Allg. Chem.* **1984**, *519*, 165.
80. Boxhoorn, G.; Sudmeijer, O.; van Kasteren, P.H.G. *J. Chem. Soc., Chem. Comm.* **1983**, 1416.
81. (a) Friebolin, H. *Basic One- and Two-Dimensional NMR Spectroscopy*; VCH: New York, **1991**, pp. 149-153, pp. 263-291. (b) Saunders, J.K.M.; Hunter, B.K. *Modern NMR Spectroscopy. A Guide for Chemists*; Oxford University: Oxford, **1989**, pp. 234,181.
82. Lazarev, A.N. *Vibrational Spectra and Structure of Silicates*; Consultants Bureau: New York: **1972**, pp. 47.
83. Hasegawa, I.; Sakka, S. *Zeolite Synthesis*. (196th National Meeting of the American Chemical Society); ACS: Washington, **1989**, pp. 28.
84. Hasegawa, I.; Sumio, S.; Sugahara, Y.; Kuroda, K.; Kato, C. *J. Chem. Soc., Chem. Commun.* **1989**, 208.
85. Knight, C.T.; Kirkpatrick, R.J.; Oldfield, E. *J. Am. Chem. Soc.* **1987**, *109*, 1632.
86. Mortlock, R.F.; Bell, A.T.; Chakraborty, A.K.; Radke, C.J. *J. Phys Chem.* **1991**, *95*, 4501.
87. Mortlock, R.F.; Bell, A.T.; Radke, C.J. *J. Phys Chem.* **1991**, *95*, 372.

88. Mortlock, R.F.; Bell, A.T.; Radke, C.J. *J. Phys Chem.* **1992**, *96*, 2968.
89. Mortlock, F.R.; Bell, A.T.; Radke, C.J. *J. Phys. Chem.* **1991**, *95*, 7847.
90. Knight, C.T.G. *Zeolites* **1989**, *9*, 448.
91. Connors, K.A. *Chemical Kinetics. The Study of Reaction Rates in Solution*; VCH: New York, **1990**, pp. 261-263, pp. 59-132.
92. Laidler, K.J. *Chemical Kinetics*, 3rd ed.; Harper & Row: New York, **1987**, pp. 206-209.
93. van't Hoff, J.H. *Vorlesungen uber theoretische und physikalische Chemie*; Braunschweig: **1898**.
94. van Eldik, R.; Asano, T.; le Noble, W.J. *Chem. Revs.* **1989**, *89*, 549.
95. Asano, T.; le Noble, W.J. *Chem. Revs.* **1978**, *78*, 407.
96. McCabe, J.R.; Eckert, C.A. *Acc. Chem. Res.* **1974**, *7*, 251.
97. Kirk Marat. University of Winnipeg's NMR Operator.
98. Chandler, W.D.; Lee, E.J.; Lee, D.G. *J. Chem Educ.* **1987**, *64*, 878.
99. SigmaPlot® curve fitting program by Jandel Scientific Corporation.
100. Schlenkrich, F.; Rademacher, O.; Scheler, H. *Anorg. Allg. Chem.* **1990**, *582*, 169.
101. Hoffman, R.A.; Forsén, S., *Prog. NMR Spectrosc.* **1966**, *1*, 15.
102. Sanders, J.K.M.; Mersh, J.D., *Prog. NMR Spectrosc.* **1982**, *15*, 353.

Appendix to Chapter 3, Section 3.2

Selective Population Transfer NMR

Population transfer NMR experiments were first described by Hoffman and Forsén.^[101] Consider two spin 1/2 nuclei A and B which are at equilibrium (chemically and magnetically) and are exchanging (Figure 1). If the exchange rate is on the chemical shift time scale and is comparable with the T_1 relaxation rate, then the rate of interchange can be calculated using selective saturation or selective inversion recovery methods.

We can assume that exchange between A and B occurs without change of spin state.^[102] Selective saturation or selective inversion of the spin sites on A will result in an increase the transfer rate of spins from the upper level of A to B and decrease the rate of transfer from the lower level (see Figure 1).

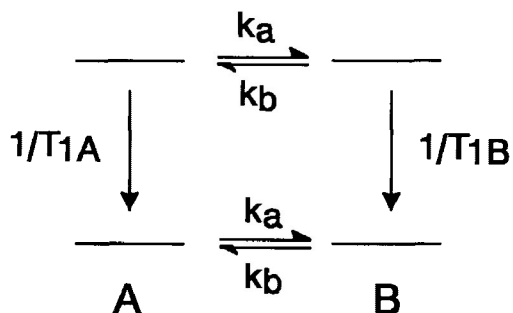


Figure 1. Transfer of spin population between two species A and B where k_a and k_b are the first order rate constants and $1/T_{1A}$ and $1/T_{1B}$ are the spin lattice relaxation rates of the species, respectively.

Saturation of A will increase the signal intensity of B. However, spin lattice relaxation will tend to restore the equilibrium population of B thus

decreasing the signal intensity. There is a competition between chemical exchange and spin lattice relaxation. By monitoring the changes in signal intensity of species B with respect to saturation time, the exchange rates can be calculated.

Silicate solutions contain a complex mixture of mutually exchanging oligomers (see Section 3.2.2) and, thus, a multi-site exchange mechanism would have to be used. Also, each exchange process will have a unique rate constant and T_1 relaxation rate. Therefore, a complete analysis of the exchange processes involving silicate oligomers would not be trivial.

